

This file is part of the following work:

**Al-Saadi, Ali Yasseen Nasir (2020) *Biodiesel production using a SrO-ZnO/Al<sub>2</sub>O<sub>3</sub> bifunctional heterogeneous catalyst*. PhD Thesis, James Cook University.**

Access to this file is available from:

<https://doi.org/10.25903/w7bw%2D7r13>

Copyright © 2020 Ali Yasseen Nasir Al-Saadi.

The author has certified to JCU that they have made a reasonable effort to gain permission and acknowledge the owners of any third party copyright material included in this document. If you believe that this is not the case, please email

[researchonline@jcu.edu.au](mailto:researchonline@jcu.edu.au)

# **Biodiesel production using a SrO-ZnO/Al<sub>2</sub>O<sub>3</sub> bifunctional heterogeneous catalyst**

A thesis submitted for the degree of

Doctor of Philosophy

by

**Ali Yasseen Nasir Al-Saadi (MSc)**

July 2020

College of Science and Engineering

James Cook University

Australia





*“He gives wisdom to whomever He wills. Whoever is given wisdom has been given much good”.*

*The Quran, Al-Baqarah, 269*

## Dedication

To man of patience and struggle ... To man who established human values and principles ...  
To man who spent all his life raising and support his children ... My beloved father (may God have  
mercy on you) ...

To the beating heart ... To the symbol of tenderness, love and sacrifice ... To that whose  
prayers were the reason of my success ... My dear mother (may God protect you from all  
misfortune) ...

To the symbol of loyalty ... To the love of my heart ... To my lifetime companion ... My dear  
wife **Israa** (may God bless you) ...

... this simple work is dedicated.

## Declaration

To the best of the author's knowledge, this thesis contains no material which has been accepted for the award of any other degree or diploma at any university or other institution, and contains no material previously published or written by another person except where due reference is made in the text.

-----

Ali Al-Saadi

-----

Date

## Acknowledgements

Firstly, I would like to thank God for helping me finish this study. Secondly, I would to express deep thanks to my supervisors Professor Yinghe He and Associate Professor Bobby Mathan for the continuous help, support and encouragement they have provided during the many years of work that went into preparing this thesis.

It is with immense gratitude that I acknowledge the support and help of Ruilin Liu and Melissa Norton. My sincere thanks also go to my Iraqi friends at James Cook University, especially Ahmed Abdulwahid, Madyan Yaseenn and Ahmed Al-Jumaili.

I would like to express sincere gratitude from the bottom of my heart to my family—my mother, brothers and sisters—and my friends in Iraq for their supplications and prayers to the omnipresent God, who gave me the strength to complete my study.

To my wife Israa, words are incapable of describing the extent of your sacrifice and endurance in supporting me, not only in my studies but also in all aspects of life. So, I would like to express my great gratitude for your continued encouragement to achieve my very best. Thank you so much.

Finally, I would like to thank the Iraqi Government represented by the Ministry of Higher Education and Scientific Research (MOHES) for granting me a scholarship. Also, I greatly appreciate the help of James Cook University in exempting me from tuition fees for my final year.

## Abstract

In recent years, the increasing global demand for fuel and negative impacts of fossil fuels on the environment have created the need for alternative fuels. Biodiesel is one alternative fuel that can help fill this market need and has several advantages, such as being environmentally-friendly (biodegradable and non-toxic) and made from renewable raw materials. Generally, the oils are classified into two categories: 1) acidic oils and 2) vegetable oils with low free fatty acid (FFA) contents, such as inedible and edible oils. Traditionally, acidic catalysts are preferably used with acidic oils in esterification reactions, while basic catalysts are better suited to vegetable oils via transesterification reactions. A variety of catalysts are used in the biodiesel industry; namely, basic catalysts (homogeneous and heterogeneous), acid catalysts (homogeneous and heterogeneous), bifunctional heterogeneous catalysts, and enzymatic catalysts. Recent studies indicate that bifunctional heterogeneous catalysts (BHCs) containing active base-acid sites are promising. BHCs have increasingly been applied in the biodiesel industry due to their benefits, such as having both acid and base active sites, which allows the simultaneous occurrence of esterification and transesterification reactions with high conversion and selectivity.

In this thesis, a series of novel bifunctional heterogeneous catalysts ( $\text{SrO-ZnO/Al}_2\text{O}_3$ ) were synthesized via the wet impregnation method for biodiesel production. The catalysts were synthesized with different Sr:Zn molar ratios over  $\text{Al}_2\text{O}_3$  at different calcination temperatures. The best-performing synthesized catalyst had a 2.6:1 Sr:Zn molar ratio and was calcined at a temperature of 900 °C. Physio-chemical characteristics of the synthesised catalysts were characterized with X-ray diffraction (XRD), scanning electron microscopy (SEM), energy-dispersive X-ray spectroscopy (EDS), Fourier-transform infrared spectroscopy (FT-IR), inductively-coupled plasma optical emission spectrometry (ICP-OS), and Brunauer–Emmett–Teller (BET) and Barrett–Joyner–Halenda

(BJH) techniques. Fatty acid ethyl ester (biodiesel) was analysed by proton nuclear magnetic resonance ( $^1\text{H}$  NMR).

The performance of the synthesized catalysts was characterized in two ways: firstly, corn oil was used in a transesterification reaction and oleic acid was used in an esterification reaction. The catalyst exhibited higher catalytic activity in transesterification, with 95.1% reaction conversion under operating conditions of a 10:1 ethanol-to-corn oil molar ratio, 10 wt.% catalyst loading, and reaction for 180 min at 70 °C. However, the best conversion with the esterification reaction was only 71.4 % under operating conditions of a 5:1 ethanol-to-corn oil molar ratio, 10 wt.% catalyst loading and 6 h reaction time at 70 °C. Also, the reaction kinetics of the esterification and transesterification reactions were studied to understand the influences of, and relationship between, reaction time and temperature. The kinetics were studied in transesterification and esterification reactions at temperatures of 50 °C, 60 °C and 70 °C. The transesterification and esterification reactions could be approximated well by first-order models. The activation energies required for transesterification and esterification reactions using the  $\text{ZnO-SrO/Al}_2\text{O}_3$  catalyst were 25.5 kJ/mol and 15.84 kJ/mol, respectively. This suggests that the rate of transesterification reaction increases more quickly with temperature than that of esterification.

Secondly, high-acidity waste cooking oil was used in simultaneous transesterification and esterification reactions over a bifunctional catalyst. The catalyst exhibited high catalytic activity, with 95.7% reaction conversion at the optimum conditions of a 10:1 ethanol-to-waste oil molar ratio, 15 wt.% catalyst dosage and 5 h reaction time at 75 °C. Reaction mechanisms for both the trans/esterification reactions that occur on the surface of the bifunctional catalyst are proposed. They show that the two reactions occur simultaneously on the base and acid sites on the surface of the bifunctional catalyst.

## Publications

### Journal papers:

- Al-Saadi, A., Mathan B., He Y., Esterification and transesterification over SrO–ZnO/Al<sub>2</sub>O<sub>3</sub> as a novel bifunctional catalyst for biodiesel production. *Renewable Energy*, 2020. 158: p. 388-399. <https://www.sciencedirect.com/science/article/abs/pii/S0960148120308764>
- Al-Saadi, A., Mathan B., He Y., Biodiesel production via simultaneous transesterification and esterification reactions over SrO-ZnO/Al<sub>2</sub>O<sub>3</sub> as a bifunctional catalyst using high acidic waste cooking oil. *Chemical Engineering Research and Design*, 2020. 162: p. 238-248. <https://www.sciencedirect.com/science/article/abs/pii/S0263876220304299>
- Al-Saadi, A., Mathan B., He Y., A new approach for quantification of ethyl esters (biodiesel) and triglycerides content by a nuclear magnetic resonance (<sup>1</sup>H NMR) Spectroscopy, (in preparation).
- Al-Saadi, A., Mathan B., He Y., Development of a bifunctional catalyst for simultaneous esterification and transesterification of blended oil (oleic acid and corn oil): Optimisation using RSM Methodology, (in preparation).

### Conferences:

- Al-Saadi, A., Mathan B., He Y., 2016, “Synthesis and performance characterisation of bi-functional catalyst for biodiesel production”, oral presentation at the *Biology in the Tropics – Postgraduate Students Conference*, James Cook University, Townsville, Australia, 28 – 29 September.
- Al-Saadi, A., B. Mathan, and Y. He, 2016, “Biodiesel production over bi-functional heterogeneous catalyst”, poster presentation at the *Bioenergy Australia Conference*, Brisbane, Australia, 14 – 16 November.

# Table of Contents

<b>ACKNOWLEDGEMENTS</b> .....	<b>I</b>
<b>ABSTRACT</b> .....	<b>II</b>
<b>PUBLICATIONS</b> .....	<b>IV</b>
<b>TABLE OF CONTENTS</b> .....	<b>V</b>
<b>LIST OF TABLES</b> .....	<b>IX</b>
<b>LIST OF FIGURES</b> .....	<b>X</b>
<b>NOMENCLATURE</b> .....	<b>XIV</b>
<b>CHAPTER 1: INTRODUCTION</b> .....	<b>1</b>
1.1 BIODIESEL AS A RENEWABLE FUEL .....	1
1.2 RESEARCH SCOPE .....	3
1.3 THESIS OUTLINE .....	4
<b>CHAPTER 2: DEVELOPMENT OF CATALYSTS AND PROCESSES FOR BIODIESEL PRODUCTION: A REVIEW</b> .....	<b>7</b>
2.1 INTRODUCTION.....	7
2.2 PROCESS DEVELOPMENT FOR THE CATALYTIC PRODUCTION OF BIODIESEL.....	11
2.2.1 <i>Overview of processes for biodiesel production</i> .....	11
2.2.1.1 Feedstocks in the biodiesel industry .....	11
2.2.1.2 Trans/esterification processes .....	16
2.2.1.2.1 Catalytic methods .....	17
2.2.1.2.2 Non-catalytic methods.....	17
2.2.2 <i>Catalytic biodiesel production processes</i> .....	18
2.3 CATALYST DEVELOPMENT FOR CATALYTIC BIODIESEL PRODUCTION.....	25
2.3.1 <i>Types of catalysts and their development</i> .....	25
2.3.1.1 Homogeneous catalysts .....	25
2.3.1.1.1 Basic catalysts .....	25
2.3.1.1.2 Acid catalysts .....	25

2.3.1.2 Heterogeneous catalysts .....	26
2.3.1.2.1 Base catalysts .....	26
2.3.1.2.2 Acid catalysts .....	28
2.3.1.2.3 Acid-base bi-functional metal oxide heterogeneous catalysts .....	29
2.3.1.2.4 Biocatalysts .....	32
2.3.2 <i>Synthesis methods and their impacts on the catalytic effects of heterogeneous catalysts</i> .....	34
2.3.3 <i>Catalyst longevity</i> .....	36
2.4 CONCLUDING REMARKS AND FUTURE OUTLOOK .....	38

### CHAPTER 3: ESTERIFICATION AND TRANSESTERIFICATION OVER A BIFUNCTIONAL CATALYST FOR BIODIESEL

<b>PRODUCTION .....</b>	<b>40</b>
3.1 ABSTRACT .....	40
3.2 INTRODUCTION .....	40
3.3 MATERIALS AND METHODS .....	43
3.3.1 <i>Materials</i> .....	44
3.3.2 <i>Catalyst preparation</i> .....	46
3.3.3 <i>Esterification and transesterification reactions</i> .....	47
3.3.4 <i>Characterisation</i> .....	48
3.3.4.1 Property characterisation .....	48
3.3.4.2 Biodiesel analysis by <sup>1</sup> H NMR .....	49
3.3.5 <i>Kinetic study of esterification and transesterification reaction over the bifunctional catalyst</i> .....	50
3.4 RESULTS AND DISCUSSION .....	50
3.4.1 <i>Catalytic activity</i> .....	50
3.4.1.1 Effect of calcination temperature on the catalyst .....	50
3.4.1.2 Catalytic performance in the transesterification process .....	51
3.4.1.3 Catalytic performance in esterification reaction .....	58
3.4.2 <i>Catalyst characterisation</i> .....	61
3.4.2.1 X-ray diffraction .....	61
3.4.2.2 Scanning electron microscopy and energy-dispersive X-ray spectroscopy .....	65
3.4.2.3 Fourier-transform infrared spectroscopy .....	67

3.4.2.4	Surface area (BET) and pore volume (BJH).....	68
3.4.2.5	Inductively Coupled Plasma Optical Emission Spectrometer .....	69
3.4.3	<i>Kinetic studies</i> .....	70
3.5	CONCLUSION.....	75
<b>CHAPTER 4: BIODIESEL PRODUCTION FROM HIGH-ACIDITY WASTE COOKING OIL.....</b>		<b>76</b>
4.1	ABSTRACT .....	76
4.2	INTRODUCTION.....	76
4.3	MATERIALS AND METHODS .....	79
4.3.1	<i>Materials</i> .....	80
4.3.2	<i>Feedstock characterisation</i> .....	80
4.3.3	<i>Catalyst preparation</i> .....	81
4.3.4	<i>Catalyst characterization</i> .....	82
4.3.5	<i>Biodiesel production and kinetics study</i> .....	82
4.4	RESULTS AND DISCUSSION.....	84
4.4.1	<i>Catalyst characterization</i> .....	84
4.4.2	<i>Effects of operating conditions</i> .....	85
4.4.2.1	Effect of reaction time on conversion .....	85
4.4.2.2	Effect of reaction temperature .....	86
4.4.2.3	Effect of the ethanol-to-waste cooking oil molar ratio .....	87
4.4.2.4	Effect of catalyst loading .....	88
4.4.2.5	Catalyst activity in simultaneous transesterification and esterification reactions .....	89
4.4.2.6	Effect of free fatty acid content .....	92
4.4.3	<i>Kinetic study</i> .....	93
4.4.4	<i>Reusability of catalyst</i> .....	95
4.4.5	<i>Mechanism of reaction</i> .....	97
4.5	CONCLUSION.....	99
<b>CHAPTER 5: CONCLUSIONS AND RECOMMENDATIONS .....</b>		<b>100</b>
5.1	CONCLUSIONS .....	100

5.2 FUTURE WORK.....	101
<b>BIBLIOGRAPHY .....</b>	<b>103</b>
<b>APPENDIX A: SUPPLEMENTARY MATERIALS.....</b>	<b>117</b>

## List of Tables

Table 2.1. Standard properties of petrodiesel and biodiesel and soybean methyl ester (SME) (Al-Dawody et al., 2014) .....	8
Table 2.2. Biodiesel prices according to the raw materials .....	10
Table 2.3. Specifications of the feedstocks used for biodiesel production (Lee et al., 2014) .....	12
Table 2.4. First generation feedstocks and their catalysts.....	13
Table 2.5. Second-generation feedstocks and their catalysts.....	14
Table 2.6. Oil contents of several microorganisms (Meng et al., 2009).....	14
Table 2.7. Third generation feedstocks and their catalysts .....	15
Table 2.8. Fourth generation feedstocks and required production conditions.....	16
Table 2.9. Modern integrated catalytic technologies used for biodiesel production .....	22
Table 2.10. Merits and demerits of catalytic biodiesel production processes via transesterification and esterification reactions.....	24
Table 2.11. Benefits and drawbacks of various types of catalysts used for biodiesel production .....	33
Table 3.1. Physical and chemical properties of the studied corn oil.....	45
Table 3.2. Comparison of the biodiesel production performance of the catalyst used in the current study with other bifunctional catalysts .....	60
Table 3.3. Weight ratios of the metals in catalyst 2.6SZA900 .....	67
Table 3.4. Surface area, pore volume and average pore diameter of catalysts according to BET analysis.....	69

Table 3.5. Theoretical, surface, and bulk amounts of Sr, Zn, and Al metals, as measured by ICP-OS and EDX.....	70
Table 3.6. Correlation coefficients and rate constants for trans/esterification reactions at different temperatures. ....	75
Table 4.1. Summary of research on biodiesel production from WCO using bifunctional catalysts.....	78
Table 4.2. Physical and chemical properties of the WCO used in this study .....	81
Table 4.3. Comparison of the studied SrO-ZnO/Al <sub>2</sub> O <sub>3</sub> catalyst with previous catalysts.....	91
Table 4.4. ICP-OS analysis of 2.6SZA catalysts before and after use in reaction.....	96

## List of Figures

Figure 2-1. Emission gases of biodiesel (Meshram et al., 2013).....	9
Figure 2-2. Components of biodiesel production cost (Atabani et al., 2012).....	9
Figure 2-3. Classification of all feedstocks used in the biodiesel industry (Lee et al., 2014)	12
Figure 2-4. Catalytic and non-catalytic process. (a) Transesterification reaction and (b) esterification reaction (Lee et al., 2014). ....	17
Figure 2-5. Flowchart of the enzymatic hydrolysis process (Pourzolfaghar et al., 2016) .....	18
Figure 2-6. Diagram of a reactive distillation process (Pérez-Cisneros et al., 2016) .....	19
Figure 2-7. Diagrams of membrane reactors used for a) transesterification and b) esterification reactions (Kiss et al., 2012).....	21

Figure 2-8. Flowchart of current biodiesel production processes using transesterification and esterification reactions .....	23
Figure 3-1 Catalyst preparation via a wet impregnation method.....	47
Figure 3-2 Effect of calcination temperature on FAEE conversion with catalyst 2.6SZA.....	51
Figure 3-3 Effect on FAEE conversion of catalysts with different amounts of strontium and zinc nitrate loaded on alumina oxide and calcined at 900 °C. Reaction conditions: 10:1 EtOH:oil molar ratio, reaction temperature = 70 °C, 180 min reaction time and 10 wt.% catalyst dosage.....	52
Figure 3-4 FAEE conversion with reaction time at three temperatures using catalyst 2.6SZA900. Reaction conditions: 10:1 ethanol:oil molar ratio, 10% catalyst loading, and reaction durations of 0–240 min. ....	53
Figure 3-5 FAEE conversion in relation to ethanol/corn oil molar ratio with catalyst 2.6SZA900. Reaction conditions: temperature = 70 °C, 10% catalyst dosage and 180 min reaction time.....	54
Figure 3-6. (a) Effect of 2.6SZA900 catalyst loading on FAEE conversion and (b) FAEE conversion over time at loadings of 10 wt.% and 15 wt.%.....	56
Figure 3-7. <sup>1</sup> H NMR spectra of the transesterification reaction reactant and product, with pure ethyl ester shown for comparison .....	57
Figure 3-8. <sup>1</sup> H NMR spectra of the esterification reaction's (a) reactant (pure oleic acid) and (b) final product (FAEE); (c) with pure ethyl oleate shown for comparison.....	58
Figure 3-9. XRD patterns for (a) catalysts with different Sr:Zn molar ratios calcined at 900 °C and (b) 2.6SZA catalyst calcined at different temperatures.....	64
Figure 3-10. SEM images of (a) neat aluminium oxide and (b) 2.6SZA 900 catalyst .....	66
Figure 3-11. 2.6SZA900 catalyst (a) EDS spectra and (b) EDS elemental mapping .....	66

Figure 3-12. FT-IR spectra of different Sr –Zn loading for prepared catalysts .....	68
Figure 3-13. Kinetic first-order models fitted to a) transesterification and b) esterification reactions .....	72
Figure 3-14. First-order models of the activation energies of the a) transesterification and b) esterification reactions .....	74
Figure 4-1. Effect of the catalyst metal ratio on conversion during the reaction. Reaction conditions: 10:1 ethanol:WCO molar ratio, 15 wt.%, 75 °C .....	85
Figure 4-2. Effect of reaction temperature on conversion using the 2.6SZA catalyst. Reaction conditions: 10:1 ethanol:WCO molar ratio, 15 wt.% catalyst, 5 h reaction time. ....	86
Figure 4-3. Effect of the ethanol/WCO molar ratio on conversion using catalyst 2.6SZA. Reaction conditions: 75 °C, 5 h reaction time, 15 wt.% catalyst.....	87
Figure 4-4. Effect of 2.6SZA catalyst loading on conversion. Reaction conditions: 75 °C, 5 h reaction time, 10:1 ethanol:WCO molar ratio.....	88
Figure 4-5. FAEE conversion and FFA and TG contents as a function of time. Reaction conditions: 15% catalyst, 10:1 ethanol:WCO molar ratio, 75 °C reaction temperature. ....	90
Figure 4-6. <sup>1</sup> H NMR spectra of the esterification reaction: (a) WCO; (b) final product after reaction and (c) standard ethyl ester for comparison .....	90
Figure 4-7. Conversion with reaction time with two feedstocks with different FFA contents (waste vegetable oil, WCO = 18% and corn oil = 0.05%).....	92
Figure 4-8. Catalyst recycling activity with different methods .....	96
Figure 4-9. Schematic illustrations of (a) an overview of the suggested reaction mechanism, (b) a possible mechanism for transesterification of TG with ethanol, and (c) a possible mechanism for esterification of FFA with ethanol.....	98

Figure S 1. <sup>1</sup> H NMR spectra for FAEE product with pure ethyl ester and pure triglycerides for comparison.....	117
Figure S 2. Kinetic pseudo-first-order models fitted to data from a) transesterification and b) esterification reactions .....	118
Figure S 3. Pseudo-first-order models of the activation energies of a) transesterification and b) esterification reactions .....	119

## Nomenclature

XRD = X-ray diffraction

SEM = Scanning electron microscope

EDS = Energy-dispersive X-ray spectroscopy

FT-IR = Fourier-transform infrared spectroscopy

ICP-OS = Inductively coupled plasma optical emission spectrometer

$^1\text{H}$  NMR = Proton nuclear magnetic resonance

FFA = Free fatty acid

TG = Triglycerides

WCO = Waste cooking oil

FAEE = Fatty acid ethyl ester

COD = Crystallography Open Database

$I_{TAG}$  = Integration intensities of triglycerides at 4.25–4.35 ppm

$I_{TAG+EE}$  = Integration intensities of methylene groups of ethyl esters at 4.1–4.2 ppm

EtOH = Ethanol

$r$  = Reaction rate ( $\text{mol.l}^{-1}.\text{h}^{-1}$ )

$k$  = Reaction rate constant ( $\text{min}^{-1}$ )

$[\text{TG}]_0$  = Triglyceride concentration at the beginning

$[\text{TG}]$  = Triglyceride concentration at any time

$E_a$  = Activation energy ( $\text{kJ/mol}$ )

$R$  = Universal gas constant ( $8.314 \text{ J mol}^{-1} \text{ K}^{-1}$ )

$A$  = Frequency factor ( $\text{min}^{-1}$ )

$T$  = Reaction temperature (K)

$R^2$  = Correlation coefficient

SV = Saponification value

AV = Acid value

m & n = Order of reaction

# Chapter 1: Introduction

Energy plays a vital role in society. Its consumption has increased significantly in the previous decade and will be increasingly needed in the future as the human population grows. Unfortunately, the combustion of fossil fuels has serious impacts on the environment due to emissions of carbon dioxide, which causes global warming and pollution. Accordingly, researchers around the world are searching for alternative energy sources that are environmentally friendly and renewable, such as wind, solar and biofuel. The biodiesel industry has increased over the previous decade and has become an important part of global alternative energies. Biodiesel is a type of biofuel and has several benefits, such as being produced from various renewable feedstocks, being environmentally friendly (biodegradable and non-toxic), and being able to be blended with petroleum diesel (Demirbas, 2009). Generally, biodiesel is manufactured by four methods: direct use (blending vegetable oil with diesel fuel), pyrolysis, micro-emulsion and trans/esterification reactions (Yusuf et al., 2011).

## **1.1 Biodiesel as a renewable fuel**

Transesterification and esterification processes are common methods of biodiesel production and a large number of researchers has used them recently. Chemically, biodiesel is defined as fatty acid esters and is manufactured through the esterification of free fatty acids or transesterification of triglycerides. The process is carried out by reacting oil (acidic oils, vegetable oils or blended oils) with alcohol (ethanol, methanol or any other alcohol) in the presence or absence of a catalyst (Lee et al., 2014). Transesterification reactions often preferably use basic catalysts with vegetable oils, while acidic catalysts are preferred for use with acidic oils via esterification reactions (Yan et al., 2009). Trans/esterification processes depend on two main variables: the type of oil and the catalyst.

An enormous range of raw materials has been employed in the production of biodiesel. The oils used are classified into two categories: acidic and vegetable oils. Vegetable oils with low free fatty acid contents contain Mo-, Di-, Tri- triglycerides (TGs), such as canola, corn, sunflower and

soybean oil. These kinds of oils are edible because of their very low acid value. Whereas acidic oils contain high contents of free fatty acids (FFAs), such as *Jatropha* and oleaginous microorganism oil. The acidic oils are inedible due to their high acid value.

From an economic perspective, the main obstacle to biodiesel production is cost, with the feedstock representing 60–70% of the total production cost (Kumar et al., 2017). Therefore, using low-cost and -quality raw materials such as waste cooking oil could reduce the biodiesel production cost. Biodiesel produced from waste cooking oil (WCO) costs approximately 1.2–2.5 US\$/litre and represents 2% of total production cost (Mohammadshirazi et al., 2014). After studying 81 different scenarios, Fawaz et al. (2018) reported that the average total cost of biodiesel produced from WCO is 0.57 US\$/litre. Waste cooking oil is vegetable oil that has been altered by cooking at high temperatures to become blended oil (acidic oil with vegetable oil), which are represented by FFA and Mo-, Di-, Tri- glycerides (TG), respectively. Recently, biodiesel produced from low-cost feedstock has attracted considerable attention. WCO is an inexpensive raw material that is approximately 60% cheaper than vegetable oils. Furthermore, not only is WCO a cheap feedstock, but direct disposal of WCO can harm the environment and is expensive to dispose of properly (Talebian-Kiakalaieh et al., 2013). The difficulty in producing biodiesel from WCO varies according to the acidic content of the oil. Because WCO contains TG and FFA, the preferred catalysts for this type of oil require the ability to catalyse both the transesterification and esterification reactions of TG and FFA simultaneously.

Previously, homogeneous catalysts have been widely used. However, they have major disadvantages, including the inability to be recovered (resulting in high consumption), the need for a washing process for naturalisation, and soap formation during production (Huang et al., 2010). On the other hand, heterogeneous solid catalysts have several advantages such as reusability, environmental friendliness (Pasupulety et al., 2013), safety and economy (Bharathiraja et al., 2014). A large number of heterogeneous catalysts (acid and base) are employed in biodiesel production. Bifunctional heterogeneous solid catalysts have attracted increasing interest from researchers due to

their benefits. For example, their acid-base active sites are together, allowing simultaneous esterification and transesterification reactions with high conversion and selectivity (Chang et al., 2014; Mardhiah et al., 2017). Therefore, bifunctional catalysts are suitable for use with different oils, especially WCO (Verma et al., 2016).

## 1.2 Research scope

The research scope of the present work is to develop a bifunctional catalyst that can catalyse reactions with feedstock containing acid oils (oleic acid), vegetable oils (corn oil), or blended oils (WCO) for biodiesel production. Specifically, there are two objectives in this work.

The first objective is to investigate the performance of novel heterogeneous catalysts (SrO-ZnO/Al<sub>2</sub>O<sub>3</sub>) for biodiesel production from corn oil via transesterification reaction and from oleic acid via esterification reaction. The objective is undertaken as follows:

1. Synthesising a new group of (SrO-ZnO/Al<sub>2</sub>O<sub>3</sub>) acid-base bifunctional heterogeneous catalysts with different Sr:Zn molar ratios over Al<sub>2</sub>O<sub>3</sub> at different calcination temperatures for biodiesel production using a wet impregnation method.
2. Characterising the prepared catalysts by different methods, such as XRD, SEM, EDS, FT-IR, BET, BJH and ICP-OS.
3. Investigating the influence of metal oxide composition on the acid-base sites on catalytic performance in a transesterification reaction of corn oil and an esterification reaction of oleic acid.
4. Optimising the operating conditions, such as ethanol/oil molar ratio, catalyst dosage, reaction temperature and transesterification and esterification reaction time, using a full factorial experimental design.
5. Studying the reaction kinetics of transesterification and esterification reactions to determine the order of reaction and to calculate the kinetic parameters, such as the reaction rate constant and activation energy of both reactions.

The second objective is to validate the catalytic activity of the synthesised catalyst in fatty acid ethyl ester (FAEE) production using high-acidity WCO. The objective is achieved as follows:

1. Investigating the bifunctional catalytic performance of the prepared catalyst by undertaking esterification and transesterification reactions simultaneously using high-FFA WCO for FAEE production.
2. Calculating the conversion of FAEE by the transesterification and esterification reactions separately, and the total conversion of FAEE by both reactions by  $^1\text{H}$  NMR.
3. Optimising operating conditions, such as ethanol/WCO molar ratio, catalyst loading, reaction temperature and time, by a full factorial experimental design.
4. Studying the effect of FFA content on the catalytic activity of the prepared catalyst.
5. Understanding the mechanisms of the esterification and transesterification reactions over the SrO-ZnO/Al<sub>2</sub>O<sub>3</sub> catalyst.
6. Studying the kinetics of the trans/esterification reactions simultaneously to calculate their reaction rate constants and activation energies, and determine their orders.
7. Investigating the reusability of the catalyst and possible regeneration methods.

### 1.3 Thesis outline

The thesis is presented as a series of chapters that have been published or are currently being reviewed for publication in peer-reviewed scientific journals. The authorship of the chapters is shared with my supervisory panel, Professor Yinghe He and Associated Professor Bobby Mathan. The thesis chapters are outlined as follows:

**Chapter one** provides a brief overview of the importance of finding alternative fuels and the importance of biodiesel. The research scope and objectives are also presented.

**Chapter two** presents the most relevant and recent literature on catalysts developed for biodiesel production. All types of catalytic processes and feedstock used in biodiesel production are discussed in detail. A summary of catalyst synthesis methods is presented. Also, literature on the

advantages, disadvantages and longevity of catalysts utilised in biodiesel production is reviewed in this chapter.

**Chapter three** describes a series of experiments that were conducted to synthesise a novel group of SrO-ZnO/Al<sub>2</sub>O<sub>3</sub> solid catalysts for biodiesel production. The influences of the metal oxide composition on the acid-base sites, on the transesterification reaction of corn oil, and on the esterification reaction of oleic acid are investigated, and the kinetics of both trans/esterification reactions are studied. Moreover, the parameters for both reactions, such as ethanol/oil molar ratio, catalyst amount, and reaction temperature and time, are optimised. The content of this chapter has been published in the journal *Renewable Energy* (Al-Saadi, A., Mathan B., and He Y., *Esterification and transesterification over SrO-ZnO/Al<sub>2</sub>O<sub>3</sub> as a novel bifunctional catalyst for biodiesel production*. *Renewable Energy*, 2020. 158: p. 388-399).

**Chapter four** describes a series of experiments that were conducted to validate the catalytic activity of the synthesised catalyst for fatty acid ethyl ester (FAEE) production using high-acidity WCO. Transesterification and esterification reactions of highly-acidic WCO are carried out simultaneously over bifunctional synthesised catalysts with distributions of strong acid-base active sites on their surfaces. Various parameters are optimised, such as ethanol/WCO molar ratio, catalyst loading in the reaction, and reaction temperature and time. Moreover, the bi-functionality of the prepared catalyst is validated by calculating the conversions of the transesterification and esterification reactions separately which, to the best of our knowledge, has never been done before. The content of this chapter has been published in the journal *Chemical Engineering Research and Design* (Al-Saadi, A., Mathan B., and He Y., *Biodiesel production via simultaneous transesterification and esterification reactions over SrO-ZnO/Al<sub>2</sub>O<sub>3</sub> as a bifunctional catalyst using high acidic waste cooking oil*. *Chemical Engineering Research and Design*, 2020. 162: p. 238-248).

**Chapter five** summarises the important outcomes of this PhD research project. Based on the experiences obtained from this PhD project, a number of recommendations are provided for further research in this field.

# Chapter 2: Development of catalysts and processes for biodiesel production: A review

## 2.1 Introduction

Due to the steady decline in fossil fuel resources caused by their increasing consumption, coupled with the global warming effect of fossil fuel emissions, researchers around the world have been actively searching for renewable energy sources in recent decades. Biofuels, which are produced from renewable biological feedstock, have become one of the most prominent sustainable energy sources globally. Biodiesel is a type of biofuel that is produced from a range of renewable resources such as vegetable oils (edible and non-edible), waste cooking oils (WCOs), animal fats, and oleaginous microorganisms. Chemically, biodiesel is defined as fatty acid esters and is manufactured through the esterification of free fatty acids (FFAs) or transesterification of triglycerides (Lee et al., 2014). It has similar physical and chemical properties to petroleum diesel (petro-diesel), including its energy content, viscosity and phase-change temperature (Muniyappa et al., 1996; Nyström et al., 2016). Therefore, it can be used in conventional engines without any modification or blended with petro-diesel in varying percentages, such as 20% (B20) and 80% (B80; Moser, 2009; Yilmaz et al., 2016). Table 2.1 presents a comparison of the properties of conventional biodiesel and a type of petro-diesel (Al-Dawody et al., 2014).

Table 2.1. Standard properties of petrodiesel and biodiesel and soybean methyl ester (SME) (Al-Dawody et al., 2014)

Property	No.2 Diesel fuel	SME
Chemical formula	$C_{13.77}H_{23.44}$	$C_{19}H_{35}O_2$
C/H ratio	6.90	6.51
Density at 15 °C ( $g/cm^3$ )	860	876
Viscosity at 40 °C (cst)	3.0	4.25
Molecular weight (kg/kmol)	190	292.2
Surface tension factor (N/m)	0.028	0.0433
Calorific value (MJ/kg)	42.5	36.22
Flash point (°C)	76	130
Cetane number	48	51.3
Total glycerine (%)	-	0.028
Free glycerine (%)	-	0.00

In addition to its renewable nature, biodiesel is also much more environmentally friendly than petro-diesel. Its emissions include very low levels of sulphur oxide ( $SO_x$ ; about 20–50 times less than petro-diesel; Demirbas, 2007) and it is highly biodegradable, which approximately 90% degradation of biodiesel made from sunflower seed oil in 28 days, (Demirbas, 2009) and less toxic than petro-diesel (Knothe, 2010). According to Balat (2009), sulphur dioxide emissions ( $SO_2$ ) decrease by approximately 20% when biodiesel is used in place of petro-diesel. The total unburned hydrocarbon (HC) content is also about 90% less than that of petro-diesel, and it produces lower amounts of particulate matter (PM) (Demirbas, 2007). Figure 2.1 shows the percentage change in exhaust emissions according to the percentage of biodiesel added to petro-diesel (Meshram et al., 2013). Biodiesel is also safer to use than conventional diesel because of its higher flash point, 423 K compared with about 350 K for petroleum diesel, (Balat, 2011). For internal combustion engines, biodiesel has a high cetane number (CN), leading to better combustion efficiency and engine performance (Yusuf et al., 2011). It also has a better lubricating property, which reduces engine wear and prolongs engine life (Demirbas, 2009).

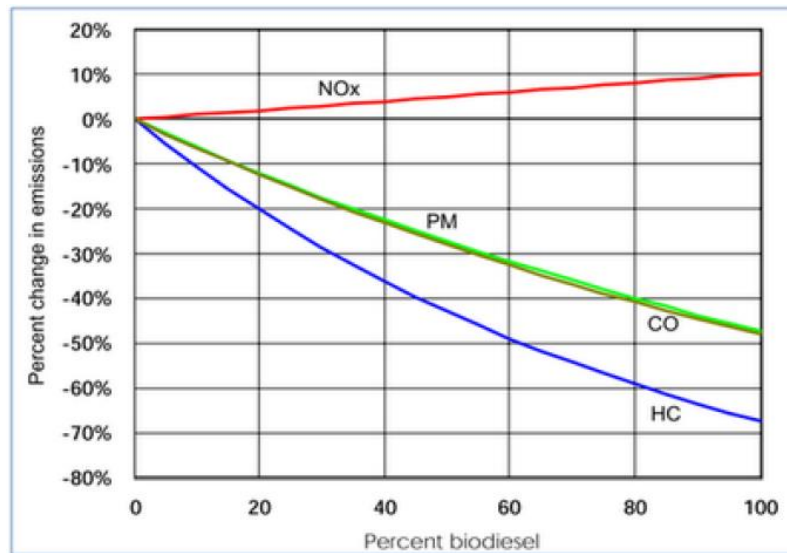


Figure 2-1. Emission gases of biodiesel (Meshram et al., 2013)

Notwithstanding the significant advantages of biodiesel, the high costs for its production present a significant hurdle for its wide uptake in the market (Go et al., 2016). Feedstock accounts for 60–70% of the total production cost (Kumar et al., 2017). A rough breakdown of biodiesel production costs is shown in Fig. 2.2 (Atabani et al., 2012). Total biodiesel production costs using different feedstocks are shown in Table 2.2.

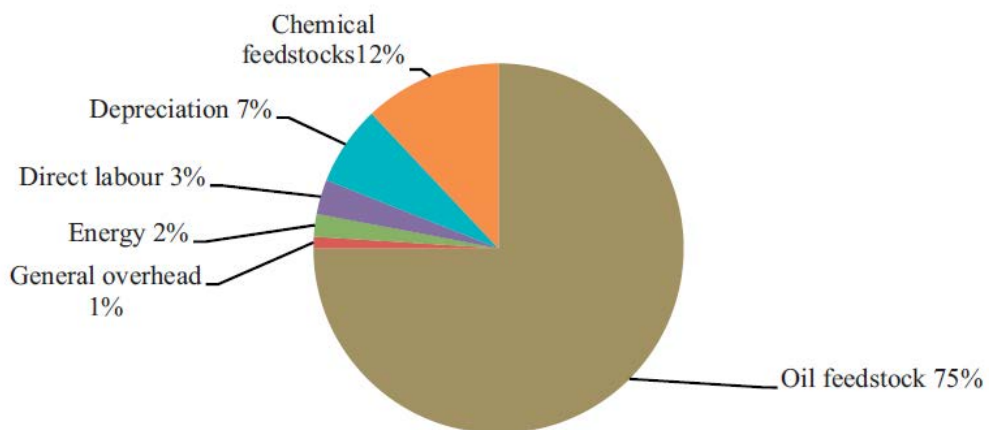


Figure 2-2. Components of biodiesel production cost (Atabani et al., 2012)

Table 2.2. Biodiesel prices according to the raw materials

Feedstock	Biodiesel production cost (US\$/litre)	The cost of raw materials to the final cost (%)	Reference
Yellow grease	0.14 – 0.32	28.6	Balat (2011)
Waste cooking oil	1.2 – 2.5	2	Mohammadshirazi et al. (2014)
Waste grease	0.34 – 0.42	NA	Demirbas et al. (2009)
Refined soy oil	0.7	77	Balat (2011)
Microalgae oil	5.3 – 8.0	NA	Pinzi et al. (2014)

A point to note about Table 2.2 is that the percentage of the cost for the feedstock in the total production cost varies with the feedstock. For low-quality feedstock such as WCO, the cost is almost negligible; however, it represents more than 75% of the total cost for refined vegetable oils. For a given feedstock, processes and technologies, including catalysts, are the keys to improving overall efficiency and reducing costs. Mustafa Balat (2011) reported that a new technology for biodiesel production could reduce the total cost of biodiesel by up to US\$ 0.3/litre. It could also improve the quality of the final products (Talebian-Kiakalaieh et al., 2013).

As the vast majority of commercial processes require the use of catalysts of some sort, this review focuses on the development of catalysts and associated processes for biodiesel production using low-cost feedstock. Section 2 provides a brief overview of biodiesel production processes using different feedstock. Section 3 critically reviews some new catalytic biodiesel production processes reported in the open literature. It will examine and compare the types of catalysts, their synthesis methods and their performance in biodiesel production. The review concludes with an outlook for future research and development directions for catalysts and associated processes for commercial biodiesel production.

## **2.2 Process development for the catalytic production of biodiesel**

### **2.2.1 Overview of processes for biodiesel production**

Diverse processes have been used for biodiesel production. The selection of a process depends on the type of feedstock, operating conditions and the availability of equipment. Go et al. (2016) reported that the biodiesel industry needs development to achieve high productivity by dealing with inexpensive and diverse raw materials under normal operating conditions and using a straightforward production process. Biodiesel made from trans/esterification reactions is produced by catalytic and non-catalytic methods through a continuous (Tran et al., 2017) or batch process (Azevêdo et al., 2018; Rafiei et al., 2018).

#### **2.2.1.1 Feedstocks in the biodiesel industry**

A large number of feedstocks and catalysts have been used for biodiesel production. The selection of a catalyst depends on the type of feedstock (acidic oil or vegetable oil), water content, catalyst effectiveness, cost of catalyst preparation, and the content of free fatty acids (FFAs) in the raw oil. For example, alkali catalysts are preferred for oils with an FFA below 3% (Atadashi et al., 2013) while the enzyme catalyst (lipase) has several benefits compared with alkali and acid catalysts, but is expensive and not industrially feasible (Sharma et al., 2008). Thus, a wide range of raw materials has been used in the biodiesel industry. Feedstocks for biodiesel production are classified into four generations, as shown in Fig. 2.3, and their specifications are tabulated in Table 2.3 (Lee et al., 2014).

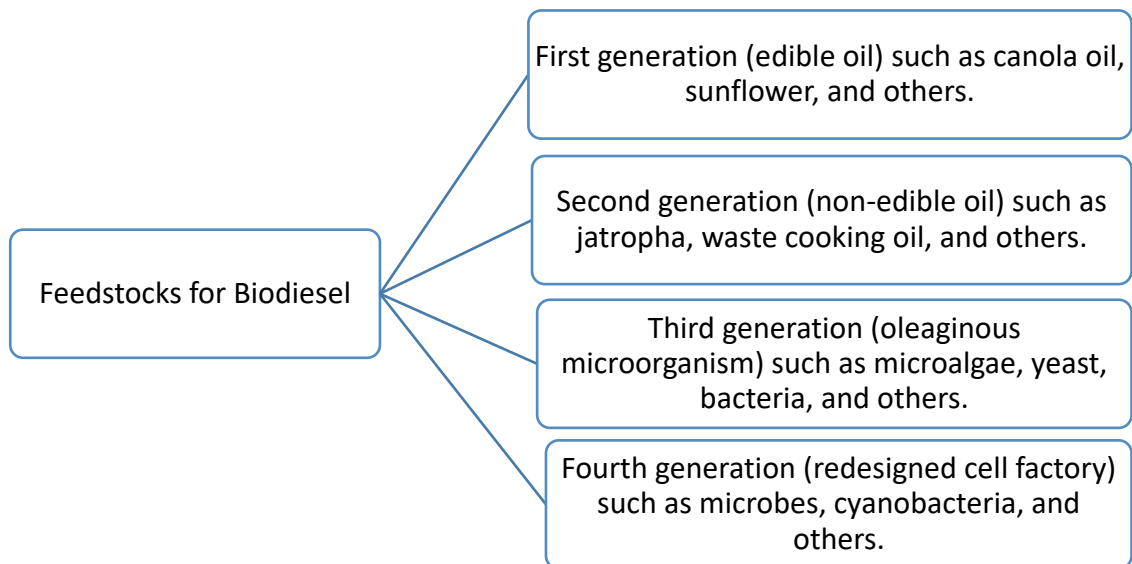


Figure 2-3. Classification of all feedstocks used in the biodiesel industry (Lee et al., 2014)

Table 2.3. Specifications of the feedstocks used for biodiesel production (Lee et al., 2014)

Generation	Level of complexity	Feedstock / catalyst	Scale applied	Limitations and challenges
First	Simple process	Pure oil / required catalyst	Commercialised	Facing food crisis
Second	More sophisticated than the 1st generation	Low-cost oil / required catalyst	Commercialised	High capital cost of production and technology
Third	Complicated process	Expensive to cultivate and harvest with high productivity / required catalyst	Pilot plant	High-cost technology and more development needed
Fourth	High level of biotechnology and genetic technology	Sugar or lignocellulose / catalyst not required	Laboratory	Complex to understand the mechanism

The first generation of raw materials has been applied for an extended period at the laboratory and industrial scales, such as vegetable oils. An enormous number of catalysts (homogeneous, heterogeneous and biocatalysts) has been used frequently with 1<sup>st</sup> generation feedstocks (edible oil) in the biodiesel industry, as listed in Table 2.4.

Table 2.4. First generation feedstocks and their catalysts

Catalyst type	Catalyst	Oil type	Yield/conversion (w-w %)	Reference
Homogeneous base	KOH	Sunflower	96	Atadashi et al. (2013)
Homogeneous acid	H <sub>2</sub> SO <sub>4</sub>	Rice bran	98	Atadashi et al. (2013)
Heterogeneous base	Ca/Al	Rapeseed	94	Meng et al. (2013)
Heterogeneous acid	Zeolite X	Sunflower	95.1	Atadashi et al. (2013)
Heterogeneous acid-base	CaO–MoO <sub>3</sub> –SBA-15	Soybean	83.2	Chang et al. (2014)
Biocatalyst	<i>Thermomyces lanuginose</i> lipase	Soybean	96	Bharathiraja et al. (2014)

The notable features of the first generation feedstocks are their low FFA and moisture contents, which mean a purification step before production is not essential (Lee et al., 2014). Although edible oils provide high conversion and yield, they have been banned from the biodiesel process due to the world food crisis and their inflationary effect on the price of crops. Consequently, second-generation feedstock has become a crucial source for the biodiesel industry, such as non-edible oils, animal fats and WCOs (Qiul et al., 2011). Second generation raw materials have become important feedstocks for biodiesel production at the laboratory and commercial scales despite their high FFA and water contents and low yield (Atadashi et al., 2013). To date, biodiesel production from low-cost feedstock has attracted considerable attention. For example, the use of WCO as a feedstock achieves economic and environmental benefits, as the price of WCO is approximately 60% lower than that of vegetable oils. WCOs can harm the environment and their disposal is expensive (Talebian-Kiakalaieh et al., 2013). Table 2.5 lists the types of catalysts used in biodiesel production from 2<sup>nd</sup> generation feedstocks.

Table 2.5. Second-generation feedstocks and their catalysts

Catalyst type	Catalyst used	Oil type	Yield/conversion (w-w %)	Reference
Homogenous base	KOH	Jatropha	96.8	Verma et al. (2016)
Homogeneous acid	H <sub>2</sub> SO <sub>4</sub>	Palm fatty acid	99.6	Atadashi et al. (2013)
Heterogeneous base	CaO – La <sub>2</sub> O <sub>3</sub>	<i>Jatropha curcas</i>	82.8	Taufiq-Yap et al. (2014)
Heterogeneous acid	Mn <sub>3.5x</sub> Zr <sub>0.5y</sub> Al <sub>x</sub> O <sub>3</sub>	Waste cooking oil	93	Amani et al. (2014)
Heterogeneous acid-base	ZnO-La <sub>2</sub> O <sub>3</sub>	Frying oil	96	Yan et al. (2009)
Biocatalyst	<i>Chromobacterium viscosum</i> lipase	Jatropha	92	Atadashi et al. (2013)

Third generation feedstocks are oleaginous microorganism oils such as bacillus, fungi, yeast, and microalgae with different lipid contents. They have attracted considerable attention due to their exceptional benefits, as shown in Table 2.6 (Meng et al., 2009). For example, microalgae grow under reasonable conditions, such as sunlight, carbon dioxide and seawater; therefore, they make a vital contribution to reducing the CO<sub>2</sub> concentration in the atmosphere (Rodolfi et al., 2009). Furthermore, microalgae can grow twice as fast as other crops in small land areas (Chisti, 2008). On the other hand, the microalgal cultivation and extraction processes are expensive and have low performance. In addition, the significant challenges of microalgal oils are their high water content (Sani et al., 2013), low volatility and high viscosity (Ramachandran et al., 2013). Selection of microalgae depends on not only their lipid content but also on their local availability (Chisti, 2007).

Table 2.6. Oil contents of several microorganisms (Meng et al., 2009)

Microorganisms	Oil content (% dry wt)	Microorganisms	Oil content (% dry wt)
<b>Microalgae</b>		<b>Yeast</b>	
<i>Botryococcus braunii</i>	25–75	<i>Candida curvata</i>	58
<i>Cylindrotheca</i> sp.	16–37	<i>Cryptococcus albidus</i>	65
<i>Nitzschia</i> sp.	45–47	<i>Lipomyces starkeyi</i>	64
<i>Schizochytrium</i> sp.	50–77	<i>Rhodotorula glutinis</i>	72
<b>Bacterium</b>		<b>Fungi</b>	
<i>Arthrobacter</i> sp.	>40	<i>Aspergillus oryzae</i>	57
<i>Acinetobacter calcoaceticus</i>	27–38	<i>Mortierella isabellina</i>	86
<i>Rhodococcus opacus</i>	24–25	<i>Humicola lanuginosa</i>	75
<i>Bacillus alcalophilus</i>	18–24	<i>Mortierella vinacea</i>	66

Moreover, several catalysts have been applied to produce biodiesel from 3<sup>rd</sup> generation feedstocks. They are still relatively novel in terms of research (Baskar et al., 2016). Acid-base heterogeneous catalysts have not been used with oleaginous microorganisms for biodiesel production. Table 2.7 lists third generation feedstocks and their common catalysts.

Table 2.7. Third generation feedstocks and their catalysts

Catalyst type	Catalyst	Oil type	Yield/ conversion (w-w %)	Reference
Homogeneous base	NaOH	Yeast <i>Rhodospiridium toruloides</i> Y4	97.7	Thliveros et al. (2014)
Homogeneous acid	H <sub>2</sub> SO <sub>4</sub>	Microalgae	60	Atabani et al. (2012)
Homogeneous acid	HCl	Yeast	53	Shi et al. (2011)
Heterogeneous base	CaO/Al <sub>2</sub> O <sub>3</sub>	<i>Nannochloropsis oculata</i> algae	80	Umdu et al. (2009)
Heterogeneous acid	Hierarchical zeolites	<i>Nannochloropsis gaditana</i> algae	NA	Carrero et al. (2011)
Heterogeneous acid-base	NA	NA	NA	NA
Biocatalyst	<i>Rhizomucor miehei</i> lipase	Microalgae	90	Huang et al. (2015)

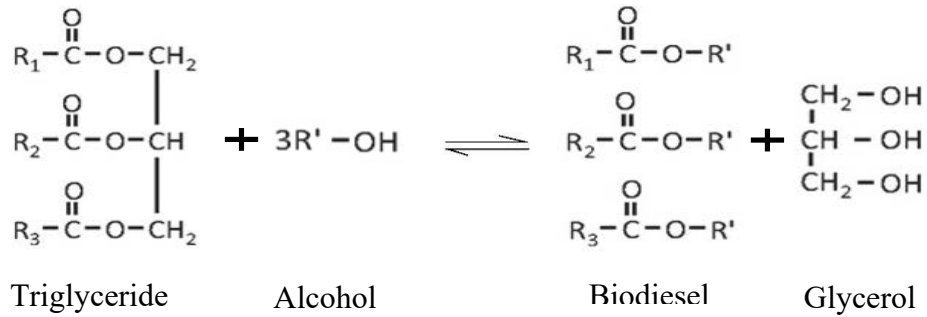
The fourth generation is the latest source of biodiesel raw materials. These raw materials include sugar and related forms, as listed in Table 2.8. The production process occurs inside microorganisms by a cellular metabolism process that produces wax esters (biodiesel; ) (Steen et al., 2010). The outstanding merits of 4<sup>th</sup> generation feedstocks are their environmental friendliness, direct production, inexpensive costs and availability. On the other hand, this feedstock has some limitations, such as difficulties in understanding their mechanisms, and requirements for complex and expensive technical equipment, large laboratories and lengthy development times (Lee et al., 2014). It is noteworthy that the first three types of feedstock (first, second and third generation) need catalysts for reaction, whereas the fourth generation of feedstock does not.

Table 2.8. Fourth generation feedstocks and required production conditions

Raw material	Microbes	Alcohol	Production rate (mg/L/h)	Reference
Sugar	<i>Escherichia coli</i>	Ethanol and isobutanol	13.75	Wierzbicki et al. (2016)
Sugar	<i>Saccharomyces cerevisiae</i>	Ethanol, isobutanol, isoamyl alcohol, and active amyl alcohol	4.8	Teo et al. (2015)
Lignocellulosic	<i>Escherichia coli</i>	Ethanol	83.8	Duan et al. (2011)
Glucose	<i>Saccharomyces cerevisiae</i>	Ethanol	6.3	Shi et al. (2012)
Hemicellulose	<i>Escherichia coli</i>	Ethanol	8.3	Steen et al. (2010)

### 2.2.1.2 Trans/esterification processes

The trans/esterification technique is classified into catalytic and non-catalytic processes. The process occurs by reacting oils (triglycerides or FFAs) with alcohol (ethanol, methanol or any other alcohol) in the presence or absence of a catalyst, as shown in Fig. 2.4. Non-catalytic, including supercritical processes, require high temperature and pressure to achieve successful reactions. The processes use various catalysts, such as homogeneous (acid, base and acid-base combined), heterogeneous (acid, base and acid-base one-step), homogeneous with heterogeneous sequential, and biocatalysts (enzymes).



(a)



(b)

Figure 2-4. Catalytic and non-catalytic process. (a) Transesterification reaction and (b) esterification reaction (Lee et al., 2014).

### 2.2.1.2.1 Catalytic methods

A large number of catalytic processes have been used for biodiesel production. They can be divided into conventional, enzymatic hydrolysis, and reactive separation processes. The conventional process uses a stirrer for mixing and an external heating source for heating during the reaction.

### 2.2.1.2.2 Non-catalytic methods

Non-catalytic methods of biodiesel production are modern techniques that do not require any catalysts at the supercritical conditions of the alcohol. Within this category, three arrangements can be made: 1) one-step supercritical alcohol with or without a co-solvent; 2) two-step supercritical

alcohol, and 3) supercritical reactive distillation. The supercritical process has recently become a preferred technique for biodiesel production.

### 2.2.2 Catalytic biodiesel production processes

The catalytic process has diversified in recent times with innovative and sophisticated methods used to facilitate and improve production. Microwaves (Ruhul et al., 2015) and ultrasound (Ramachandran et al., 2013) have been used for both heating and mixing. There are two new catalytic method processes that have been used recently, namely, hydroesterification and reactive separation. Hydroesterification consists of two steps. The first is the hydrolysis of raw materials with water at supercritical conditions to produce FFAs, and the second step is esterification of the FFAs in the presence of alcohol and acid catalysts (dos Santos et al., 2019) or enzyme catalysts (Pourzolfaghar et al., 2016), as shown in Fig. 2.5.

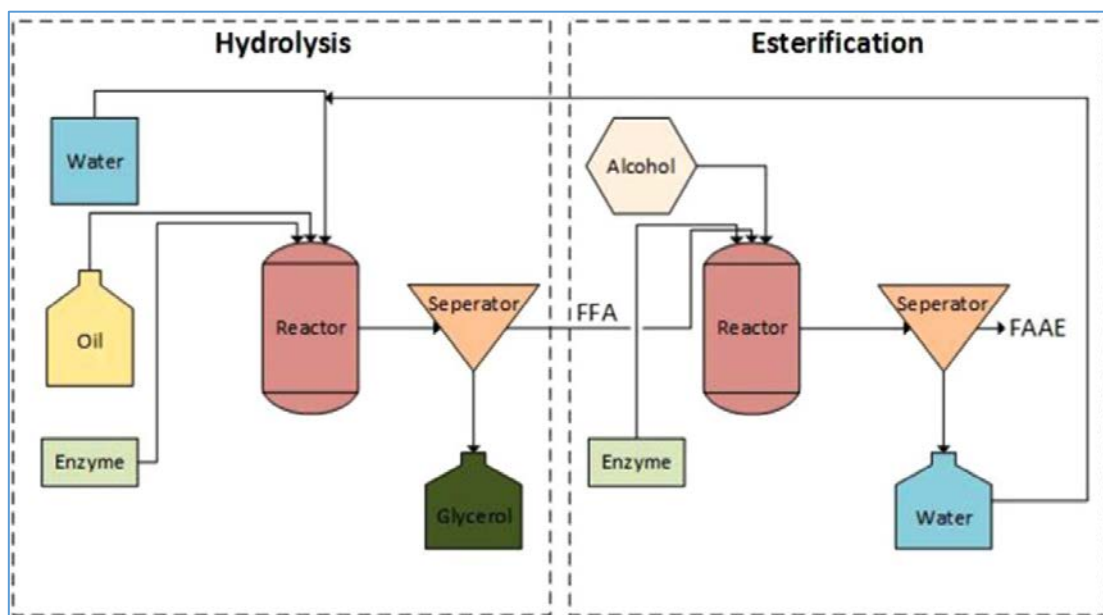


Figure 2-5. Flowchart of the enzymatic hydrolysis process (Pourzolfaghar et al., 2016)

A reactive separation process combines the production and separation of the final product (biodiesel) in a single-unit operation (Talebian-Kiakalaieh et al., 2013). The operation includes a range of processes, such as reactive or catalytic distillation (single or double columns), reactive absorption, and a membrane reactor. The reactive distillation uses a single column (Muthia et al., 2018) or double columns (Petchsoongsakul et al., 2017) to produce biodiesel via reaction and separation simultaneously. Reactive distillation consists of two zones, which are the reactive and separation zones, as shown in Fig. 2.6. The reaction takes place in the reactive section, which is located in the middle of the tower, then alcohol is separated from the top of the distillation column by the separation section for recycling. The heavy products, which are esters, separate from the bottom of distillation column through the separation section (Budiman, 2009). A variety of catalysts (homogeneous or heterogeneous) and feedstocks have been utilised in this process, including oleic acid (Pérez-Cisneros et al., 2016), WCO (Petchsoongsakul et al., 2017), palm oil (Pradana et al., 2017), acetic acid (Deng et al., 2018) and dodecanoic acid (Kiss et al., 2006).

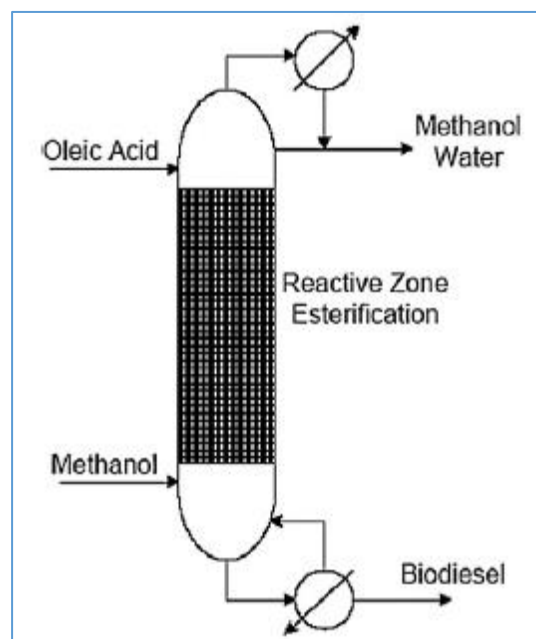
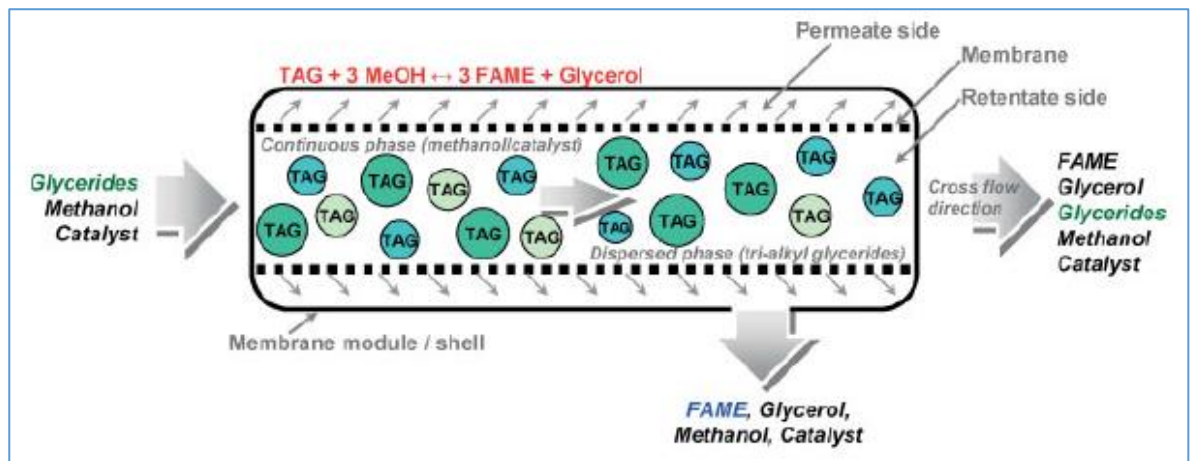


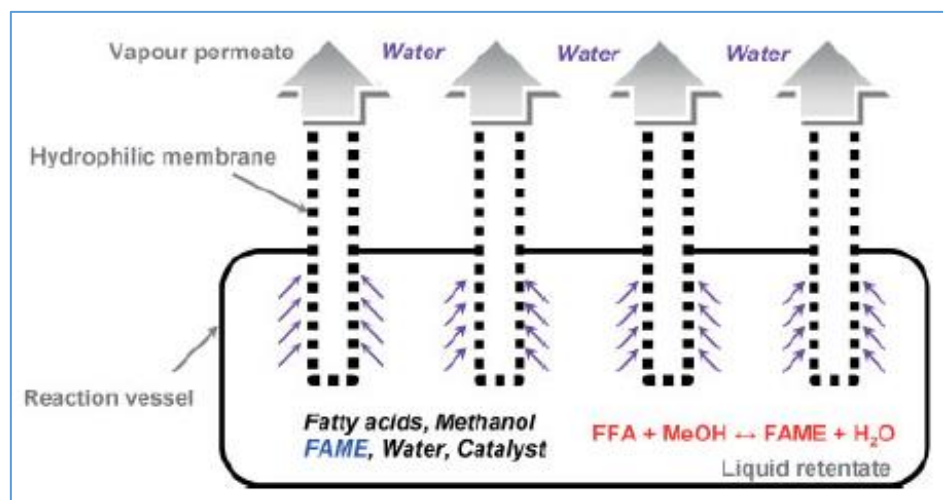
Figure 2-6. Diagram of a reactive distillation process (Pérez-Cisneros et al., 2016)

Reactive absorption is similar to the reactive distillation concept but does not use a condenser and boiler, which saves a large amount of energy (Bildea et al., 2011). Reactive absorption needs approximately  $1/9^{\text{th}}$  of the energy of catalytic distillation (Talebian-Kiakalaieh et al., 2013). Reactive absorption absorbs water and solvent continuously from the final product and can use heterogeneous catalysts in the process (Kiss et al., 2012).

A membrane reactor also can combine the reaction and separation processes in a single step. Homogeneous and heterogeneous catalysts have been used in this process, such as NaOH, KOH, H<sub>2</sub>SO<sub>4</sub>, enzymes (Kiss et al., 2012), sulfonic acid (Aca-Aca et al., 2018) and Amberlyst-15 (Catia Cannilla et al., 2018). Membrane reactors are fabricated using a permeated membrane that immobilises a heterogeneous catalyst in its pores (Aca-Aca et al., 2018), while homogenous catalysts are soluble in alcohol (Kiss et al., 2012). For transesterification reaction, the reaction occurs inside the membrane at the interface between the oil and alcohol in the presence of the catalyst. Biodiesel, glycerol, alcohol and catalyst can pass through the permeated membrane, while oil molecules flow in a retentate stream, as shown in Fig. (2.7a) (Kiss et al., 2012). For esterification reaction, the reaction occurs in a pervaporation catalytic membrane reactor (PVCMR). The PVCMR allows the water produced from the esterification reaction to permeate through the membrane while the product passes through the retentate stream (Aca-Aca et al., 2018), as shown in Fig. (2.7b). Table 2.9 lists modern catalytic processes that use different catalysts.



(a)



(b)

Figure 2-7. Diagrams of membrane reactors used for a) transesterification and b) esterification reactions (Kiss et al., 2012)

Table 2.10 lists the merits and demerits of all the catalytic processes used for biodiesel production by trans/esterification reactions. Figure 2.8 shows the current processes used for biodiesel production by transesterification and esterification reactions.

Table 2.9. Modern integrated catalytic technologies used for biodiesel production

Technology	Catalyst type	Catalyst	Yield/Conversion (%)	Reference
Reactive distillation	Homogeneous base	KOCH <sub>3</sub>	96.8 – 98.6	He et al. (2005)
Reactive distillation	Homogeneous base	H <sub>3</sub> PW <sub>12</sub> O <sub>40</sub> _6H <sub>2</sub> O	93.94	Noshadi et al. (2012)
Reactive distillation	Homogeneous acid	H <sub>2</sub> SO <sub>4</sub>	NA	Cossio-Vargas et al. (2011)
Reactive distillation	Heterogeneous acid	Nafion-SiO <sub>2</sub> /SS-fibre	78.1	Deng et al. (2018)
Reactive distillation	Heterogeneous	Activated carbon (K/AC)	82.69	Pradana et al. (2017)
Reactive distillation	Heterogeneous acid and base	Amberlyst 15 and CaO/Al <sub>2</sub> O <sub>3</sub>	98	Petchsoongsakul et al. (2017)
Reactive distillation	Phantom catalyst	Ozone micro-bubbles	80	Zimmerman et al. (2018)
Reactive absorption	Heterogeneous acid	Ion-exchange resins and sulphated zirconia	NA	Bildea et al. (2011)
Membrane reactors	Heterogeneous acid	Amberlyst 15	60	Cannilla et al. (2018)
Membrane reactors	Homogeneous base	NaOH	99.3	Noriega et al. (2018)
Membrane reactors	Homogeneous acid and base	Acid and base catalysts	95	Abdurakhman et al. (2018)

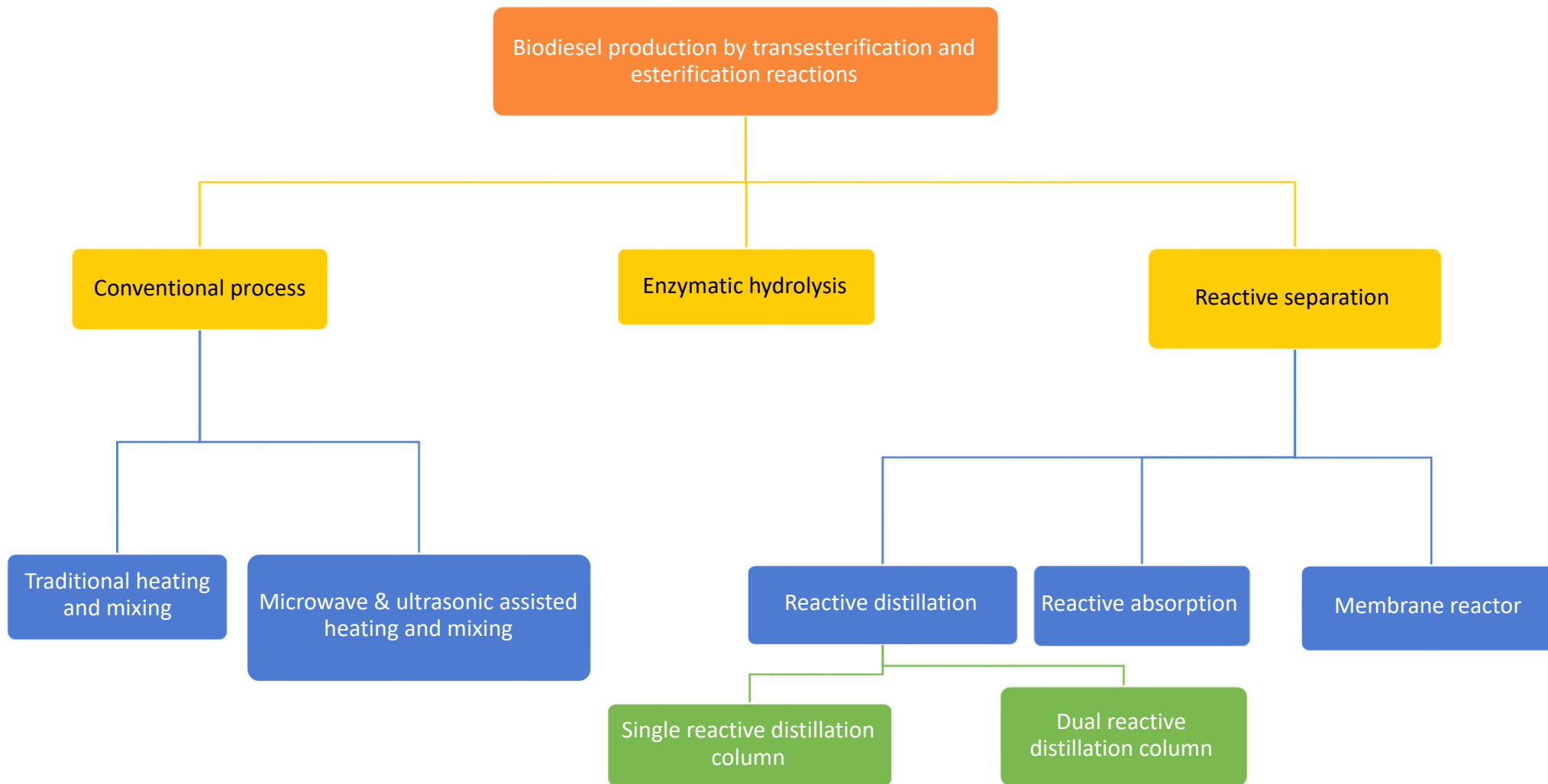


Figure 2-8. Flowchart of current biodiesel production processes using transesterification and esterification reactions

Table 2.10. Merits and demerits of catalytic biodiesel production processes via transesterification and esterification reactions

Process	Merits	Demerits	References
Catalytic conventional	-Low energy demand, excellent yield depending on the catalyst used, minor temperature and pressure needed.	-High cost of catalysts, catalyst preparation difficulties.	Ruhul et al. (2015)
Microwave-assisted	-Superior yield and grade product, little energy required, environmentally friendly, fast reaction, low alcohol needed, low amount of undesired products.	-Inappropriate for all industrial scales.	Talebian-Kiakalaieh et al., (2013)
Ultrasonic-assisted	-Minimum reaction time, low alcohol consumption, less power required, high reaction rate, high yield, high grade of glycerol, does not need any change in equipment facilities.	-Not suitable for long reaction, large amount of catalysts loading required, soap formation for the fast reaction.	Talebian-Kiakalaieh et al. (2013)
Hydroesterification	-High purity glycerol gained. -Appropriate for any feedstock including high free fatty acids and moisture. -Low power demanded.	-Not utilized at industrial scales yet.	dos Santos et al. (2019) Pourzolfaghar et al. (2016)
Reactive distillation	-Reduction in total energy and cost of the process - High selectivity, less catalysts needed. -Less conversion limitations, lower process total cost.	-Limited application. -Boiling point limitation. -Thermal degradation of biodiesel, vapour of products and water return to the column.	Muthia et al. (2018) Pradana et al. (2017) Lee et al. (2014)
Reactive absorption	-High yield and selectivity, straightforward and tight, low cost, can remove water continuously.	-Ineffective along the process, thermal limitations, solvent regeneration difficulties, more development needed.	Talebian-Kiakalaieh et al. (2013) Lee et al. (2014)
Membrane separation	-Improvement in chemical equilibrium -Low energy required. -High selectivity, increased catalytic activity -No thermal limitations, higher selectivity, high surface area contact between the reactants.	-High cost of membrane formation, fouling problems, high-performance catalysts required, more development needed for industrial scale.	Catia Cannilla et al. (2018) Noriega et al. (2018) Aca-Aca et al. (2018) Lee et al. (2014)
In-situ (reactive extraction)	-No feedstock extraction step needed, low capital cost, continuous glycerol separation, high yield.	-Low mixing between alcohol and nonpolar oil, more development required for reusability of the catalyst.	Lee et al. (2014)

## **2.3 Catalyst development for catalytic biodiesel production**

### **2.3.1 Types of catalysts and their development**

#### **2.3.1.1 Homogeneous catalysts**

##### **2.3.1.1.1 Basic catalysts**

Homogeneous alkali catalysts are commonly used in transesterification reactions, such as sodium hydroxide (NaOH) and potassium hydroxide (KOH). They are appropriate for industrial use because they have several advantages, such as high activity, low cost (Pasupulety et al., 2013) and the ability to work under normal conditions (Sharma et al., 2008). Also, homogeneous base catalysts are non-corrosive and can achieve high conversion with rapid reaction (Huang et al., 2010), and can produce more than 98% conversion in a short time about 30 minutes (Ye et al., 2014). However, the process also faces several challenges, including high consumption of water from washing the catalyst and glycerol (Pasupulety et al., 2013), and difficulties in separating the catalyst (Lee et al., 2014). In addition, homogeneous base catalysts are not suitable for raw materials that contain high amounts of FFA (from neutralisation) and water due to the formation of soap and hydration of the catalyst (Endalew et al., 2011). The soap process comes from the reaction of FFA and the alkali catalyst.

##### **2.3.1.1.2 Acid catalysts**

Homogenised acidic catalysts, such as sulphuric acid (H<sub>2</sub>SO<sub>4</sub>), are used for biodiesel production via an esterification reaction. Acid catalysts are appropriate for feedstocks with high FFA contents and still provide a high yield. The use of acid catalysts eradicates the problem of soap formation (da Silva et al., 2008). However, homogeneous acid catalysts require a long time to complete the reaction (Huang et al., 2010). Further, homogeneous acid and alkali catalysts have the same issue: difficulties in separation from the final product. The inability to separate acidic catalysts from biodiesel can lead to the corrosion of engines (Canakci et al., 1999) and other equipment.

### **2.3.1.2 Heterogeneous catalysts**

Recently, biodiesel production using heterogeneous catalysts has attracted increasing interest (Di Serio et al., 2008). Heterogeneous solid catalysts overcome all the impediments and limitations of homogeneous catalysts, such as separation from the final product (Pasupulety et al., 2013), and saponification (Mythili et al., 2014). In addition, they have several benefits, such as reusability, environmental friendliness (Pasupulety et al., 2013), and excellent safety and economy (Bharathiraja et al., 2014).

#### **2.3.1.2.1 Base catalysts**

Biodiesel production over base catalysts shows high performance in transesterification reactions using different vegetable (edible) oils (Mardhiah et al., 2017) and is potentially low-cost (Bharathiraja et al., 2014; Correia et al., 2015). Various types of heterogeneous alkaline solid catalysts have been used in biodiesel production. Heterogeneous alkaline solid catalysts, such as alkaline earth oxides, alkali doped materials, transition metal oxides, and hydrotalcite, have been commonly applied to biodiesel production (Lee et al., 2014). One of the most common types is the alkaline earth oxides, such as CaO, MgO, BaO, and SrO. In general, alkaline earth oxides are inexpensive, low toxicity, have low solubility in alcohol, and high catalytic performance in transesterification reaction (Roschat et al., 2016). Alkali-doped materials have also been applied in biodiesel production. Different alkaline earth metals doped with zinc oxide have been used for biodiesel production from soybean oil. A SrO/ZnO catalyst showed high catalytic activity with 94.7% conversion, but the reused catalysts exhibited lower catalytic performance (Yang et al., 2007). Pasupulety et al. (2013) studied the effect of biodiesel yield over CaO loading on different alumina oxide catalysts using soybean oil with methanol. The catalyst showed 90% yield using 20% CaO/n-Al<sub>2</sub>O<sub>3</sub> due to the presence of calcium diglycerate (CDG). Moreover, Al-Ca hydrotalcite catalyst loaded with K<sub>2</sub>CO<sub>3</sub> was utilised

in a transesterification reaction with soybean oil feedstock. It achieved a 95.1% biodiesel yield in the first cycle and about 87.4% after four cycles of the catalyst (Sun et al., 2014).

Recently, new categories of catalysts have been applied in biodiesel production, such as nano-catalysts and magnetic base catalysts. Nano-catalysts have nano-dimensional and morphological structural characteristics that can provide high catalytic performance and selectivity. Gurunathan et al. (2015) reported that nano-catalysts have become more efficient in the transesterification reaction of vegetable oils, achieving 97.81% biodiesel yield using neem oil over a copper-doped zinc oxide nano-catalyst. Magnetic catalysts provide a high surface area and an enormous amount of active base sites. Dai et al. (2018) used a magnetic  $\text{LiFe}_5\text{O}_8\text{-LiFeO}_2$  catalyst and obtained 96.5% biodiesel conversion from soybean oil. Another magnetic catalyst ( $\text{Na}_2\text{SiO}_3@\text{Ni/C}$ ) achieved a 98.1% biodiesel yield from soybean oil (Zhang et al., 2016). Also, Zhang et al. (2015) claim that magnetic catalysts can achieve recovery rates 1.8 times greater than those of ordinary catalysts. Besides, magnetic catalysts are easily and highly recoverable (Xue et al., 2014). Base catalysts can be reused with only a slight decrease in catalyst activity (Endalew et al., 2011; Sharma et al., 2008). Boonyuen et al. (2018) achieved more than 99% biodiesel conversion from edible palm oil over a CaO catalyst driven from the outer lips of waste *Turbo jourdani* (Gastropoda: Turbinidae) shells, and the catalyst still obtained more than 90% conversion after eight cycles. The main issue in using CaO is soap formation when using a high-acidity oil such as *Jatropha curcas* oil (JCO) (Endalew et al., 2011). Generally, the main disadvantages of base heterogeneous catalysts are that they are highly influenced by moisture, are unsuitable for feedstocks containing water and high FFA contents (Mardhiah et al., 2017), and are prone to high leaching (Lee et al., 2010). Also, the leaching of alkaline earth metals and hydrotalcite catalysts is significantly affected when they are used with high amounts of FFA and water (Di Serio et al., 2010).

### 2.3.1.2.2 Acid catalysts

A large number of heterogeneous acid catalysts have been applied to biodiesel production, such as heteropolyacids, acidic polymers and resins, waste carbon-derived solid acids, and acidic metal oxides (Lee et al., 2014). Heterogeneous acid catalysts are highly compatible with esterification reactions, are easily separated, and most of them can be used with high-FFA-content feedstocks (Mardhiah et al., 2017; Ramu et al., 2004). Each type of heterogeneous acid catalyst has advantages.  $\text{WO}_3/\text{ZrO}_2$  and  $\text{SO}_4^{2-}/\text{ZrO}_2$  catalysts have high acidity and stability but high leaching for  $\text{SO}_4^{2-}$ , which reduces the catalytic activity (Park et al., 2010). An  $\text{SO}_4^{2-}/\text{TiO}_2\text{-SiO}_2$  catalyst showed high catalytic performance and was environmentally friendly, produced from cheap feedstock, stable during production, and could be used in continuous processes (Peng et al., 2008). (NKC-9, 001 x 7 and D61) cation-exchange resins (co-polymer) catalyst has high catalytic performance due to the abundance of acid sites, high selectivity, high acidity, and high reusability (Feng et al., 2010). ( $\text{H}_3\text{PMo}_{12}\text{O}_{40}$ ) supported on an alumina ( $\text{Al}_2\text{O}_3$ ) heteropolyacid catalyst can be used in high-moisture-content raw materials with high catalytic performance because of its high acidity; however, the catalyst requires further development for utilisation with inexpensive feedstocks for biodiesel production (Carvalho et al., 2017). 12-tungstophosphoric heteropolyacid over zirconia also showed high performance in esterification reaction due to having very strong Bronsted acids and low solubility in polar solvents; however, clogging of micropores by organic matter reduces the catalytic activity (Alcañiz-Monge et al., 2018). Recently, sulfonated carbon-based acid catalysts that produce biodiesel from lignocellulosic biomass raw materials have attracted interest from researchers because of their economic and ecological benefits (Tang et al., 2018). A C-SO<sub>3</sub>H catalyst was produced from glucose as a carbon source to produce biodiesel from WCO. The catalyst showed high catalytic activity due to its high acidity and thermal stability (Nata et al., 2017). The main demerits of heterogeneous acid catalysts include decreased activity due to leaching (Lee et al., 2010; Kiss et al., 2012), the need for high reaction temperatures, and long reaction times (Mardhiah et al., 2017).

Moreover, the use of acid catalysts requires large quantities of alcohol, which carries high costs due to corrosion.

### **2.3.1.2.3 Acid-base bi-functional metal oxide heterogeneous catalysts**

In recent years, there has been a growing trend in the application of bi-functional heterogeneous solid catalysts to biodiesel production. Several researchers consider bi-functional catalysts to be promising for the biodiesel industry because of their many benefits (Mardhiah et al., 2017). Chemically, bi-functional catalysts include two forms of active sites: base and acid sites. In other words, they combine the two types of heterogeneous catalysts (acid and base) into a single catalyst. A significant role of dual-functional catalysts is to enable both esterification and transesterification reactions to occur in a single step (Chang et al., 2014) with high yield and selectivity (Mardhiah et al., 2017). In addition, acid-base catalysts are suitable for low-cost and high FFA feedstocks (Verma et al., 2016). Heterogeneous mixed-metal-oxide catalysts can offer new acid-base-attracting properties, depending on the types of metals and preparation methods used (Borges et al., 2012). Yan et al. (2009) reported a Zn-La bi-functional heterogeneous catalyst to be more effective than either acid or base catalysts. The acid and base sites in a  $Mn_{0.5}Ce_{0.5}$  catalyst were also found to provide higher conversion reactions than single-type catalysts (Cannilla et al., 2010).

Yan et al. (2009) studied ZnO-La<sub>2</sub>O<sub>3</sub> heterogeneous catalysts with different molar ratios of Zn:La to produce biodiesel from WCO. The catalyst was prepared from cheap materials and a Zn:La ratio of 3:1 gave the catalyst acid and base properties, which increased its ability to participate in simultaneous transesterification and esterification reactions. The catalyst achieved 96% biodiesel yield from WCO, crude soybean oil, crude palm oil, and food-grade soybean oil with a 5% oleic acid and 3% moisture content. However, the required processing temperature was high at 170–200 °C. Wen et al. (2010) tested the catalytic performance of a TiO<sub>2</sub>-MgO bifunctional heterogeneous catalyst, which was prepared by a sol-gel method, for biodiesel production from WCO. They found that the titanium ions dispersed on the catalyst's surface enhanced its stability so that it could maintain

good catalytic activity. The catalyst was able to obtain a 92.3% yield from WCO with a 3.6 mg KOH g<sup>-1</sup> acid value, so it is suitable for biodiesel production on an industrial scale. Nevertheless, the catalytic activity decreased slightly during use; thus, it needs regeneration to maintain its performance.

Macario et al. (2010) prepared a series K over ITQ-6, MCM-41, and SiO<sub>3</sub> to obtain bifunctional heterogeneous catalysts by a hydrothermal synthesis method. The synthesised catalysts were tested for transesterification and esterification efficacy using waste fruit oilseed with a 5.58% FFA content. The KITQ-6 catalyst showed a higher catalytic activity without any soap formation but needed a 180 °C process temperature and 24 h reaction time. Also, the catalytic activity decreased and needed regeneration due to potassium leaching. Endalew et al. (2011) reported a simultaneous esterification and transesterification process over a Fe<sub>2</sub>(SO<sub>4</sub>)<sub>3</sub>+(CaO or Li-CaO) bifunctional catalyst for biodiesel production from *Jatropha curcas* oil (JCO). The Ca: Fe<sub>2</sub>(SO<sub>4</sub>)<sub>3</sub> and Li-CaO: Fe<sub>2</sub>(SO<sub>4</sub>)<sub>3</sub> catalysts achieved about 93.37% and 96% biodiesel yields, respectively, at a 3:1 ratio and obtained higher yields at a 2:1 ratio. The main issue in this process is soap formation due to calcium oxide, which causes deactivation of the catalyst and makes it unable to be recycled. The cause of catalyst deactivation is the presence of atmospheric CO<sub>2</sub>, which affects the high basicity of the catalyst's surface. Alhassan et al. (2015) carried out a simultaneous production of biodiesel from WCO containing 17.5% FFA over a Fe<sub>2</sub>O<sub>3</sub>-MnO-SO<sub>4</sub><sup>2-</sup>/ZrO<sub>2</sub> (FMSZ) bifunctional catalyst. Dispersion of iron-manganese-sulphate particles enhanced the surface area and acidity of the prepared catalyst as it prevented the agglomeration of zirconia particles, thereby providing high catalytic activity. Also, the catalyst was used in six consecutive runs without any reduction in its activity.

Lee et al. (2015) studied CaO-La<sub>2</sub>O<sub>3</sub> as a bifunctional mixed-metal-oxide catalyst. In this catalyst, La<sup>2+</sup> ions provide acidic properties while Ca<sup>2+</sup> ions provide basic properties. The catalyst was synthesised by a co-precipitation method and used for biodiesel production via a transesterification reaction using inedible *Jatropha* oil with methanol. Good interaction between Ca

and La particles and high CaO dispersion increases the acidic and basic active sites on the catalyst surface, which enhances the simultaneous esterification and transesterification reaction of Jatropha oil with a high FFA content. The highest biodiesel yield was 98.76% at a reaction temperature of 160 °C, reaction time of 3 h, and a 25:1 methanol to oil molar ratio. However, the catalyst was significantly affected by  $\text{Ca}^{2+}$  leaching in the first run due to the partial solubility of calcium oxide, which did not link with the catalyst's binary system. Tamborini et al. (2016) investigated biodiesel production from acidic oil (acetic and oleic acid oil) and vegetable oil (sunflower oil) with ethanol over sulfonated porous carbons (PCs-SO<sub>3</sub>H) as a bifunctional catalyst prepared by a sol-gel method. The PC200S-SO<sub>3</sub>H bifunctional catalyst showed high catalytic activity in both transesterification and esterification reactions, in which it achieved 90% and 94% biodiesel conversions, respectively. The increasing sulfonation on the porous carbons enhanced the catalytic activity in the esterification and transesterification reactions and improved the catalyst's reusability.

Moreover, Wang et al. (2017) found that the carbonaceous bifunctional magnetic catalyst Zr-CMC-SO<sub>3</sub>H@3Fe-C<sub>400</sub> can produce biodiesel from acidic and vegetable oils. The catalyst was prepared by a four-step method of iron ion chelation, calcination, zirconium ion chelation and embedding, and sulfonation. The catalyst achieved 97% biodiesel yield from oleic acid and 95% from soybean oil, as well as providing easy separation of ions, stable catalytic efficiency, and high reusability over ten consecutive runs with catalyst regeneration. Pirouzmand et al. (2018) studied different doped metal oxides, such as Mg, CO, and Zn, on MCM-41 for the production of biodiesel from WCO with methanol by simultaneous esterification and transesterification reactions. The bifunctional catalyst [CTA]MCM-41 was made by direct synthesis and obtained high catalytic activity with a 93% biodiesel yield. A high dispersion of hydrophobicity on the MCM mesoporous induced by a cetyltrimethylammonium bromide CTA template enhances the catalyst activity of the process.

#### **2.3.1.2.4 Biocatalysts**

Enzyme catalysts (lipase) have been utilised as heterogeneous catalysts for biodiesel production. Lipases are extracted from various microorganisms such as bacteria, fungi and algae. Commercially, the extracted lipases are immobilised inside supporting biomass particles and can be used as catalysts in transesterification reactions (Bharathiraja et al., 2014). Enzyme catalysts used in the biodiesel industry can be divided into two categories: free enzyme and immobilised enzyme. Free enzyme (non-immobilized enzyme) catalysts can be used once only because of the inability to separate them from the product, while immobilised enzyme catalysts have the advantages of reusability, operational stability and ease of handling (Nielsen et al., 2008), environmental friendliness (Lee et al., 2010) and low energy requirements (Mardhiah et al., 2017). Careful selection of an appropriate enzyme according to the conditions of the process is essential to ensure good yields with different types of feedstocks and FFA levels (Huang et al., 2010; Nielsen et al., 2008). Researchers have also developed enzymes with high thermal stability (Songstad et al., 2009), high insolubility in alcohol which minimises catalyst leaching (Marchetti et al., 2007), no soap formation, and that do not require a purification process (Leung et al., 2010).

However, biodiesel yields using lipase catalysts have been found to decline significantly with increasing temperature, moisture content, and feedstock impurity (Parawira, 2009; Nielsen et al., 2008). The economic aspect is still the biggest obstacle to using enzyme catalysts industrially due to their high costs, long reaction times, deactivation (Sbihi et al., 2015), low yields (Pasupulety et al., 2013) and stability and performance difficulties (Hwang et al., 2014). Commercially, lipase is still unable to reach the standard specifications of fuel according to the American Society for Testing and Materials (ASTM) (Huang et al., 2010).

The advantages and drawbacks of all types of catalysts used in biodiesel production are summarised in Table 2.11.

Table 2.11. Benefits and drawbacks of various types of catalysts used for biodiesel production

Process	Benefits	Drawbacks	References
Homogeneous basic catalysts	-Effortless to operate, high yield, and normal operating conditions. -Appropriate for transesterification, inexpensive, suitable for industrial scale.	-Inappropriate for feedstocks contain high free fatty acid and water contents. -Not economical, difficulty in separating from the final product.	Lee et al. (2014) Pasupulety et al. (2013)
Homogeneous acid catalysts	-Suitable for high free fatty acid raw materials, high performance for esterification reaction.	-Very slow for transesterification reaction. -Highly corrosive, neutralization needed. -Difficulty separating from the final product.	Lee et al. (2014) Lee et al. (2010) Pasupulety et al. (2013)
Heterogeneous alkali catalysts	-Simple separation, reactivity and reusability, long lifetime. -High performance for transesterification reaction under normal conditions.	-High moisture attraction during storage, inappropriate for feedstocks containing high free fatty acids. -Not tolerant of free fatty acid and water, high leaching, not economical.	Sharma et al. (2008) Mardhiah et al. (2017) Lee et al. (2010)
Heterogeneous acid catalysts	-Reusability, easy separation, long lifetime. -Compatible for esterification reaction, environmentally friendly.	-Low activity and reaction rate. -Low catalytic performance, high temperatures and long reaction times needed.	Lee et al. (2010) Mardhiah et al. (2017)
Heterogeneous acid-base catalysts	-A high potential for esterifying FFA and transesterifying triglycerides in one step. -Appropriate for low-quality raw materials, high yield and stability.		Chang et al. (2014) Mardhiah et al. (2017)
Enzyme catalysts	-Environmentally friendly, simple separation and reusability. -Low energy requirement.	-Highly expensive, highly sensitive to operating conditions. -Long reaction time. -Inappropriate for the industrial scale.	Lee et al. (2010) Mardhiah et al. (2017) Ruhul et al. (2015)
Enzymatic hydro-esterification	-High-purity glycerol gained, appropriate for feedstocks with high free fatty acids and moisture contents, lower power demand.	-Not utilized at the industrial scale yet.	Pourzolfaghar et al. (2016)

### **2.3.2 Synthesis methods and their impacts on the catalytic effects of heterogeneous catalysts**

Heterogeneous catalysts have been prepared by various techniques. No researcher has reported that catalyst synthesis methods depend directly on the type of catalyst and its performance in biodiesel production. Rather, the efficiency of biodiesel production depends directly on the type of catalyst and the technique's conditions. Catalytic features such as selectivity, activity and stability within chemical reactions (Campanati et al., 2003) depend on the catalyst preparation technique (Lee et al., 2014), calcination temperature (Sharma et al., 2011), the metal (molar or weight) ratios of the synthesised catalyst, and the physicochemical properties of the material, such as its oxidation state, crystal phase, exposed facet, and metal deposit size.

Firstly, the catalyst preparation method may play a significant role in the performance of biodiesel production. Yogesh et al. (2011) and Lee et al., (2010) reported two different methods of preparing an MgO/SBA-15 catalyst: impregnation and in situ coating. In situ coating produces a high surface area and pore volume, but little catalytic activity compared to the impregnation technique, because of low MgO loading on SBA-15. Magnesium oxide loading is higher in the impregnation method, resulting in significantly higher catalytic activity by the final catalyst. Also, sulphated zirconia (S-ZrO<sub>2</sub>) was synthesised using solvent-free (mixing the precursors without any solvent) and precipitation methods for transesterification and esterification reactions. It was reported that the solvent-free route is more efficient than the precipitation method. The solvent-free technique achieved a 98.6% biodiesel conversion under optimum conditions (Semwal et al., 2011).

Secondly, one of the significant factors that affect catalytic activity is calcination temperature. Vieira et al. (2018) studied the activity of SO<sub>4</sub><sup>2-</sup>/La<sub>2</sub>O<sub>3</sub> supported on HZSM-5 for

biodiesel production by esterification reaction using oleic acid. The catalytic activity strongly depends on the content of  $\text{SO}_4^{2-}$  in the structure, which enhances the acidity and surface area. The sulphated content increases with decreasing calcination temperature, and it was found that the best calcination temperature is 350 °C. The authors claimed that the lowest tested temperature (350 °C) would induce the best catalytic results because of the decomposition of sulfate groups at temperatures above 400 °C. Roschat et al. (2016) studied the effect of calcination temperature on the catalytic activity of sodium silicate for biodiesel production from palm oil. The catalyst showed catalytic activity at different temperatures; however, the best biodiesel yield was 98.04% at a calcination temperature of 300 °C because of the presence of sodium silicate crystalline phase. A low calcination temperature produced low-intensity peaks while a high one produced a low biodiesel yield due to the influence of sintering, which led to a decrease in surface area. The authors claimed that incomplete conversion of the sample to the sodium silicate crystalline phase provides a low conversion rate, as the formation of sodium silicate crystals is important in biodiesel production. Dai et al. (2018) investigated the effect of catalytic activity on calcination temperature using  $\text{LiFe}_5\text{O}_8\text{-LiFeO}_2$  as a magnetic solid basic catalyst for biodiesel production via transesterification reaction using soybean oil. The results showed that the prepared catalyst achieves the highest biodiesel conversion of 96.5% at an 800 °C calcination temperature because of the abundance of basic active sites on the catalyst surface. Any further increase in temperature leads to decreases in the basic active sites due to the sublimation and agglomeration in the structure, which decreases the reaction conversion. Meanwhile, the lower calcination temperature was insufficient to complete the decomposition of  $\text{Fe}_2\text{O}_3$  and  $\text{Li}_2\text{CO}_3$ .

Thirdly, the mole or weight ratio of the metals used in catalyst preparation is significant. In this regard, Alsharifi et al. (2017) studied the influence of the LiO-to- $\text{TiO}_2$  percentage weight ratio on catalytic activity in a transesterification reaction of canola oil for biodiesel production.

The findings showed that the highest reaction conversion was achieved when 30 wt%  $\text{LiNO}_3$  was added to  $\text{TiO}_2$ . The 30LT450 catalyst obtained a 98% biodiesel yield due to its high surface area. Wan et al. (2010) studied the effect of Mg/Ti molar ratio on biodiesel production from WCO over a  $\text{TiO}_2$ -MgO catalyst. The results show that increases in Ti lead to decreases in biodiesel conversion due to metal leaching. The catalyst exhibited increasing catalytic activity with increases in the Mg/Ti molar metal ratio from 0.5 to 1, but the Mg showed high leaching. Increasing the metal ratio above one did not significantly increase biodiesel yield, whilst Mg leaching increased considerably.

### **2.3.3 Catalyst longevity**

Re-usability is an essential feature for heterogeneous catalysts used in biodiesel production (Talebian-Kiakalaieh et al., 2013). The catalytic activity is generally reduced after recycling due to deactivation. In heterogeneous catalysts used for biodiesel production, there are five deactivation mechanisms; namely, fouling, mechanical alteration, sintering, poisoning, and leaching or lixiviation. (Sádaba et al., 2015).

Leaching is a significant problem in solid catalysts used in the biodiesel industry. Low leaching of catalyst produces high-purity biodiesel and glycerine (Atadashi et al., 2013) and prolonged catalyst life (Lee et al., 2014). Talebian-Kiakalaieh et al. (2013) reported that the leaching problem still occurs with a large number of catalysts. Therefore, further research is needed to investigate the causes and mechanisms of leaching in heterogeneous catalysts. For example, mixed-metal-oxide catalysts have proven high catalytic performance, but their effectiveness decreases continuously with each reaction cycle because of the influence of leaching. In addition, leaching of active  $\text{Ca}^{+2}$  from a  $\text{CaO-La}_2\text{O}_3$  bi-functional catalyst was reported to be the main reason for its deteriorating catalytic activity and inability to be reused after the first batch (Mardhiah et al., 2017). The performance of a  $\text{K}_2\text{O}/\gamma\text{Al}_2\text{O}_3$  catalyst

decreased dramatically after the second cycle due to leaching of the potassium active sites (Chang et al., 2014). Moreover, leaching of sodium from a  $\text{Na}_2\text{SiO}_3$  catalyst had a significant effect on the rate of transesterification reaction, with its conversion decreasing from 98% to 60% after four runs. In addition, after four re-uses of a K/KLC catalyst, the conversion of the process decreased steadily from 98% to 82% due to potassium leaching. Although transition metal oxide catalysts show high effectiveness, soap formation occurs regularly due to leaching of the active sites on the surface of the MnO-TiO catalyst (Lee et al., 2014).

In contrast, there are a vast number of catalysts with proven and robust re-usability that are unaffected by leaching. For example, KSF and Amberlyst-15 showed relatively constant activity after five re-uses (Mardhiah et al., 2017). The magnetic catalysts ( $\text{S}_2\text{O}_8^{2-}/\text{ZrO}_2\text{-TiO}_2\text{-Fe}_3\text{O}_4$ ) and Amberlyst-15 were reused successfully for eight cycles (Go et al., 2016), whereas Ca-Mg-Al hydrotalcite was reused 12 times (Ramachandran et al., 2013). Furthermore, Jeong et al. (2017) reported a bifunctional solid Zn-Al catalyst that was able to achieve 40 consecutive reactions without decreasing its catalytic activity. The catalyst was utilised with oleic acid and soybean oil for biodiesel production via esterification and transesterification reactions.

A tungsten oxide zirconia ( $\text{WO}_3/\text{ZrO}_2$ ) catalyst exhibited high effectiveness without leaching when used with vegetable oils (Borges et al., 2012), while a  $\text{WO}_3/\text{SO}_3$  (miscellaneous solid acids) catalyst did not show any leaching after five re-uses as there were no losses of  $\text{WO}_3$  (Lee et al., 2014). In the same context,  $\text{K}_2\text{CO}_3/\text{MgO}$  (Lee et al., 2014) and  $\text{Na}/\text{SiO}_2$  (Ramachandran et al., 2013) catalysts exhibited high catalytic activity with a slight leaching effect after six and five batches, respectively. For  $\text{K}_2\text{CO}_3/\text{MgO}$ , little change in base amount occurred after the catalyst was recycled and calcined, which indicates that there is little leakage of the active sites on the catalyst during the reaction. In general, solid basic hydrotalcite catalysts (Lee et al., 2014) and cation-exchange resin catalysts (Borges et al., 2012) show high reusability. Some studies have investigated methods for eliminating the leaching phenomenon.

For example, filling the mesoporous structure of CaO with ZnO particles to create a CaO-ZnO catalyst is one way to prevent leaching, because zinc oxide helps protect the catalyst from CO<sub>2</sub> and H<sub>2</sub>O. In addition, adding MgO leads decreases CaO leaching in KF/CaO-MgO catalyst, thereby increasing the catalytic activity and stability (Chang et al., 2014). Evaluation of the stability and recyclability of solid synthesised catalysts in biodiesel production is economically and environmentally important.

Leaching of heterogeneous catalysts can be measured by various techniques, such as inductively coupled plasma-mass spectrometry (ICP-MS) and atomic absorption spectrometry (AAS). ICP-MS was used to examine CaO leaching from a CaO/Al<sub>2</sub>O<sub>3</sub> catalyst (Atadashi et al., 2013). Potassium leaching from a K-pumice catalyst was analysed by the AAS method. Lee et al. (2014) applied AAS to detect tungsten (W) leaching from an MCM-48 catalyst. The main reason for using AAS instead of ICP-MS is its higher sensitivity.

## **2.4 Concluding remarks and future outlook**

Energy is an important component in the climate system and plays a vital role in pollution. The increase in energy consumption influence significantly and negatively the climate change. The deleterious effects of fossil fuels have prompted studies aimed to find alternative energy sources that are environmentally friendly. Biodiesel has attracted considerable attention because of its benefits over petroleum diesel. However, biodiesel is still unable to compete with petroleum diesel commercially because of the higher cost of its production. The total cost is dependent on three essential factors: the raw materials, catalysts and technology used. Compatibility between these factors can achieve high yields and allow biodiesel to be competitive both industrially and globally.

A very broad range of raw materials has been used for biodiesel production. Recent research has shown that low-quality feedstock, such as WCO, is among the most valuable resources for the biodiesel industry. The increasing focus on WCOs in recent research has

several explanations: its availability, accessibility, very low cost and lack of need for extraction as it is a waste product. Therefore, WCOs could be a promising feedstock for biodiesel in the future.

A vast number of studies on different catalysts for trans/esterification reactions state that heterogeneous catalysts are far better than homogeneous catalysts. Upcoming heterogeneous catalysts for the biodiesel industry need the characteristics of high production, high catalytic activity, Multi-usability which means the recycling of catalyst (longevity), low cost, and usability under standard conditions which refers to the ability to use a catalyst with high catalytic activity under moderate operating conditions (such as reaction temperatures less than the boiling point of the alcohol used, and atmospheric pressure). In recent years, there has been increasing interest in bi-functional catalysts because of their high activity, high yield, suitability for both triglycerides and FFA, and ability to deal with various raw materials. Further studies will be needed to better understand the effectiveness and reusability of different types of bi-functional catalysts.

For industrial-scale biodiesel production, feedstocks often contain both triglycerides and free fatty acids. Therefore, the development and synthesis of an inexpensive heterogeneous bifunctional catalyst with high catalytic activity for both trans/esterification reactions under mild operating conditions that can be used for the production of biodiesel are highly desirable.

## Chapter 3: Esterification and transesterification over a bifunctional catalyst for biodiesel production

### 3.1 Abstract

In this chapter, a series of novel bifunctional catalysts (SrO-ZnO/Al<sub>2</sub>O<sub>3</sub>) for biodiesel production were synthesised via the wet impregnation method. The basic and acidic activities of the prepared catalysts were investigated using corn oil and oleic acid, respectively. The physio-chemical characteristics of the synthesised catalysts were analysed by XRD, SEM-EDS, and FT-IR. The <sup>1</sup>H NMR technique was used to analyse fatty acid ethyl esters and free fatty acids. The catalyst exhibited higher catalytic activity in transesterification reaction, with 95.1% reaction conversion under operating conditions of a 10:1 ethanol-to-corn oil molar ratio, 10 wt.% catalyst loading, and 180 min reaction at 70 °C. Conversion via esterification reaction was only 71.4 % with a 5:1 ethanol-to-corn oil molar ratio, 10 wt.% catalyst loading, and 6 h reaction time at 70 °C. Kinetic study revealed that the transesterification and esterification reactions were in good agreement with a first-order model.

### 3.2 Introduction

In recent years, increasing global demand for fuel and the negative impacts of fossil fuels on the environment have raised the need for alternative fuels. Biodiesel is one alternative fuel that can help fill market demand and has several advantages, such as being environmentally-friendly (biodegradable and non-toxic) and made from sustainable raw materials (Demirbas, 2009). Generally, biodiesel (mono-alkyl ester) can be produced from different oils (edible or inedible), either by esterification or transesterification reactions with alcohol (methanol, ethanol or any other alcohol; Lee et al., 2014). The raw materials for esterification reactions are usually acidic oils, while vegetable oils are used in

transesterification reactions. With feed materials that consist of a blend of acidic and vegetable oils, both reactions can occur simultaneously.

Conventionally, homogenous catalysts (acid and base) have been used extensively in biodiesel production. However, the main disadvantages of these types of catalysts are their inability to be recovered, which results in their high consumption, the need for a washing process for naturalisation, and soap formation during production (Huang et al., 2010). Within this context, heterogeneous solid catalysts have attracted increasing interest to overcome all the impediments and limitations of homogeneous catalysts. The essential advantages of heterogeneous catalysts are reusability, environmental friendliness (Pasupulety et al., 2013), safety and economy (Bharathiraja et al., 2014). A large number of heterogeneous catalysts (acid and base), such as mesoporous silica, alkaline earth metal oxides, transition metal oxides, alkaline doped materials, solid acid waste carbon, and hetero-poly acids, have been applied to biodiesel production (Lee et al., 2014).

Recent studies indicate that bifunctional heterogeneous catalysts containing active base-acid sites are promising. Bifunctional heterogeneous catalysts have increasingly been applied in the biodiesel industry due to their benefits, such as their co-occurrence of acid-base active sites, which allows simultaneous esterification and transesterification reactions with high conversion and selectivity (Chang et al., 2014; Mardhiah et al., 2017). Bifunctional catalysts are particularly suitable for low-cost feedstocks with high contents of free fatty acids (FFAs) such as waste cooking oil (WCO; Verma et al., 2016) and inedible oils such as *Jatropha* oil (Wang et al., 2018). Heterogeneous mixed-metal-oxide catalysts can be made bi-functional to offer attractive acid-base properties depending on the types of metals and preparation methods involved (Borges et al., 2012). Also, the chemical structures of combined metal oxides provide different oxygen contents on the catalyst surface, which makes bifunctional catalysts highly effective and widespread (Kondamudi et al., 2011).

However, to the best of our knowledge, there has been no research on biodiesel production using strontium oxide (SrO) with zinc oxide (ZnO) over alumina oxide ( $\text{Al}_2\text{O}_3$ ) as catalysts. Previously, alkaline earth metal oxides (AMOs), including magnesium oxide (MgO), calcium oxide (CaO), barium oxide (BaO) and SrO, have been doped on ZnO and prepared by an impregnation method. The prepared catalysts have high catalytic activity in transesterification reactions using soybean oil with methanol, due to their alkalinities. The  $\text{Sr}(\text{NO}_3)_2/\text{ZnO}$  combination achieved the highest conversion of 93.7%, which is better than other AMO catalysts (Yang et al., 2007). Notably, strontium oxide (SrO), prepared from calcination of  $\text{SrCO}_3$ , is a high performer in biodiesel production, with a yield higher than 95% using soybean oil (Liu et al., 2007). Su et al. (2013) reported that the catalytic performance of Cu/SrO in transesterification reaction is, in general, better than that of other Cu/AMOs with Cu/SrO catalysts prepared by the chemisorption-hydrolysis method, and can achieve a 96% biodiesel yield using hemp seed oil.

Zinc oxide (ZnO), on the other hand, is known to be able to provide high Lewis acid with the zinc ion  $\text{Zn}^{+2}$  (Lee et al., 2014). Yan et al. (2009) reported that a ZnO- $\text{La}_2\text{O}_3$  bifunctional catalyst with a 3:1 molar ratio of Zn/Li achieved a high 96% biodiesel yield from waste or unrefined oils. In this catalyst, the zinc oxide and lanthanum oxide represent the Lewis acid and base sites, respectively. Moreover, the authors found that fatty acid methyl ester (FAME) conversion is better when using Zn-La than when using individual acid or base catalysts. Bancquart et al. (2001) examined the basicity and acidity of different solid metal oxide catalysts. The results showed that ZnO has a strong acidity of 455  $\mu\text{mol/g}$  and a weak basicity of 21  $\mu\text{mol/g}$ , as determined by temperature-programmed desorption of  $\text{NH}_3$  and  $\text{CO}_2$ , respectively.

Combining alumina with zinc or strontium can enhance the acidic-basic properties of a catalyst. Mierczynski et al. (2015) investigated biodiesel production using strontium aluminate ( $\text{SrAl}_2\text{O}_4$ ) synthesised by the co-precipitation method. This catalyst showed strong base sites and obtained a 90% yield using rapeseed oil. Additionally, a zinc aluminate catalyst ( $\text{ZnAl}_2\text{O}_3$ ) was prepared by combustion of urea with aluminium nitrate and zinc nitrate. The catalyst exhibited the same acid-base strength and achieved a 95% yield using waste frying oil (Alves et al., 2012).

In industrial-scale biodiesel production, feedstocks often contain both triglycerides and FFAs. Hence, the development of a bifunctional heterogeneous catalyst with high catalytic activity for both trans/esterification reactions under mild operating conditions is of great interest to the biodiesel industry.

In this study, a new group of  $\text{SrO-ZnO/Al}_2\text{O}_3$  solid catalysts with different Sr:Zn molar ratios over  $\text{Al}_2\text{O}_3$  were used for biodiesel production. The influence of the metal oxide composition on the acid-base sites, on the transesterification reaction of corn oil, and on the esterification reaction of oleic acid were investigated, and the kinetics for both trans/esterification reactions were studied. Moreover, the parameters were optimised for both reactions, including the ethanol/oil molar ratio, catalyst amount, and reaction temperature and time.

### **3.3 Materials and methods**

This study used a full factorial experimental design to optimise the reaction conditions and was implemented in two stages. Briefly, three catalysts were prepared with different metal ratios and calcined at three different temperatures. The metal ratio and calcination temperature that resulted in the highest conversion were taken as indicative of the best-performing catalyst. This catalyst was then selected for further investigation to determine the optimum reaction conditions in the same manner.

### 3.3.1 Materials

All materials were obtained from Sigma-Aldrich, Australia. Corn oil was purchased as vegetable oil and its physicochemical properties (as provided by Sigma-Aldrich) are shown in Table 3.1. Technical grade oleic acid and analytical grade ethanol (EtOH) were used for the esterification and transesterification reactions, respectively. For catalyst preparation, activated neutral Brockmann I alumina with a specific surface area of 155 m<sup>2</sup>/g, strontium nitrate Sr(NO<sub>3</sub>)<sub>2</sub>, and zinc nitrate hexahydrate Zn(NO<sub>3</sub>)<sub>2</sub>·6H<sub>2</sub>O were obtained.

Table 3.1. Physical and chemical properties of the studied corn oil

Test	Specification	Result
Appearance (turbidity)	Clear	Clear
Appearance (form)	Liquid	Liquid
Appearance (colour)	Very faint yellow to yellow	Yellow
Heavy metals (as lead)	$\leq 0.001$ %	$< 0.001$ %
Peroxide	$\leq 10.0$	0.4
Acid value	$\leq 0.2$	0.1
Water content	$\leq 0.1$ %	$< 0.1$ %
Alkaline phosphatase impurity	Pass	Pass
Brassicasterol	$\leq 0.3$ %	$< 0.1$ %
Fatty acid (c14)	$\leq 0.1$ %	$< 0.1$ %
Fatty acid (c14)	$\leq 0.1$ %	$< 0.1$ %
Fatty acid (c16)	8.6 – 16.5 %	11.8 %
Fatty acid (c16:1)	$\leq 0.5$ %	0.1 %
Fatty acid (c18)	1.0 – 3.3 %	1.4 %
Fatty acid (c18:1)	20.0 – 42.2 %	29.3 %
Fatty acid (c18:2)	39.4 – 62.0 %	55.7 %
Fatty acid (c18:3)	0.5 – 1.5 %	0.9 %
Fatty acid (c20)	$\leq 0.8$ %	0.3 %
Fatty acid (c20:1)	$\leq 0.5$ %	0.2 %
Fatty acid (c22)	$\leq 0.3$ %	0.1 %
Fatty acid (c22:1)	$\leq 0.1$ %	$< 0.1$ %
Fatty acid (c24)	$\leq 0.4$ %	0.1 %

### 3.3.2 Catalyst preparation

The catalysts were prepared according to the procedure shown in Fig. 3.1. All catalysts were synthesised through impregnation of an aqueous solution of metal nitrates onto a natural alumina support. In a conventional catalyst preparation method, the desired amounts of  $\text{Sr}(\text{NO}_3)_2$  and  $\text{Zn}(\text{NO}_3)_2 \cdot 6\text{H}_2\text{O}$  were added to 100 ml of deionised water until completely dissolved. Aluminium oxide (powder) was added after the strontium and zinc nitrate were dissolved completely. The mixture was agitated for two h at room temperature then, to remove the excess water, evaporated slowly by hot oil bath at 75 °C until the mixture was mostly dry. The product was heated in an oven for 6 h at 120 °C and, finally, calcined at 700 °C, 900 °C, and 1100 °C for 6 h in a muffle furnace. A series of catalysts with different Sr-Zn molar ratios of (1) 65:25, (2) 45:45, and (3) 25:65 mol% (with respect to 10 mol% aluminium) were prepared, with corresponding Sr/Zn molar ratios of 2.6, 1, and 0.4. The catalysts are denoted as  $x\text{SZA}y$ , where  $x$  represents the molar ratio of Sr/Zn and  $y$  represents calcination temperature; for example, 2.6SZA900 means a Sr/Zn molar ratio of 2.6 and calcination temperature of 900 °C.

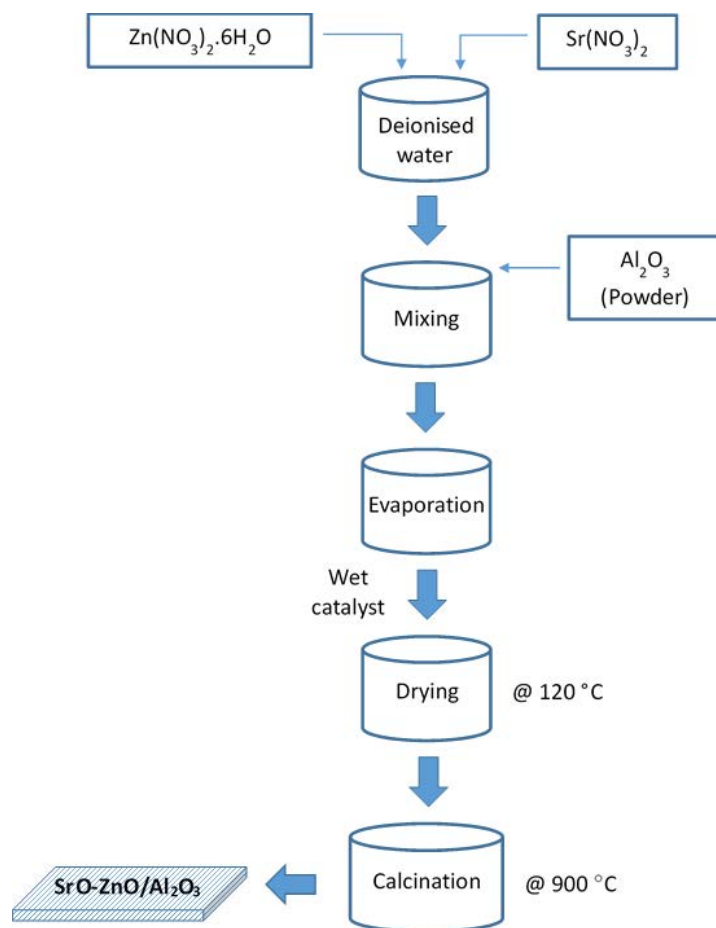


Figure 3-1 Catalyst preparation via a wet impregnation method

### 3.3.3 Esterification and transesterification reactions

Esterification and transesterification reactions were conducted in a two-necked 250 ml round-bottom glass reactor with a water-cooled condenser, with a thermocouple in the oil bath to control the reaction temperature. For the transesterification reaction, the glass reactor was filled with 10 g corn oil and the desired amount of catalyst (5 – 15% of oil weight), then heated to a suitable temperature (50 – 70 °C). Various ethanol-to-oil molar ratios (4:1 – 15:1) were added and various reaction times were applied (0 – 240 min). The same procedure was applied to the esterification process with oleic acid, only the reaction time was changed (1 – 6 h). At the completion of each reaction, the collected sample was placed in an ice bath to stop the

reaction, then the used catalyst was separated from the product by filtration. Due to the small particle sizes of the catalyst, however, not all catalyst particles were recovered by filtration. The mixture was further processed in a centrifuge at 10,000 rpm for 3 min to separate the remaining catalyst, and the reaction mixture was later loaded into an oil bath at 125 °C to remove the excess ethanol. After that, the obtained product, fatty acid ethyl esters (FAEEs), was analysed by  $^1\text{H}$  NMR.

It should be noted that the vast majority of the experiments were carried out twice or sometimes three times, especially those that gave high yield (> 90%). Most of the relative errors are around 2% with the maximum being < 3%. Also, the biodiesel conversions were measured twice via  $^1\text{H}$  NMR analysis.

### **3.3.4 Characterisation**

#### **3.3.4.1 Property characterisation**

The crystal structures of the calcined catalysts were examined by powder X-ray diffraction (XRD) using a D2 Phaser Bruker AXS diffractometer equipped with nickel-filtered Cu  $K\alpha_1$  radiation ( $\lambda = 1.5406 \text{ \AA}$ ). The standard scan parameters were  $45^\circ/\text{min}$  within a  $2\theta$  range of  $10^\circ - 80^\circ$  for 1 h and a  $0.010^\circ$  step size. The phases were identified using the powder diffraction file (PDF) database (COD, Crystallography Open Database) and by *DIFFRAC.EVA* software version 4.0 diffraction file data. The morphology of catalysts prepared with different amounts of metals was analysed by high-resolution scanning electron microscopy (SEM) (Hitachi SU5000 FE-SEM). An energy dispersive spectrometer (EDS) was utilised to characterise the morphology and the elemental distributions of the (SrO)(Al<sub>2</sub>O<sub>3</sub>)(ZnO) ternary systems were estimated using Oxford *AZtec* software *X-MAX*. The functional groups of the prepared catalysts were determined using Fourier-transformed infrared (FTIR) spectroscopy (Perkin Elmer Spectrum 100). The spectra were obtained in the wavelength range of 650 –

4000 cm<sup>-1</sup>. The physical properties of the prepared catalysts were investigated by different analyses. The specific surface area of samples was measured by N<sub>2</sub> adsorption-desorption isotherms using the BET surface area method, and the BJH model was used for the determination of pore size and pore volume. Elemental analysis was carried out with an inductively coupled plasma optical emission spectrometer (ICP-OS; Agilent 5100). The samples were dissolved using concentrated HCl. A series of multi-element standard solutions was used to calibrate the instrument. The wavelengths used for quantification were 396.15 nm for aluminium, 215.283 nm for strontium, and 213.857 nm for zinc.

### 3.3.4.2 Biodiesel analysis by <sup>1</sup>H NMR

An <sup>1</sup>H NMR analysis of the final ethyl oleate product was carried out at 400 MHz using a Bruker spectrometer with 5 mm probes. For sample preparation, 10 μL of the product was mixed with 600 μL chloroform (CDCl<sub>3</sub>). *MestReNova* software was employed to analyse the spectra. Calibrations were carried out using standard samples of FAEE, corn oil (TG) and oleic acid (FFA). For transesterification reaction, the conversion of FAEE was quantified using Equation (1) (Ghesti et al., 2007):

$$\text{FAEE conversion \%} = \left( \frac{(I_{TAG+EE} - I_{TAG})}{(I_{TAG+EE} + 2I_{TAG})} \right) \times 100 \quad (3.1)$$

Where  $I_{TAG}$  is the integration intensities of triglycerides at 4.25 – 4.35 ppm, and  $I_{TAG+EE}$  is the integration intensities of methylene groups of ethyl esters at 4.1 – 4.2 ppm.

For esterification reactions, the conversion of FAEE was determined by calculating the FFA content of oleic acid before and after reaction via Equation (2) (Kondamudi et al., 2011):

$$\text{FAEE conversion} = \left( \frac{(FFA_{Initial} - FFA_{Final})}{FFA_{Initial}} \right) \times 100 \quad (3.2)$$

The FFA content (wt %) was calculated with Equation (3) (Satyarthi et al., 2009):

$$\text{FFA (wt \%)} = \left( \frac{4 \times \text{area of unmerged peak of } \alpha\text{-CH}_2 \text{ of FFA}}{\text{total area of } \alpha\text{-CH}_2 \text{ of both FFA and ester}} \right) \times 100 \quad (3.3)$$

Where the area of the unmerged peak of the  $\alpha$ -CH<sub>2</sub> of FFA is the integration intensity at 2.37 – 2.41 ppm, the total area of  $\alpha$ -CH<sub>2</sub> of both FFAs, and ester is the integration intensities at 2.2 – 2.41 ppm.

In summary, biodiesel conversion by transesterification reaction was calculated by Equation 3.1, while conversion by esterification reaction was calculated by Equations 3.2 and 3.3. The <sup>1</sup>H NMR analyses of the final products for both reactions are shown in Figs. 3.7 and 3.8.

### **3.3.5 Kinetic study of esterification and transesterification reaction over the bifunctional catalyst**

The reaction kinetics of the esterification and transesterification reactions were studied to understand the relationship between reaction time and temperature and their influences on the reaction. The kinetics were studied at different temperatures (50 °C, 60 °C and 70 °C) for the transesterification and esterification reactions using the first-order model.

## **3.4 Results and discussion**

### **3.4.1 Catalytic activity**

#### **3.4.1.1 Effect of calcination temperature on the catalyst**

The impact of calcination temperature on the catalytic activity of the 2.6SZA catalyst was investigated at different temperatures (700 °C, 900 °C, 1100 °C), as shown in Fig. 3.2. The reaction was conducted at a catalyst loading of 10 wt.%, an ethanol/oil molar ratio of 10:1, a 70 °C reaction temperature, and reaction time of 180 min. All three calcination temperatures showed different activities in catalysing the transesterification reaction. The conversion of

FAEE increased with increases in calcination temperature up to 900 °C and further increases in temperature did not increase FAEE conversion. The high conversion at the calcination temperature of 900 °C was because of the appearance of the active phases  $\text{Al}_4\text{O}_7\text{Sr}$  and  $\text{Al}_2\text{O}_6\text{Sr}_3$ , whereas the low performance at 700 °C was probably due to the low intensity of the same phases. Also, the decomposition of the phases of binary oxide  $(\text{SrO})(\text{Al}_2\text{O}_3)$   $\text{Al}_4\text{O}_7\text{Sr}$  and  $\text{Al}_2\text{O}_6\text{Sr}_3$  was likely the cause of the decline in the reaction conversion at the 1100 °C calcination temperature (further explained in Section 3.2.1).

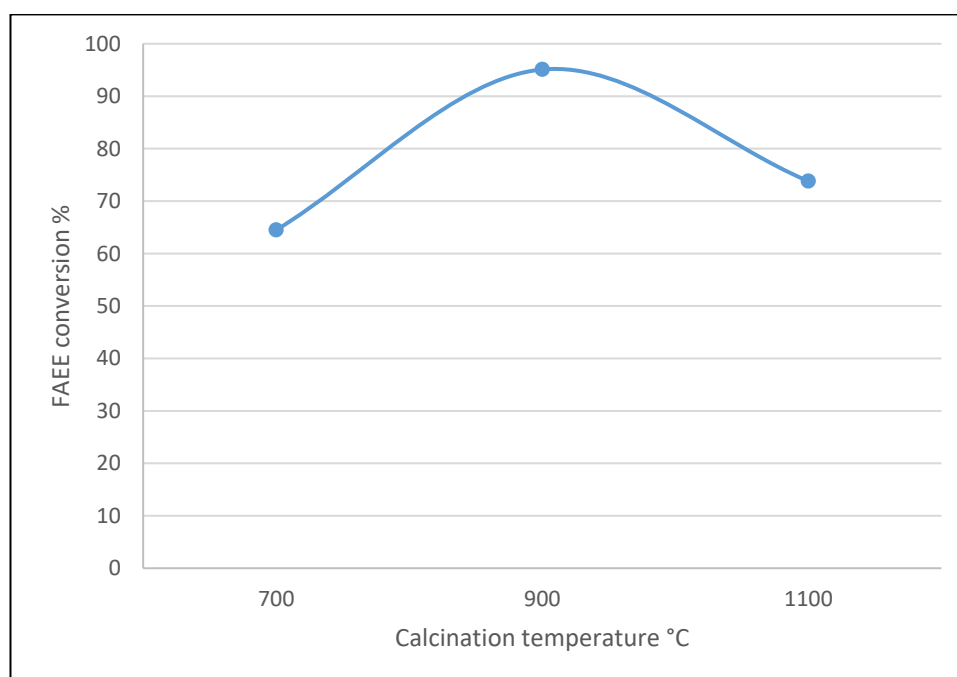


Figure 3-2 Effect of calcination temperature on FAEE conversion with catalyst 2.6SZA

### 3.4.1.2 Catalytic performance in the transesterification process

A series of prepared catalysts (0.4, 1, and 2.6SZA900) were employed to evaluate their catalytic performance. The prepared catalysts were applied to the corn oil as a base oil source under various reaction temperatures (50, 60, 70 °C), catalyst loadings (5, 10, 15 wt.%), EtOH:oil molar ratios (4:1, 7:1, 10:1, 15:1) and reaction times (0 to 240 min).

Figure 3.3 shows the effect of different strontium (Sr) to zinc (Zn) molar ratios ranging from 0.4 to 2.6 with calcination at 900 °C. The results show that the highest FAEE conversion was for catalyst 2.6SZA900 under the reaction conditions of 10:1 EtOH:oil molar ratio, reaction temperature 70 °C, 180 min reaction time and 10 wt.% catalyst dosage. The influence of Sr addition on the conversion of FAEE is obvious because of the high activity of Sr in the transesterification reaction (Liu et al., 2007). Increasing the strontium content in the metal mixture leads to an increase in the Lewis base feature of the prepared catalyst. The ions  $\text{Sr}^{2+}$  and  $\text{O}^{2-}$ , which are strong Lewis bases, are expected to facilitate the transesterification reaction (Yang et al., 2010).

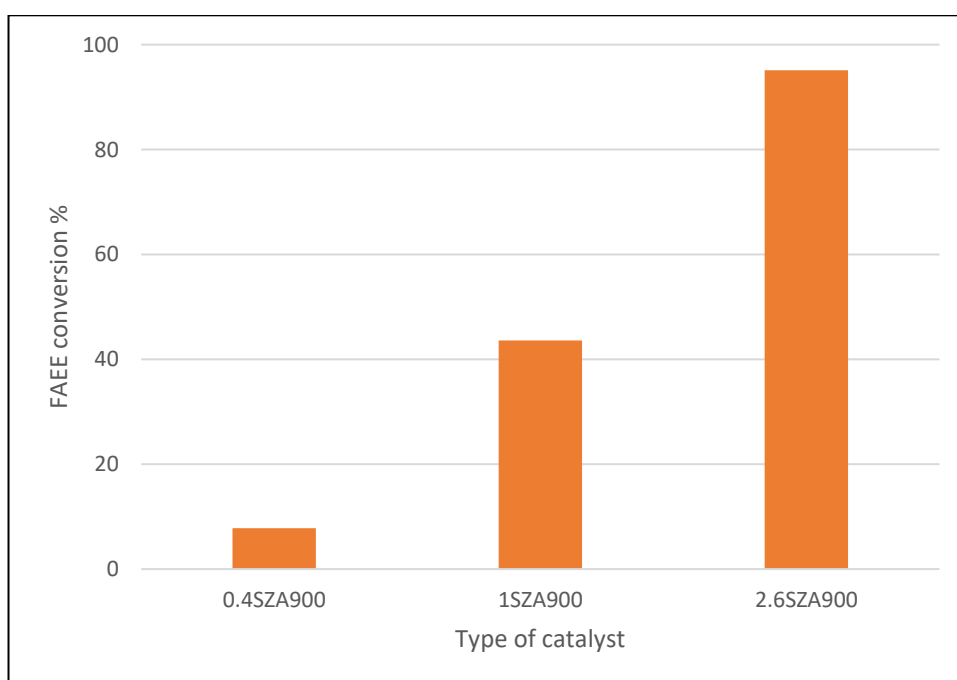


Figure 3-3 Effect on FAEE conversion of catalysts with different amounts of strontium and zinc nitrate loaded on alumina oxide and calcined at 900 °C. Reaction conditions: 10:1 EtOH:oil molar ratio, reaction temperature = 70 °C, 180 min reaction time and 10 wt.% catalyst dosage.

The reaction temperature has an essential influence on transesterification reactions (Encinar et al., 2016). Figure 3.4 shows the influence of reaction temperature on catalyst activity at temperatures of 50 – 70 °C. The reaction was carried out at a 10:1 ethanol:oil molar

ratio, 10% catalyst loading, and reaction durations of 0 – 240 min with samples withdrawn every 30 min. The highest FAEE content of 95.1% was achieved at 70 °C and 180 min, after which the conversion remained almost constant. The finding suggests that the increase in reaction temperature increases collisions between reactant molecules (Yadav et al., 2018) and improves mass transfer by lowering the viscosities of the reactants and reducing the activation energy limitation (Wu et al., 2016). In addition, the conversion of FAEE was discovered to increase with reaction time and peak at 180 min. Extending the reaction time further did not influence FAEE conversion, which remained nearly constant as the reaction had reached an equilibrium state (Al-Sharifi et al., 2019).

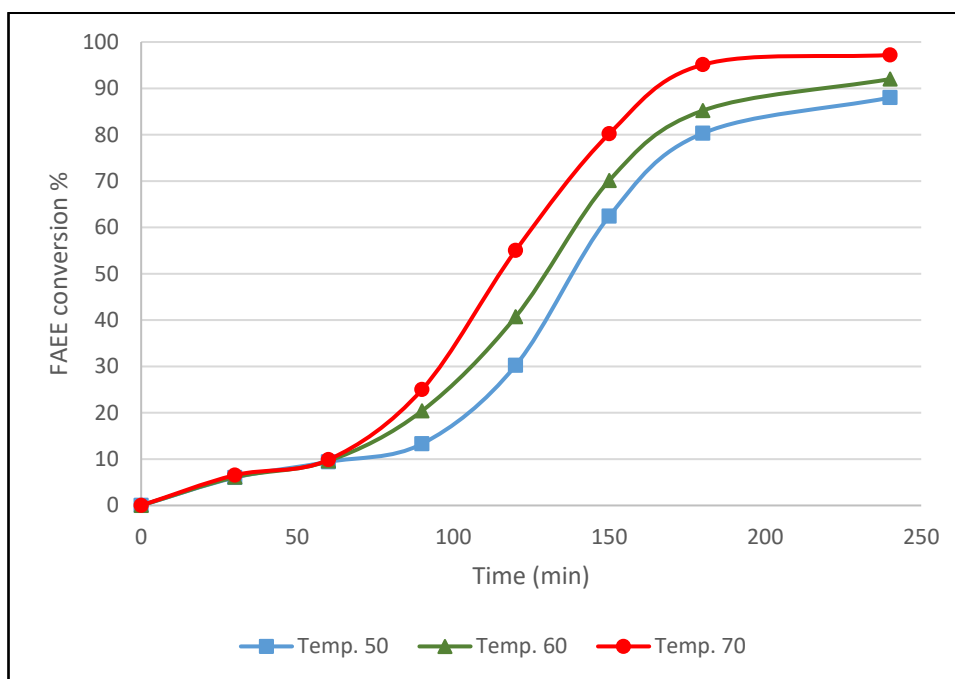


Figure 3-4 FAEE conversion with reaction time at three temperatures using catalyst 2.6SZA900. Reaction conditions: 10:1 ethanol:oil molar ratio, 10% catalyst loading, and reaction durations of 0–240 min.

The effect of the ethanol-to-corn oil molar ratio was investigated under reaction conditions of 70 °C, 10% catalyst dosage and 180 min reaction time. An excessive amount of ethanol was favoured to drive the reaction towards its completion. The conversion of the reaction increased from 15% to 95.1% as the ethanol-to-oil molar ratio increased from 4:1 to

10:1, as illustrated in Fig. 3.5. However, further increases in the ratio caused a decline in conversion. The reason being that the presence of excessive ethanol probably dilutes the contact between the catalyst and reactants (Zhang et al., 2017). Additionally, excess ethanol might also dissolve the glycerol (by-product) and prevent reaction between the catalysts and reactants (Yadav et al., 2018).

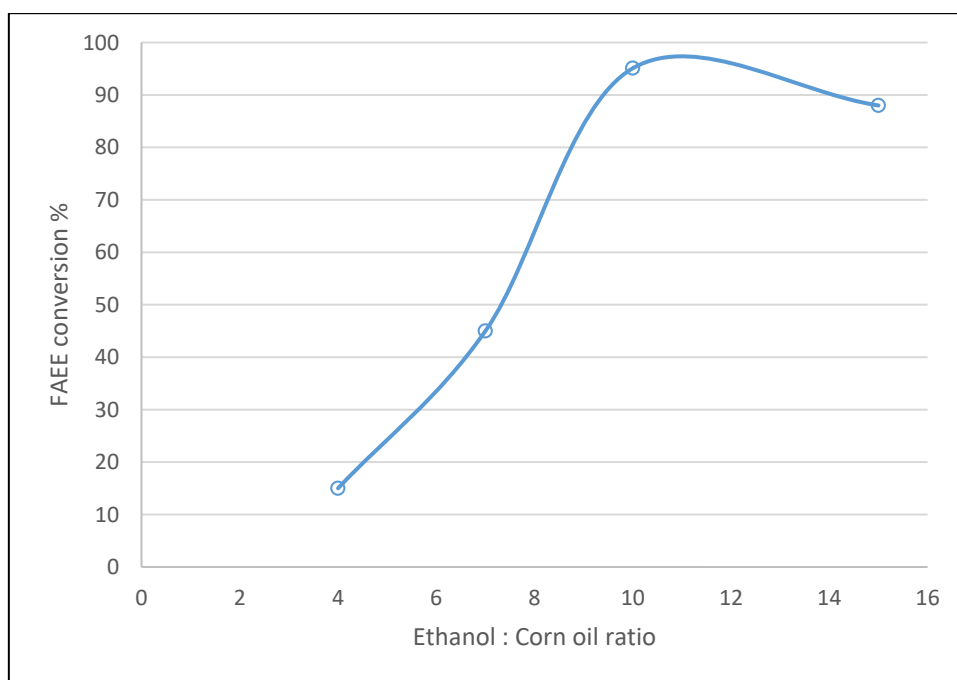
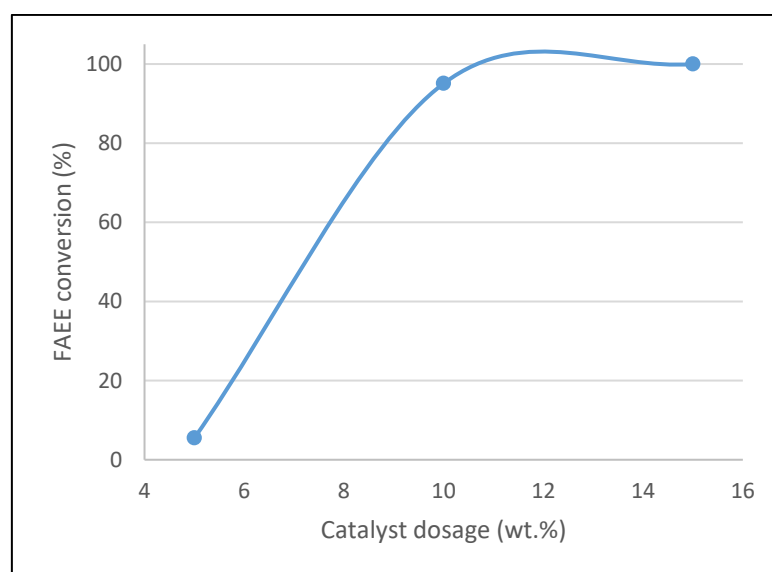


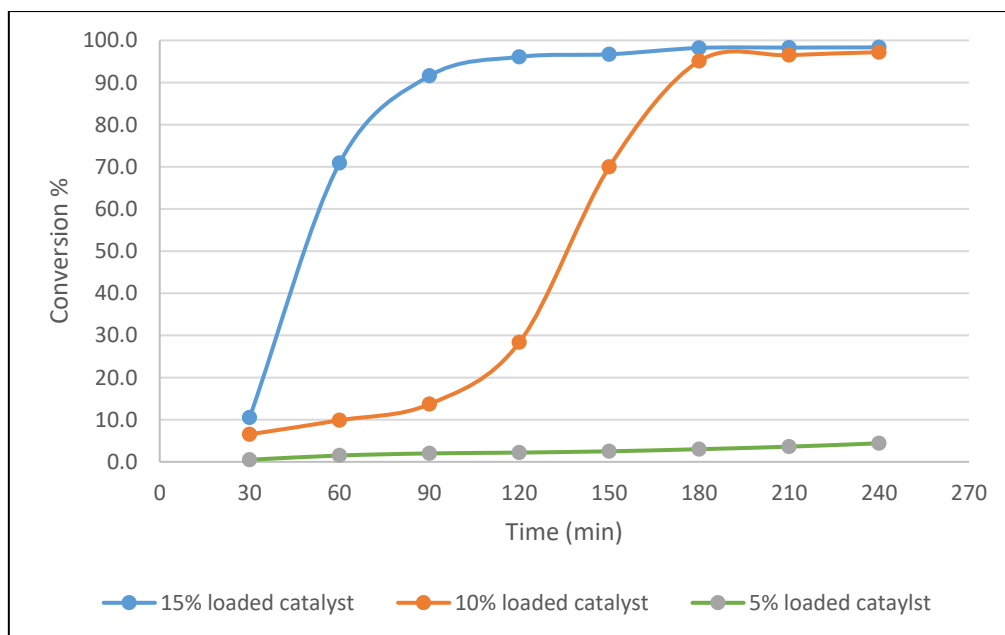
Figure 3-5 FAEE conversion in relation to ethanol/corn oil molar ratio with catalyst 2.6SZA900. Reaction conditions: temperature = 70 °C, 10% catalyst dosage and 180 min reaction time.

The effect of the amount of catalyst 2.6SZA900 on its performance in transesterification reaction with corn oil was investigated at 70 °C with a 10:1 ethanol-to-oil ratio for 3 h using catalyst loadings of 5, 10, and 15%. Figure 3.6a illustrates the significant impact of the catalyst amount in this reaction: conversion increased from 5.5% to 100% with increases in loading from 5% to 15%. This is because increased catalyst loading provides increased contact between reactants and the catalyst surface (Wang et al., 2017) and increases the active sites in the mixture (Kaur et al., 2018).

The time required for complete transesterification (> 99% FAEE conversion) decreased from 240 min to 120 min on increasing the catalyst loading from 10 wt.% to 15 wt.%. Moreover, the catalyst achieved more than 90% biodiesel conversion within 90 min with the 15 wt.% loading, while the conversion was less than 15% with the loading 10% during the same period, as shown in Fig. 3.6b. The results indicate that the loading of the prepared catalyst plays a crucial role in the reaction; this is consistent with a previous report that transesterification conversion depends strongly on the catalyst dosage (Yadav et al., 2018). Figure 3.6b also shows that the reaction reached the steady state very quickly at the 15 wt.% catalyst dosage, while the reaction took longer at the lower dosage because of the low surface area of the 2.6SZA900 catalyst. This is because an increased catalyst dosage leads to an abundance of active sites for reaction and enhances mass transfer (Yahya et al., 2018).



(a)



(b)

Figure 3-6. (a) Effect of 2.6SZA900 catalyst loading on FAEE conversion and (b) FAEE conversion over time at loadings of 10 wt.% and 15 wt.%

Although a 15 wt.% loading of 2.6SZA900 catalyst caused faster kinetics and a higher reaction conversion, the cost and time taken for catalyst preparation were significant. When this was taken into account, the 10 wt.% catalyst dosage was determined to be more economical for this reaction (using corn oil). In addition, an EtOH:oil molar ratio of 10:1, reaction time of 180 min and reaction temperature of 70 °C were the best operating conditions. Figure 3.7 shows the  $^1\text{H}$  NMR spectrum of the FAEE produced by the transesterification reaction under these operating conditions.

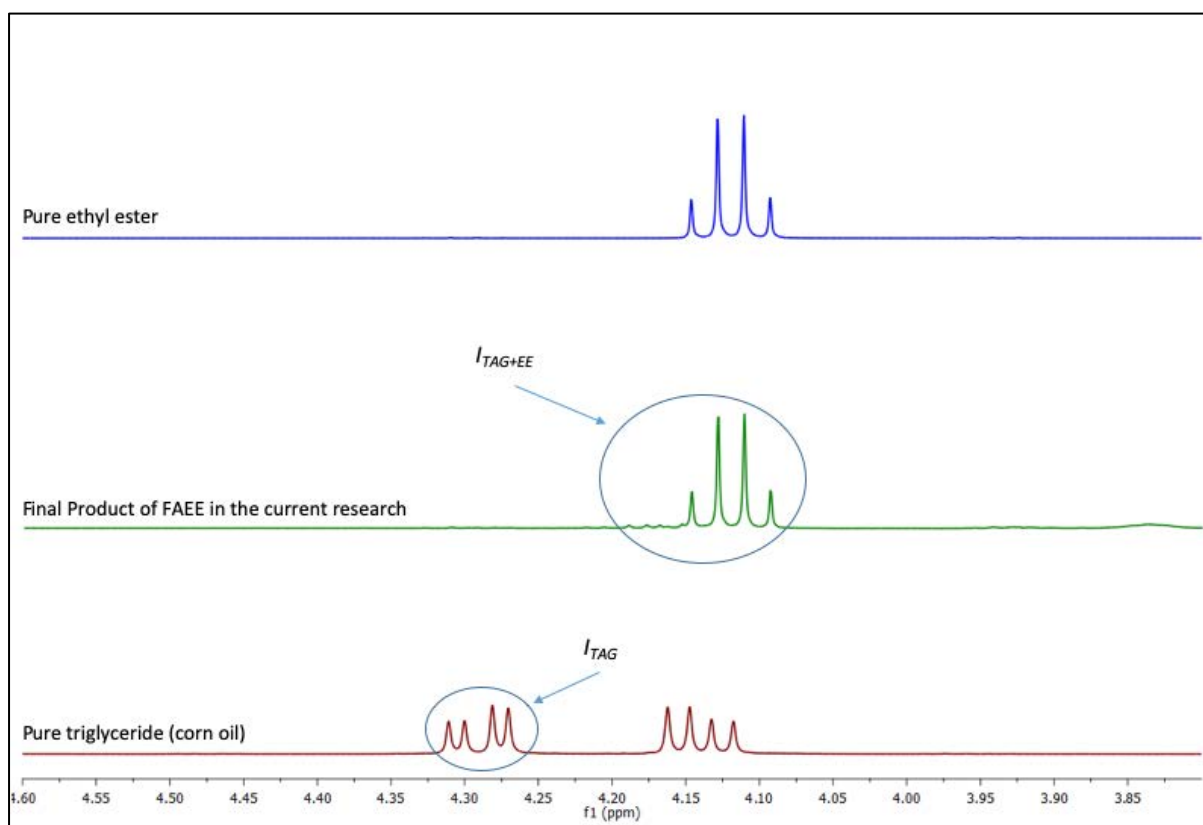


Figure 3-7.  $^1\text{H}$  NMR spectra of the transesterification reaction reactant and product, with pure ethyl ester shown for comparison

### 3.4.1.3 Catalytic performance in esterification reaction

Due to its high catalytic performance in a transesterification reaction, the 2.6SZA900 catalyst was also studied in an esterification reaction. The esterification process was carried out with oleic acid as a standard FFA. The maximum conversion of FAEE in the esterification reaction was 71.4% at 70 °C, with a 5:1 ethanol-to-oleic acid molar ratio, 10% catalyst dosage and 6 h reaction time. The  $^1\text{H}$  NMR spectrum of the final product shown in Fig. 3.8 confirms the production of FAEE from the esterification reaction.

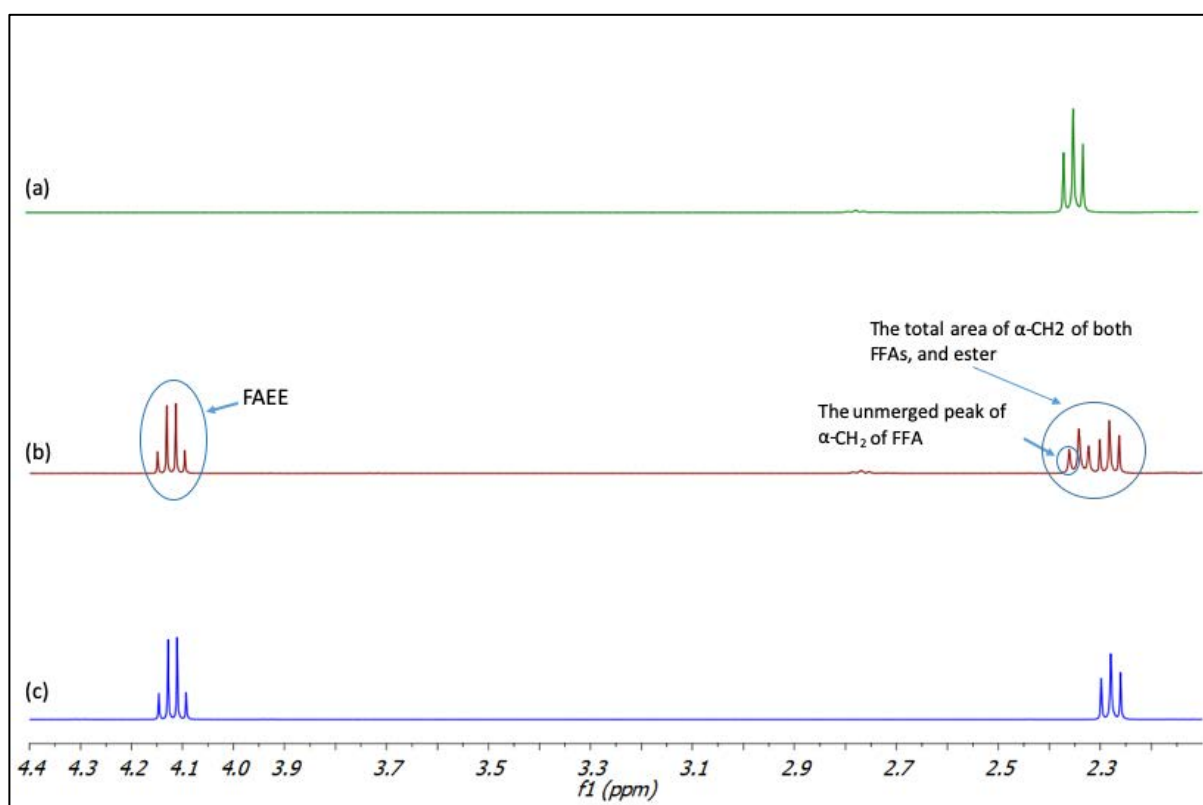


Figure 3-8.  $^1\text{H}$  NMR spectra of the esterification reaction's (a) reactant (pure oleic acid) and (b) final product (FAEE); (c) with pure ethyl oleate shown for comparison

The synthesized 2.6SZA900 catalyst exhibited acid and base properties because of the mixed metal oxides of strontium oxide SrO, zinc oxide ZnO, and aluminium oxide  $\text{Al}_2\text{O}_3$ . The presence of ZnO provided Lewis acid properties to the catalyst.  $\text{Zn}^{+2}$  and  $\text{O}^{-2}$ , which are strong Lewis acids (Pirouzmand et al., 2018), and  $\text{Al}^{+3}$  and  $\text{O}^{-2}$ , which are medium Lewis acids

(Kondamudi et al., 2011), are expected to enhance the esterification reaction. As mentioned in the XRD analysis, the various polar crystal phases of ZnO enhance the efficiency of the catalyst in the esterification reaction. In contrast, the presence of SrO is expected to enhance the transesterification reaction. The metal ions  $\text{Sr}^{+2}$  and  $\text{O}^{-2}$  work as a strong Lewis base due to the high density of basic active sites (Rashtizadeh et al., 2014).

The bifunctionality of the catalyst was confirmed experimentally by esterification of oleic acid and transesterification of corn oil. Also, the performance of the current catalysts was tested via separate esterification and transesterification reactions, with reasonable results from both. As is known, the basicity of a catalyst enhances transesterification reactions while its acidity enhances esterification reactions.

Table 3.2 compares the performance of catalyst 2.6SZA900 with some bifunctional catalysts reported in the literature. Two catalysts performed better than our catalyst 2.6SZA900. The ZnO-La<sub>2</sub>O<sub>3</sub> catalyst reported by Yan et al. (2009) achieved a conversion of 96% for transesterification with soya bean oil, and 96.7% for esterification with oleic acid at a reaction temperature of 200 °C. Similarly, the CMC-SO<sub>3</sub>H@3Fe-C400 catalyst reported by Wang et al. (2017) achieved a 95.4% conversion for transesterification and 97.39% for esterification using the same feedstock as Yan et al. but at a reaction temperature of 90 °C. It is worth noting that the reaction temperatures of 200 °C and 90 °C used in Yan et al. and Wang et al., respectively, are much higher than that used in the current study (70 °C).

Table 3.2. Comparison of the biodiesel production performance of the catalyst used in the current study with other bifunctional catalysts

Catalyst	Transesterification			Esterification			Reference
	Feedstock	Reaction conditions	Conversion or yield (%)	Feedstock	Reaction conditions	Conversion or yield (%)	
ZnO-La <sub>2</sub> O <sub>3</sub>	Soybean oil	200 °C, 60 min	96	Oleic acid	200 °C, 110 min	96.7	Yan et al. (2009)
Na-Q-3T	Canola oil	75 °C, 2 h	60	Octanoic acid	75 °C, 6 h	100	Kondamudi et al. (2011)
Zr-CMC-SO <sub>3</sub> H@3Fe-C400	Soybean oil	90 °C, 4 h	95.4	Oleic acid	90 °C, 4 h	97.39	Wang et al. (2017)
PCs-SO <sub>3</sub> H	Sunflower oil	90 °C, 2 h	70	Oleic acid	75 °C, 10 h	71	Tamborini et al. (2016)
2.6SZA900	Corn oil	70 °C, 180 min	95.1	Oleic acid	70 °C, 6 h	71.4	This study

### 3.4.2 Catalyst characterisation

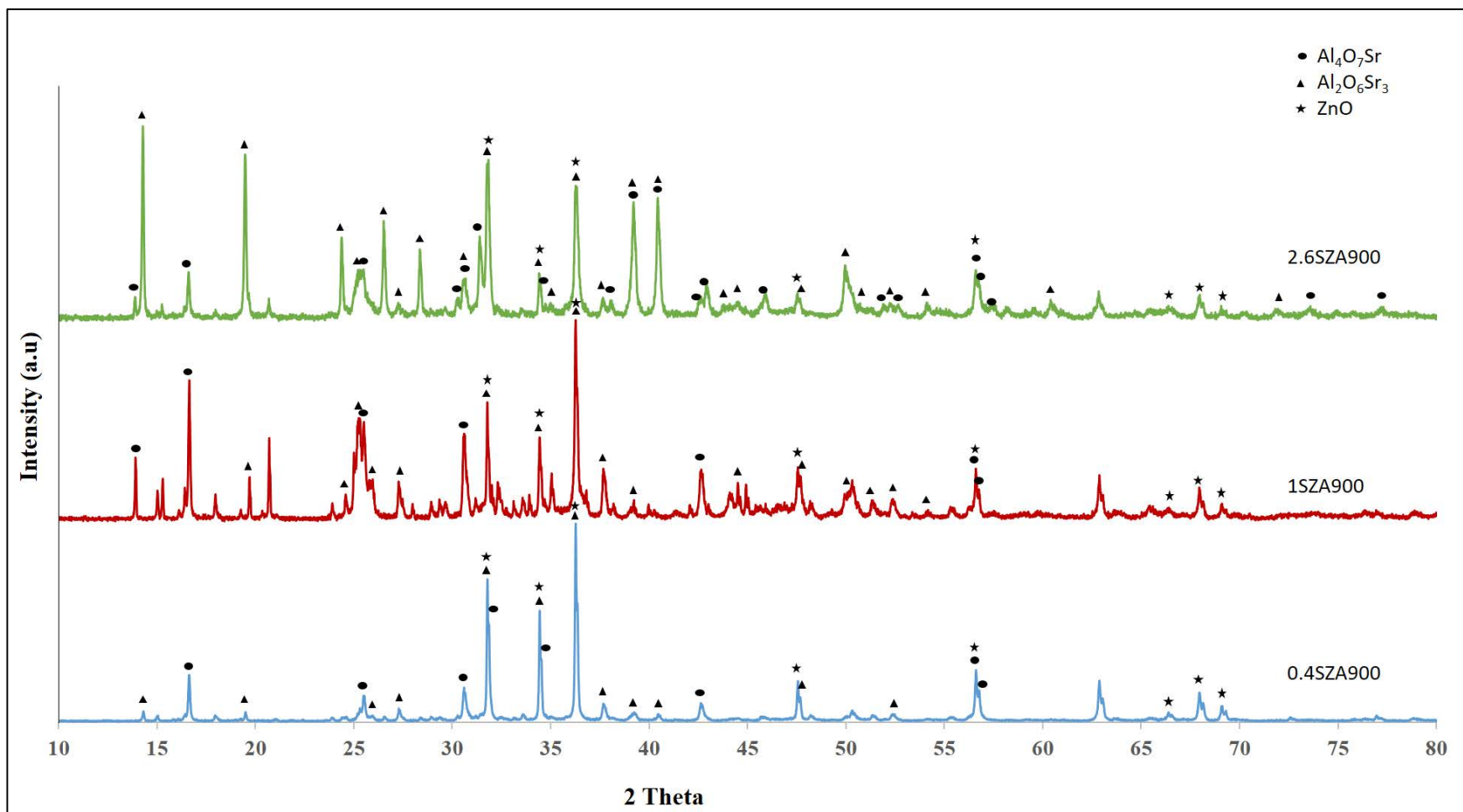
#### 3.4.2.1 X-ray diffraction

The diffraction patterns of catalyst SZA900 made with different Sr:Zn molar ratios are illustrated in Figure 3.9a. The XRD data show high interaction between Sr and Al<sub>2</sub>O<sub>3</sub> and confirm the presence of different phases of strontium aluminium oxide, including Al<sub>4</sub>O<sub>7</sub>Sr and Al<sub>2</sub>O<sub>6</sub>Sr<sub>3</sub>, which correspond with the data reported in COD file Nos. 9007445 and 2000991, respectively. The results also identify the formation of zinc oxide in the zincite phase, which matches the data reported in COD file No. 9008877. The result shows that several diffraction peaks of binary oxide Al<sub>4</sub>O<sub>7</sub>Sr clearly emerge with increases in the Sr:Zn molar ratio from 0.4 to 2.6, including Al<sub>4</sub>O<sub>7</sub>Sr (2 0 0), (2 2 0), (4 0 0), (0 2 2), (2 0 2), and (3 1 3) at 2θ of 14.16°, 24.33°, 28.53°, 39.29°, 40.41°, and 63.34°, respectively. Also, two peaks of Al<sub>2</sub>O<sub>6</sub>Sr<sub>3</sub> (4 4 4) and (7 1 1) arise at 2θ of 39.34° and 40.6°, respectively. On the other hand, the peaks of ZnO phases slightly decrease with decreases in the amount of zinc in the catalysts.

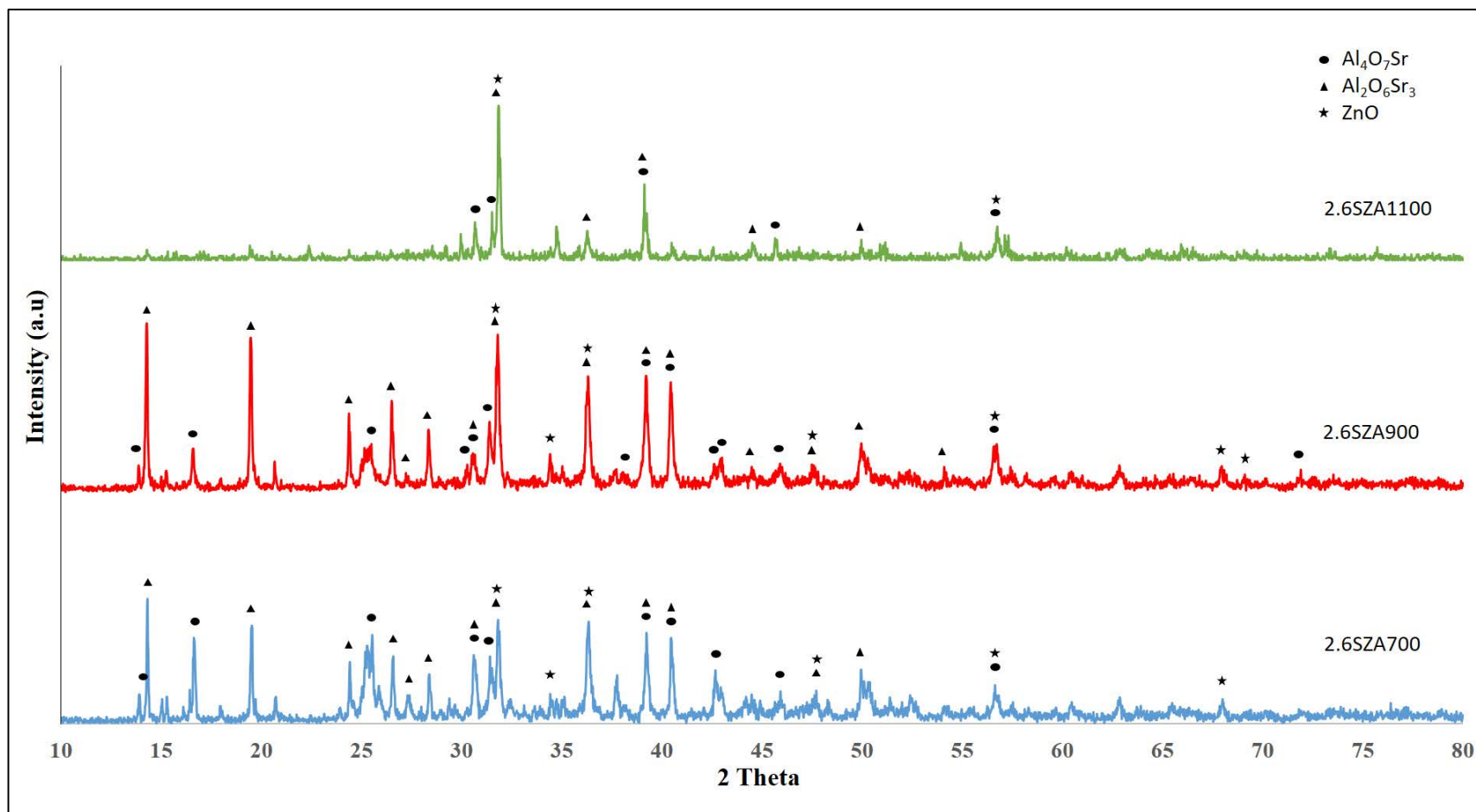
Figure 3.9b shows the XRD patterns of triple metal oxides of SrO, Al<sub>2</sub>O<sub>3</sub>, and ZnO for catalyst 2.6SZA at calcination temperatures of 700, 900, and 1100 °C. The XRD findings show the significant effects of calcination temperature on the intensity of the phases of binary oxide (SrO)(Al<sub>2</sub>O<sub>3</sub>) and ZnO. For the 2.6SZA700 catalyst, the intensity of Al<sub>4</sub>O<sub>7</sub>Sr and Al<sub>2</sub>O<sub>6</sub>Sr<sub>3</sub> were observed to be very low, while some phases were not prominent. The same trend was reported by Xu et al. (2006). Furthermore, increasing the calcination temperature to 1100 °C caused disappearance of the peaks of binary oxide (Al-O-Sr) of Al<sub>4</sub>O<sub>7</sub>Sr and Al<sub>2</sub>O<sub>6</sub>Sr<sub>3</sub> at 2θ of 14° to 30°, and the peak at 40.4° of the Al<sub>4</sub>O<sub>7</sub>Sr phase, which is most likely the reason for the decrease in effectiveness of the catalyst. Therefore, the 2.6SZA900 catalyst exhibited the highest intensity for the different phases formed and, hence, has better catalytic performance than the other catalysts synthesized in the current study.

Mierczynski et al. (2015) obtained different phases of binary oxide SrO-Al<sub>2</sub>O<sub>3</sub> prepared via a co-precipitation technique at a 0.5 Sr:Al molar ratio. The researchers distinguished the presence of different crystal phases in the prepared catalyst at calcination temperatures of 600 °C, 900 °C, and 1200 °C. Diffraction analysis of the mixed-metal oxides proves the existence of various crystal phases, including Al<sub>2</sub>O<sub>6</sub>Sr<sub>3</sub>, Al<sub>2</sub>SrO<sub>4</sub>, and Al<sub>2</sub>O<sub>6</sub>Sr<sub>3</sub>.2H<sub>2</sub>O. Xu et al. (2011) prepared different mixed oxides of Sr-Al, including Al<sub>2</sub>O<sub>6</sub>Sr<sub>3</sub> and Al<sub>4</sub>O<sub>7</sub>Sr phases from a nitrate precursor. Rashtizadeh et al. (2014) obtained a nanocomposite Al<sub>2</sub>O<sub>6</sub>Sr<sub>3</sub> phase prepared from strontium nitrate and an aluminium isopropoxide precursor by a sol-gel method at a 900 °C calcination temperature. The XRD findings in the current study are in line with these results.

The XRD analysis confirms that catalyst 2.6SZA900 has different phases of strontium aluminium oxide and the polar crystal phase of ZnO. The binary oxide (SrO)(Al<sub>2</sub>O<sub>3</sub>) phases were proven to be highly active for the transesterification reaction. Mierczynski et al. (2015) achieved 90.5% conversion of methyl ester from rapeseed oil using an SrAl<sub>2</sub>O<sub>4</sub> catalyst. Rashtizadeh et al. (2014) used an Al<sub>2</sub>O<sub>6</sub>Sr<sub>3</sub> catalyst with soybean oil and obtained a biodiesel of yield about 95.7%. Moreover, the polar crystal phases of ZnO at 47.54°, 62.86°, and 67.95° were confirmed as being high-performing in the esterification reaction (Yan et al., 2009). Consequently, the polar surfaces of strontium aluminium oxide and (ZnO) can provide active sites for transesterification and esterification reactions.



(a)

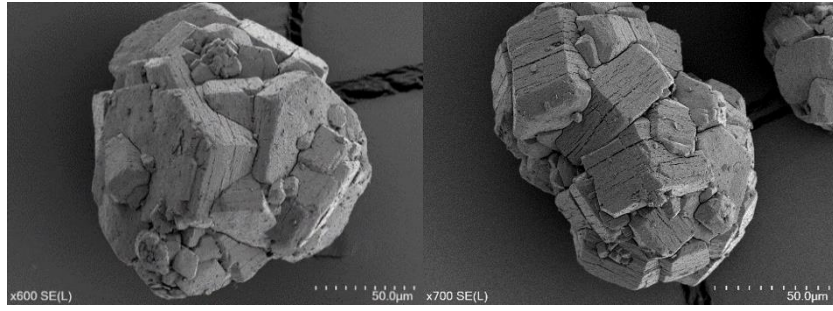


(b)

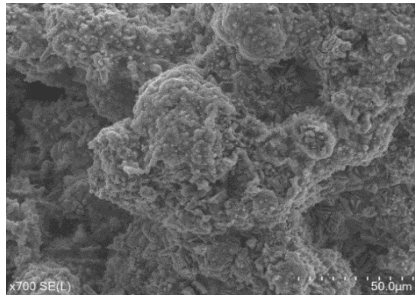
Figure 3-9. XRD patterns for (a) catalysts with different Sr:Zn molar ratios calcined at 900 °C and (b) 2.6SZA catalyst calcined at different temperatures

### 3.4.2.2 Scanning electron microscopy and energy-dispersive X-ray spectroscopy

Figure 3.10 shows the fresh  $\text{Al}_2\text{O}_3$  and the final synthesised catalyst. Figure 3.10(a) exhibits the surface morphology of fresh  $\text{Al}_2\text{O}_3$  before the loading of any metal. The  $\text{Al}_2\text{O}_3$  particles have irregular rock-like shapes. Figure 3.10(b) demonstrates the effect of Sr and Zn loading on the surface morphology of alumina at a calcination temperature of 900 °C. The SEM image of the surface of the synthesised catalysts reveals a major transformation of the rocky particles of the  $\text{Al}_2\text{O}_3$  into fine particle agglomerates as a result of surface coverage by metal oxides (ZnO and SrO). The EDS image in Fig. 3.11 and data in Table 3.3 illustrate the distribution of Sr, Al, Zn and O on the calcined catalyst surface at 900 °C. The distributions of each element show that SrO (red), ZnO (blue) and  $\text{Al}_x\text{O}_y\text{Sr}_z$  (yellow) are clearly visible in the same location on the surface, where  $x$ ,  $y$ , and  $z$  represent the compositions of metals for  $(\text{SrO})(\text{Al}_2\text{O}_3)$  binary oxides in different phases (further explained in Section 3.2.1). As SrO and ZnO represent active base and acid sites, this result suggests that the final synthesised catalyst calcined at 900 °C includes both acidic and basic metal oxide forms and is expected to exhibit bifunctional activities.



(a)



(b)

Figure 3-10. SEM images of (a) neat aluminium oxide and (b) 2.6SZA 900 catalyst

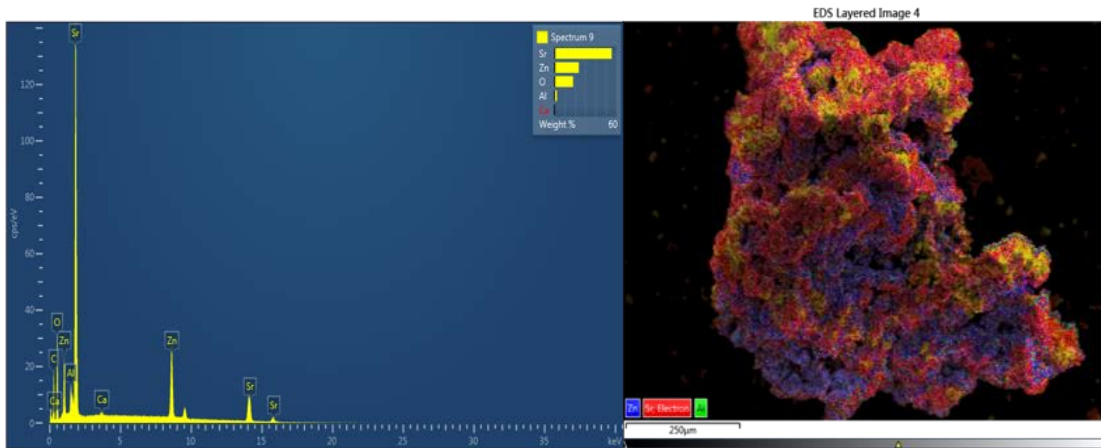


Figure 3-11. 2.6SZA900 catalyst (a) EDS spectra and (b) EDS elemental mapping

Table 3.3. Weight ratios of the metals in catalyst 2.6SZA900

Element	Wt.%	Oxide %
O	18.13	
Al	2.36	4.5
Zn	23.74	29.6
Sr	55.77	65.9
Total	100.00	100.00

### 3.4.2.3 Fourier-transform infrared spectroscopy

The FT-IR spectra of SrO, ZnO, and Al<sub>2</sub>O<sub>3</sub> metal oxides at different Sr loadings calcined at 900 °C are illustrated in Fig. 3.12. The FT-IR spectra show that peaks appear around 855 cm<sup>-1</sup> and in the region of 1446 cm<sup>-1</sup>, which correspond to the vibrations of Sr-O and become more intense with Sr addition (Chroma et al., 2005). Intensities of the absorption peaks of Sr-O around 700 cm<sup>-1</sup> are increased in companion with the increasing Sr/Zn molar ratio (Li et al., 2016). Moreover, the peak at 700 cm<sup>-1</sup> might be related to strontium aluminate (Guo et al., 2004; Vijaya et al., 2008). The peak which appears at around 3662 cm<sup>-1</sup> corresponds to the Zn-O. The intensity increases with increasing amounts of zinc in the 0.4SZA900 catalyst (Borah et al., 2019).

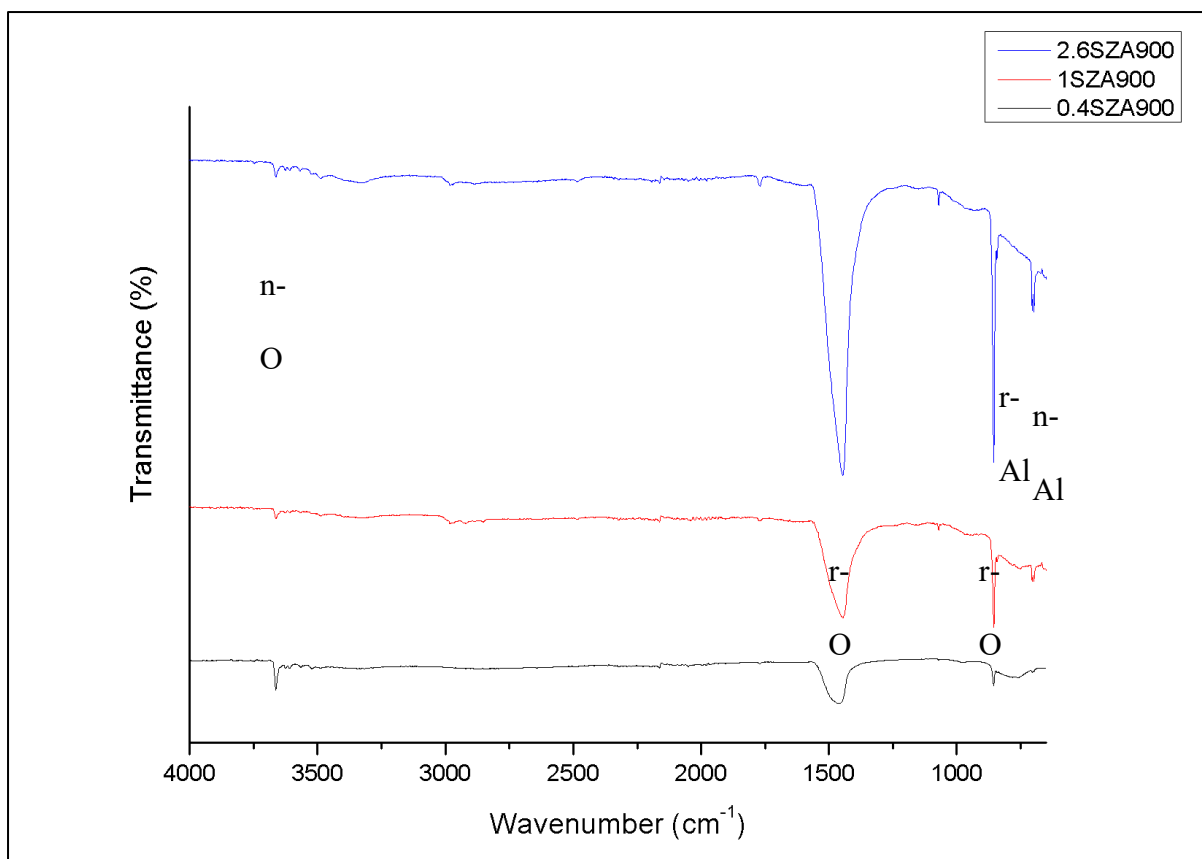


Figure 3-12. FT-IR spectra of different Sr –Zn loading for prepared catalysts

#### 3.4.2.4 Surface area (BET) and pore volume (BJH)

The specific surface area, pore volume, and pore diameter of catalysts synthesised with different Sr/Zn molar ratios and calcination temperatures are listed in Table 3.4. The surface area results confirm significant reductions in the specific surface areas of the prepared catalysts as a result of loading strontium and zinc ions onto the  $Al_2O_3$ , possibly blocking some of its pores. Furthermore, increasing the calcination temperature from 700 °C to 1100 °C had the same consequence because of the phase crystallization change and the sintering process. The result suggests that the catalyst's activity does not only depend on its specific surface area but on the metal active sites of strontium aluminium oxide and zinc oxide. Yan et al. (2009) and Al-Sharif et al. (2019) have also reported achieving high conversion with low surface area.

Table 3.4. Surface area, pore volume and average pore diameter of catalysts according to BET analysis

Catalyst	Surface area (m <sup>2</sup> /g)	Pore volume (cm <sup>3</sup> /g)	Pore diameter (nm)
Al <sub>2</sub> O <sub>3</sub>	155	0.283	5.800
0.4ZSA900	1.371	0.014	3.519
1ZSA900	3.132	0.049	3.411
2.6ZSA900	3.515	0.054	3.516
2.6ZSA700	3.540	0.039	3.174
2.6ZSA1100	1.214	0.013	3.414

### 3.4.2.5 Inductively Coupled Plasma Optical Emission Spectrometer

The surface and bulk weight percentages of Sr, Zn, and Al metals were determined by EDS and ICP-OS analyses; respectively, as listed in Table 3.5. The results show that the experimental surface and bulk metal amounts have the same trends as the theoretical amounts, which are Sr > Zn > Al. The amount of Sr in the experimental surface analysis was lower than the theoretical amount, probably due to the good dispersion of Sr on the catalyst surface. The result indicates that Sr atoms were incorporated into the Al-species lattice and rendered an excess exposure of Al on the catalyst surface. The same trend was reported by Lee et al. (2015). However, the bulk amounts of Sr and Al were found to be lower than the intended amounts, maybe because of incomplete dissolution of the (SrO)(Al<sub>2</sub>O<sub>3</sub>) sample during its preparation for analysis.

Table 3.5. Theoretical, surface, and bulk amounts of Sr, Zn, and Al metals, as measured by ICP-OS and EDX

Metal	Theoretical amount (wt.% actually prepared)	Experimental bulk amount (wt.% measured by ICP-OS)	Experimental surface amount (wt.% measured by EDX)
Sr	74.9	70.8	65.9
Zn	21.5	26.3	29.6
Al	3.6	2.9	4.5
Total	100	100	100

### 3.4.3 Kinetic studies

Kinetic studies of transesterification and esterification reactions were conducted at different temperatures to gain a better understanding of the relationships between reaction time and temperature in each reaction. Kinetic studies are also important in understanding the reaction mechanism. Before conducting the kinetic studies, the following assumptions were made: (1) The reaction is forward, because excess ethanol is used, and the backward reaction is not considered. (2) The reaction is first-order with respect to the feed oil, as reported by previous researchers (Al-Sharifi et al., 2019). (3) Intermediate reactions are ignored. (4) There is perfect mixing of reactants and products in the reactor and mass transfer does not limit the reactions.

A kinetic study of the transesterification reaction of corn oil was investigated at reaction temperatures of 50, 60, and 70 °C and reaction times of 30 to 240 min. A kinetic study of the esterification reaction of oleic acid was made at the same temperatures but with reaction times of 1 to 6 h.

For the first-order model of transesterification reaction:

$$r = \frac{d[TG]}{dt} = -k[TG]$$

Where  $r$  is the reaction rate and  $k$  is the reaction rate constant.

Integration of the above equation from 0 to  $t$  for time and  $[TG]_0$  to  $[TG]$  for triglyceride concentration yields:

$$\ln[TG] = -kt + \ln[TG]_0 \quad (3.4)$$

Substituting the conversion equation:

$$\frac{[TG]_0 - [TG]}{[TG]_0} = x$$

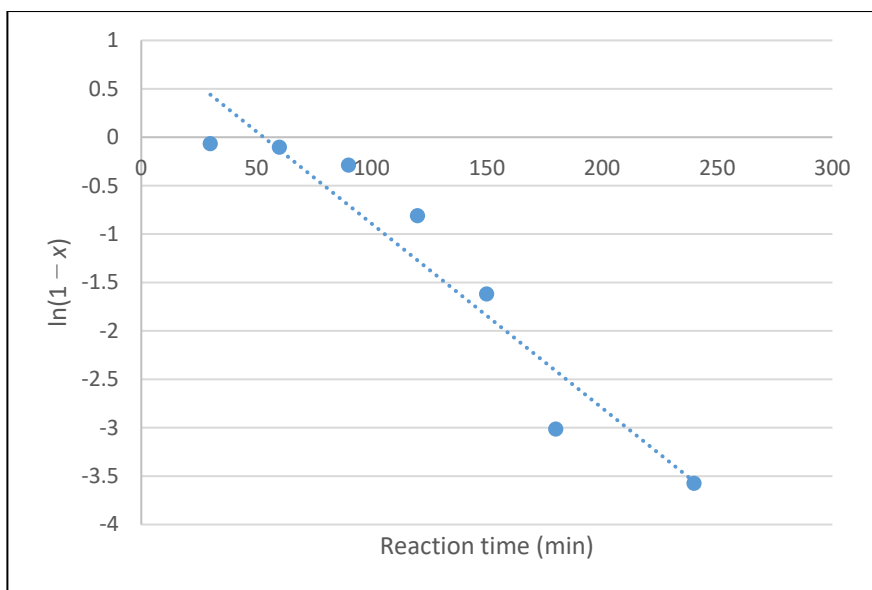
results in:

$$\ln(1 - x) = -kt \quad (3.5)$$

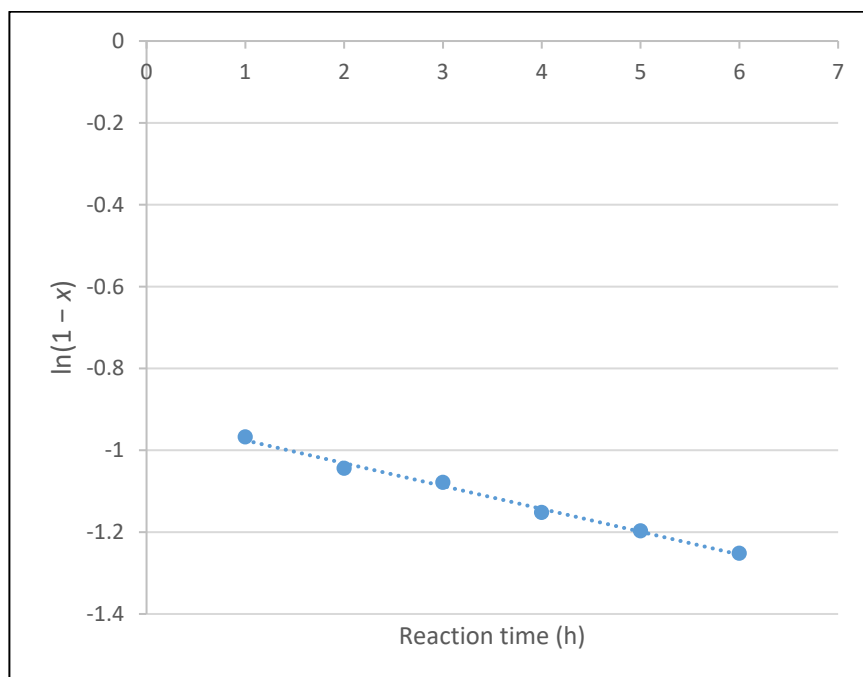
The rate constant  $k$  can be obtained by plotting  $\ln(1 - x)$  against time  $t$ , where the slope of the linear equation represents  $k$ .

For the esterification reaction, the same calculations can be applied, and Equation 3.5 can be used to find the constant of the reaction ( $k$ ).

The fitting of the kinetic first-order model of the transesterification reaction took into account all data points obtained from 30 to 240 min. For the esterification reaction, the data points were taken from 1 to 6 h. The high  $R^2$  value demonstrates the adequacy of the first-order reaction model. Regression of the experimental results for the transesterification and esterification reactions are shown in Figs 3.13 (a) and (b), respectively.



(a)



(b)

Figure 3-13. Kinetic first-order models fitted to a) transesterification and b) esterification reactions

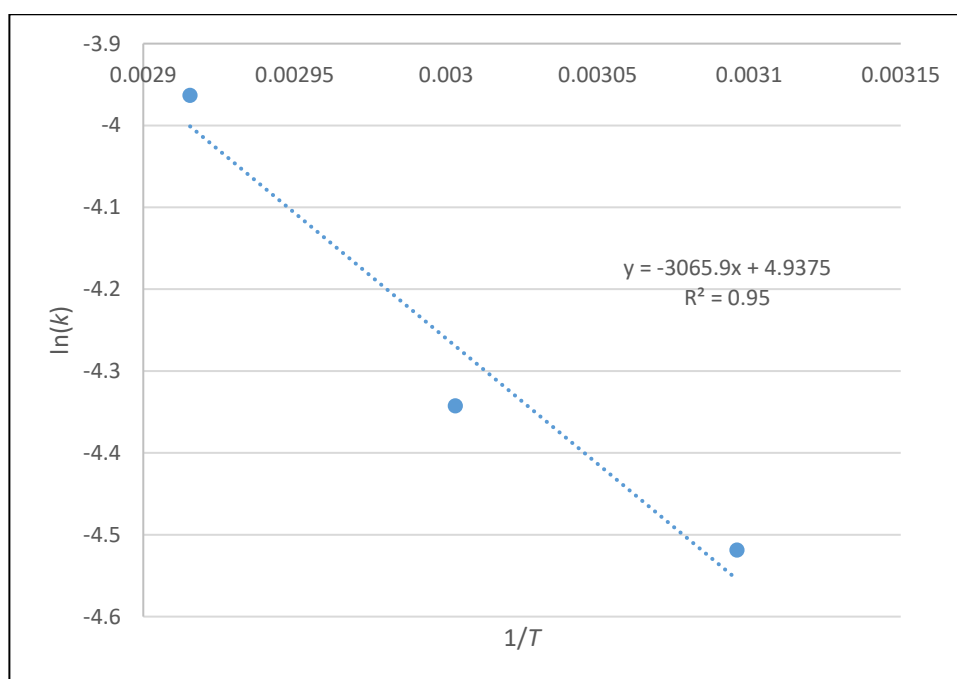
The Arrhenius equation was applied to calculate the activation energy for further investigation of the change in reaction rate at different reaction temperatures, as shown below:

$$k = A \cdot e^{-E_a/RT} \quad (3.7)$$

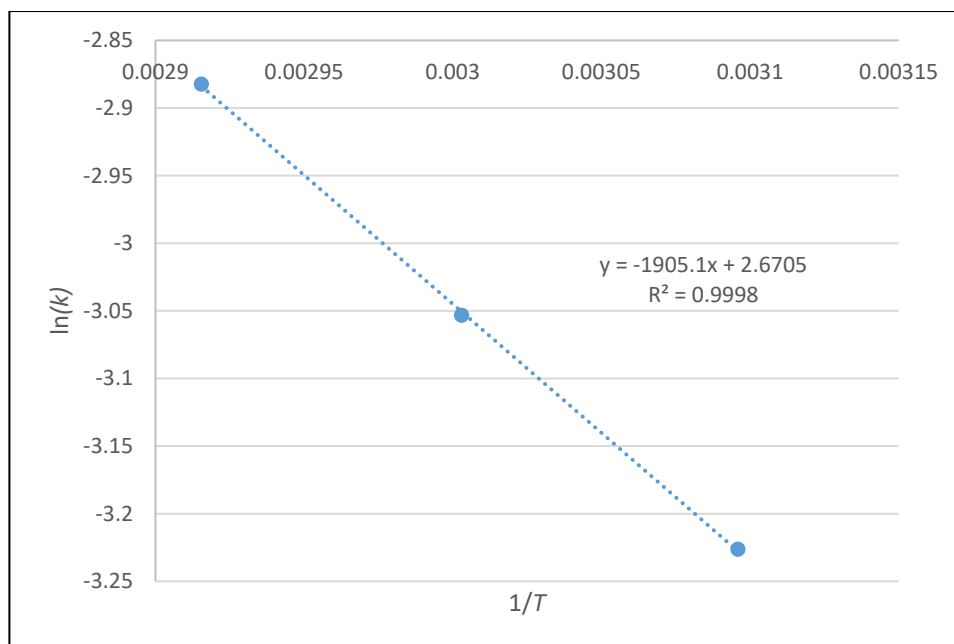
By simplifying the equation, we obtain:

$$\ln k = -\frac{E_a}{RT} + \ln A \quad (3.8)$$

where  $E_a$  is the activation energy (kJ/mol),  $R$  is the universal gas constant ( $8.314 \text{ J mol}^{-1} \text{ K}^{-1}$ ),  $k$  is the reaction rate constant ( $\text{min}^{-1}$ ),  $A$  is a frequency factor ( $\text{min}^{-1}$ ), and  $T$  is the reaction temperature (K). The activation energy ( $E_a/R$ ) was obtained by plotting  $\ln(k)$  against the reciprocal of temperature ( $1/T$ ), where the slope of the linear equation represents ( $-E_a/R$ ), and the intercept represents  $A$ , as shown in Fig. 3.14.



(a)



(b)

Figure 3-14. First-order models of the activation energies of the a) transesterification and b) esterification reactions

Table 3.6 presents the values of the correlation coefficient ( $R^2$ ) for the trans/esterification reactions at each reaction temperature. The values of  $R^2$  show that the transesterification and esterification reaction observations are in good agreement with the first-order model. Furthermore, increases in reaction temperature lead to a higher rate constant and, thus, an improved reaction rate, which can be explained in terms of enhanced collisions between molecules (Alsharifi et al., 2017). The activation energies required for transesterification and esterification reactions using the ZnO-SrO/Al<sub>2</sub>O<sub>3</sub> catalyst were 25.5 and 15.84 kJ/mol, respectively.

Table 3.6. Correlation coefficients and rate constants for trans/esterification reactions at different temperatures.

Temperature (°C)	Transesterification		Esterification	
	Correlation coefficient (R <sup>2</sup> )	Rate constant (min <sup>-1</sup> )	Correlation coefficient (R <sup>2</sup> )	Rate constant (h <sup>-1</sup> )
50	0.91	0.0109	0.937	0.0397
60	0.93	0.013	0.93	0.0472
70	0.92	0.019	0.99	0.0558

### 3.5 Conclusion

This study synthesised a novel bifunctional catalyst by loading an acid metal (Zn) and alkali metal (Sr) on alumina oxide using the wet impregnation method. The efficiency of the synthesised catalyst was then evaluated under mild reaction conditions. A series of SrO-ZnO/Al<sub>2</sub>O<sub>3</sub> catalysts were prepared and used in esterification and transesterification processes. Oleic acid and corn oil were used for esterification and transesterification reactions for biodiesel production. The study showed that the prepared catalyst has catalytic activity with both reactions. The obtained 2.6SZA900 catalyst achieved more than 95.1% conversion for biodiesel production under the transesterification conditions of a 10:1 ethanol-to-oil molar ratio, 10% catalyst loading, and a reaction time of 180 min at 70 °C. The operating conditions for the esterification process were a 5:1 ethanol-to-corn oil molar ratio, 10% catalyst loading, and reaction time of 6 h at 70 °C, which achieved a 71.4% biodiesel conversion. Kinetic studies showed that the prepared 2.6SZA900 catalysts could be employed for trans/esterification under moderate temperature and atmospheric pressure.

# Chapter 4: Biodiesel production from high-acidity waste cooking oil

## 4.1 Abstract

A simultaneous transesterification and esterification process was applied for production of biodiesel from high-acidity waste cooking oil containing 18 wt% free fatty acids (FFAs) using a range of heterogeneous bifunctional strontium-zinc-aluminium catalysts. The influences of the molar ratio of metal oxide, the ethanol-to-waste oil molar ratio, reaction temperature and time, catalyst dosage, and feedstock FFA content on biodiesel conversion were studied. High interaction between strontium, aluminium and zinc metals was recognised to promote catalyst performance. High interaction and mixing of strontium, aluminium and zinc oxides enhanced and increased the acid and base active sites on the surface of catalyst. The catalyst with a 2.6:1 molar ratio of strontium to zinc was found to perform best in simultaneously transesterifying the glycerides and esterifying the fatty acids in the used oil. The catalyst exhibited higher catalytic activity with high-acidity waste cooking oil, with 95.7% reaction conversion at the optimum conditions of a 10:1 ethanol-to-waste oil molar ratio, 15 wt% catalyst dosage, and 5 h reaction time at 75 °C. The used catalyst showed low reusability due to high leaching of strontium.

## 4.2 Introduction

Biodiesel is produced from a range of renewable resources, such as plant oils (edible and non-edible), waste cooking oils, animal fats, and oleaginous microorganisms. The main obstacle to biodiesel production is cost, with the feedstock comprising 60 – 70 % of the total production cost (Kumar et al., 2017). Therefore, using low-cost and -quality raw materials such as waste cooking oil (WCO) could reduce the biodiesel production cost. Biodiesel production

from WCO costs approximately 1.2 – 2.5 US\$/litre, with the WCO comprising only 2% of the total production cost (Mohammadshirazi et al., 2014). Also, Fawaz et al. (2018) reported that the average total cost of biodiesel produced from WCO is 0.57 US\$/litre after studying 81 different scenarios.

Oils are generally classified into two categories: 1) acidic oils and 2) vegetable oils with low FFA contents, including inedible and edible oils. Traditionally, acidic catalysts are often preferably used with acidic oils in esterification reactions, while the vegetable oils prefer to use basic catalysts via a transesterification reaction (Endalew et al., 2011). WCOs were originally vegetable oils that were changed by cooking at high temperatures and then blended (acidic oil with vegetable oil). They are comprised of free fatty acids (FFAs) and Mo-, Di-, and Tri-glycerides (TGs). Accordingly, bifunctional heterogeneous catalysts that can produce biodiesel from FFAs and TGs simultaneously are highly desirable and have the potential to increase biodiesel productivity.

Heterogeneous bifunctional catalysts are solid catalysts that have acidic and basic features due to the presence of acid-base active sites on their surface. This allows them to participate in trans/esterification reactions simultaneously. Several heterogeneous bifunctional catalysts have been used for biodiesel production from WCOs with different FFA contents, as listed in Table 4.1. It is clear that WCOs contain different quantities of FFAs, and that all catalysts used for biodiesel production from WCO require high reaction temperatures to achieve good conversion. This is because FFAs can inhibit transesterification reactions (Yan et al., 2009). Therefore, an inexpensive heterogeneous bifunctional catalyst capable of achieving high conversion of high-acidity WCO to biodiesel under moderate operating conditions is highly desirable. The bifunctional catalyst SrO–ZnO–Al<sub>2</sub>O<sub>3</sub> used in Chapter 3 has been proven to have high performance in treating both acidic and vegetable oils. Therefore, it will be applied in this chapter to treat high-acidity WCO.

Table 4.1. Summary of research on biodiesel production from WCO using bifunctional catalysts

Bifunctional catalyst	FFA (wt.%)	Reaction temperature (°C)	Yield or conversion (%)	Reference
ZnO-La <sub>2</sub> O <sub>3</sub>	3.78	200	96	Yan et al. (2009)
Sr/ZrO <sub>2</sub>	2.9	115.5	79.7	Wan Omar et al. (2011)
Fe <sub>2</sub> O <sub>3</sub> AMnOASO <sub>4</sub> <sup>2-</sup> /ZrO <sub>2</sub>	17.5	180	96.5	Alhassan et al. (2015)
γ-Al <sub>2</sub> O <sub>3</sub> -MgO	1.6	100	91.4	Farooq et al. (2016)
Na/FAP	2.5 ± 0.5	120	97	Essamlali et al. (2019)

The bifunctional SrO-ZnO-Al<sub>2</sub>O<sub>3</sub> catalyst used in our previous study (chapter 3) proved to have high performance in its ability to treat both acidic and vegetable oils. The catalyst derives its bifunctionality (acid-base) activity from the presence of zinc oxide and strontium oxide. The presence of SrO has a significant effect on transesterification reactions because of its high basicity; the basicity doubles when it is mixed with ZrO<sub>2</sub> (Yang et al., 2007). Strontium oxide (SrO) shows higher performance in transesterification reactions than other alkaline earth metal oxides, such as CaO and MgO. Also, a SrO catalyst achieved 82% conversion from olive oil, whereas conversions with CaO and MgO catalysts were only 15% and 0%, respectively, due to the high amount of active sites on the catalyst surface of strontium oxide (Chen et al., 2012). A CuO/SrO catalyst was applied to transesterification of refined hemp seed oil and achieved 92% biodiesel yield, surpassing all other alkaline earth metal oxide catalysts because of its high-basicity efficacy (Su et al., 2013). A mixed-metal-oxide catalyst of Sr-Al exhibited high catalytic activity in a transesterification reaction, achieving 90.5% conversion using rapeseed oil and methanol (Mierczynski et al., 2015).

The presence of ZnO has a significant effect on esterification reactions because of its acidity, and it has been used as a Lewis acid catalyst in various studies. Bancquart et al. (2001) reported that zinc oxide (ZnO) has strong acidity and very low basicity. Corro et al. (2013) claimed that ZnO provides a high amount of acid active sites on the surface of the catalyst (ZnO/SiO<sub>2</sub>). They used it to achieve 96% conversion of *Jatropha curcas* crude oil with a high FFA content via an esterification reaction. Furthermore, ZnO enhances the acidic active sites on the surface a ZnO-La<sub>2</sub>O<sub>3</sub> catalyst when it is used as a bifunctional catalyst (Yan et al., 2009).

In the current paper, template of SrO-ZnO-Al<sub>2</sub>O<sub>3</sub> heterogeneous catalysts with different Sr:Zn ratios were synthesized via the wet impregnation method, where Zn<sup>2+</sup> O<sup>2-</sup> was chosen as a strong Lewis acid and Sr<sup>2+</sup> O<sup>2-</sup> as a strong Lewis base. The template used was Sr-Zn-Al, which was prepared in the previous chapter. Transesterification and esterification reactions of high-acidity WCO were carried out simultaneously over bifunctional synthesised catalysts with strong acid-base active sites distributed on their surfaces. Various parameters, such as ethanol/WCO molar ratio, catalyst loading in the reaction, and reaction temperature and time, were optimised. Moreover, the bi-functionality of the prepared catalyst was validated by calculating the conversions of the transesterification and esterification reactions separately which, to the best of our knowledge, has not been done before.

### **4.3 Materials and methods**

The catalyst and the reaction conditions were optimised for the production of biodiesel from WCO. To achieve this, a full factorial experimental design was implemented in two stages. Briefly, three catalysts were prepared with Sr:Zn:Al ratios of 65:25:10, 45:45:10 and 25:65:10 mol%. The metal ratio that led to the highest conversion under the targeted reaction conditions was chosen as the best-performing catalyst. This catalyst was then selected for an investigation of the optimum reaction conditions through a full factorial experimental design.

### 4.3.1 Materials

Waste cooking oil was collected from a restaurant in Townsville, Australia. Corn oil, activated neutral Brockmann I alumina oxide  $\text{Al}_2\text{O}_3$ , strontium nitrate  $\text{Sr}(\text{NO}_3)_2$ , zinc nitrate hexahydrate  $\text{Zn}(\text{NO}_3)_2 \cdot 6\text{H}_2\text{O}$ , chloroform-d  $\text{CDCl}_3$ , and ethanol were obtained from Sigma-Aldrich, Australia in analytical grade.

### 4.3.2 Feedstock characterisation

The WCO was filtered using a piece of medical cotton to remove all the solid residues, then used in the reaction without any further purification. The physical and chemical properties of the WCO are presented in Table 4.2. The FFA weight percentage of WCO was quantified via the  $^1\text{H}$  NMR spectrum using Equation (1) (Satyarthi et al., 2009):

$$\text{FFA (wt \%)} = \left( \frac{4 \times \text{area of unmerged peak of } \alpha\text{-CH}_2 \text{ of FFA}}{\text{total area of } \alpha\text{-CH}_2 \text{ of both FFA and ester}} \right) \times 100 \quad (4.1)$$

Where the area of the unmerged peak of  $\alpha\text{-CH}_2$  of FFA is the integration intensities at 2.37 – 2.41 ppm, and the total area of  $\alpha\text{-CH}_2$  of both FFA and ester is the integration intensities at 2.2 – 2.41 ppm.

The average molecular weight (Mwt) of WCO was calculated by Equation (2) (Zhu et al., 2006):

$$\text{Mwt} = \frac{56.1 \times 1000 \times 3}{(SV - AV)} \quad (4.2)$$

Where  $SV$  is the saponification value and  $AV$  is the acid value.

Table 4.2. Physical and chemical properties of the WCO used in this study

Property	Value	Method
FFA content	18 wt.%	Equation (4.1)
Total glycerides	82 wt.%	Material balance
Acid value (AV)	35.4 mg KOH/g oil	ASTM D6751 (Appendix A)
Saponification value (SV)	234.71 mg KOH/g oil	ASTM D5558 (Appendix A)
Molecular weight	844.56 g/gmol	Equation (4.2)
Water content	0.1355 wt.%	ASTM D1744 (Appendix A)
Density	0.916 g/cm <sup>3</sup>	ASTM D1298-99 (Appendix A)

### 4.3.3 Catalyst preparation

The catalysts were prepared according to the procedure shown in Fig. 3.1. Briefly, the required amounts of  $\text{Sr}(\text{NO}_3)_2$  and  $\text{Zn}(\text{NO}_3)_2 \cdot 6\text{H}_2\text{O}$  were dissolved in 100 mL of deionised water, then the required amount of aluminium oxide was added. The mixture was left to evaporate slowly until dry; afterwards, the dry mixture was placed in an oven to dry at 120 °C for 6 h; then calcined at 900 °C for 6 h. A series of catalysts with different Sr/Zn molar ratios (2.6, 1, and 0.4) were denoted as *m*SZA, where *m* represents the molar ratio. It is worth noting that all materials used to prepare the catalysts are readily available and inexpensive. Further, the preparation method is simple and requires no specialist equipment.

#### 4.3.4 Catalyst characterization

The current catalysts have been characterized extensively in Chapter 3; however, two relevant catalyst characteristics determined by XRD and EDS are mentioned here. The powder X-ray diffraction (XRD) analysis was carried out with a Bruker AXS diffractometer, and the phases were identified using the powder diffraction file database (COD, Crystallography Open Database). Scanning electron microscopy (SEM) with a high resolution was used to obtain information about the morphology of the samples. The morphological study of the catalysts was carried out using an SEM (Hitachi SU5000 FE-SEM). Elemental analysis was carried out with an inductively coupled plasma optical emission spectrometer (ICP-OS; Agilent 5100). The samples were dissolved using concentrated HCl. A series of multi-element standard solutions was used to calibrate the instrument. The wavelengths used for quantification were 396.15 nm for aluminium, 215.283 nm for strontium, and 213.857 nm for zinc.

It should also be noted that the bifunctionality of the catalyst has been confirmed experimentally by esterification of oleic acid and transesterification of corn oil in the previous chapter.

#### 4.3.5 Biodiesel production and kinetics study

Various parameters were investigated regarding the performance of a series of bifunctional catalysts on simultaneous esterification-transesterification processes for producing fatty acid ethyl ester (FAEE). The reactions were conducted under different operating conditions: reaction temperatures of 55 – 75 °C, catalyst dosages of 5 – 15 wt.%, ethanol-to-WCO molar ratios of 5:1 – 15:1, and reaction times of 1 – 6 h.

The experiments were conducted in a two-necked 250 mL round reactor equipped with a water-cooled condenser and thermocouple. A desired quantity of SrO-ZnO/Al<sub>2</sub>O<sub>3</sub> catalyst was added to the ethanol; afterwards, the reactant mixture was heated to the required

temperature under an agitation speed of 700 rpm, then WCO was added to start the reaction. At the end of the experiment, the catalyst was separated from the product using a centrifuge at 10,000 rpm for 3 min and the reaction mixture was later loaded into an oil bath at 125 °C to remove the excess ethanol. This is simpler and more efficient compared with rotary evaporation or solvent extraction, with no observable adverse effect on the biodiesel product. Afterwards, the FAEE product was analysed by its <sup>1</sup>H NMR spectrum, with the calibrations were carried out using standard samples of FAEE. FAEE was quantified by Equation (4.3) (Ghesti et al., 2007):

$$(\text{FAEE conversion \%})_{\text{Total}} = \left( \frac{(I_{TAG+EE} - I_{TAG})}{(I_{TAG+EE} + 2I_{TAG})} \right) \times 100 \quad (4.3)$$

Where  $I_{TAG}$  is the integration intensities of the glyceryl methylenic hydrogens (which includes Mono-, Di-, and Tri-glycerids) at 4.25 – 4.35 ppm,  $I_{TAG+EE}$  is the integration intensities of glyceryl methylenic hydrogens and the -OCH<sub>2</sub> of ethoxy hydrogens (methylene groups of ethyl esters) superimposed at 4.1 – 4.2 ppm. More clarification and detail are shown in Fig. S1 (Appendix A).

For the esterification reaction, the conversion of FAEE was determined by calculating the FFA concentrations in the sample at the beginning and end of reaction via Equation (4.4):

$$(\text{FAEE conversion \%})_{\text{FFA}} = \left( \frac{FFA_{\text{Initial}} - FFA_{\text{Final}}}{FFA_{\text{Initial}}} \right) \times 100 \quad (4.4)$$

Where  $(\text{FAEE conversion \%})_{\text{FFA}}$  is the conversion of the esterification reaction. The concentration of FFA was calculated with Equation (4.1).

For the transesterification reaction, the conversion of FAEE was determined by calculating the concentrations of TG in the sample at the beginning and end of the reaction via Equation (4.5):

$$(\text{FAEE conversion \%})_{\text{TG}} = \left( \frac{TG_{\text{Initial}} - TG_{\text{Final}}}{TG_{\text{Initial}}} \right) \times 100 \quad (4.5)$$

Where (FAEE conversion %)<sub>TG</sub> is the conversion of the transesterification reaction. The concentration of TG was calculated by material balance. Determination of TG content in this research depended on the FFA concentration. The WCO contained FFA and a negligible amount of water, hence, the rest in WCO is the TG concentration.

In summary, the total FAEE converted from WCO was calculated by Equation 4.3. The FAEE conversion of the esterification reaction was calculated by Equations 4.1 and 4.4, while the conversion of the transesterification reaction was calculated by Equation 4.5. Both the experiments and <sup>1</sup>H NMR analyses were performed at least twice with the greatest difference being < 3%.

Because the FAEE was produced from WCO via two reactions, it was necessary to study the kinetics of the transesterification and esterification reactions separately with the aim of finding the combined order of FAEE reaction from WCO. In the kinetics study, the order of each reaction was determined at a reaction temperature of 75 °C, then the total order of the reaction was recognized.

## **4.4 Results and discussion**

### **4.4.1 Catalyst characterization**

The powder X-ray diffraction analysis of different Sr:Zn molar ratios after calcining at 900 °C is shown in Figure 3.9a. The analysis identified two different phases of binary oxide (Sr)(Al<sub>2</sub>O<sub>3</sub>), Al<sub>2</sub>O<sub>6</sub>Sr<sub>3</sub> and Al<sub>4</sub>O<sub>7</sub>Sr, and a single phase of ZnO in the zincite form. Several diffraction peaks of Al<sub>2</sub>O<sub>6</sub>Sr<sub>3</sub> and Al<sub>4</sub>O<sub>7</sub>Sr clearly emerged with increasing strontium content, while the ZnO phase remained relatively unchanged for all catalysts. The XRD results are completely compatible with the EDS spectra and elemental mapping, as shown in Fig. 3.11. The EDS analysis shows good distributions of binary oxide (SrO)(Al<sub>2</sub>O<sub>3</sub>) and ZnO, which are shown as yellow and blue colours, respectively.

## 4.4.2 Effects of operating conditions

### 4.4.2.1 Effect of reaction time on conversion

The relationships between conversion and reaction time using catalysts with different Sr:Zn molar ratios are illustrated in Fig. 4.1. The reaction was conducted with a 10:1 ethanol:WCO molar ratio, 15 wt.% catalyst concentration, 75 °C reaction temperature, and reaction times that varied from 1 to 6 h. The FAEE conversion increased from 12.7% to 95.7% with increasing time up to 5 h, then reached the equilibrium state and remained almost constant. The main reason why the reaction reaches equilibrium within 5 h is the presence of a high content of FFAs in the WCO (as explained in Section 3.1.6). Moreover, the reaction conversion increased with increases in the Sr loading. As a result, the 2.6SZA catalyst achieved the highest conversion. Hence, 2.6SZA was selected for further investigation, with 5 h chosen as the best reaction time.

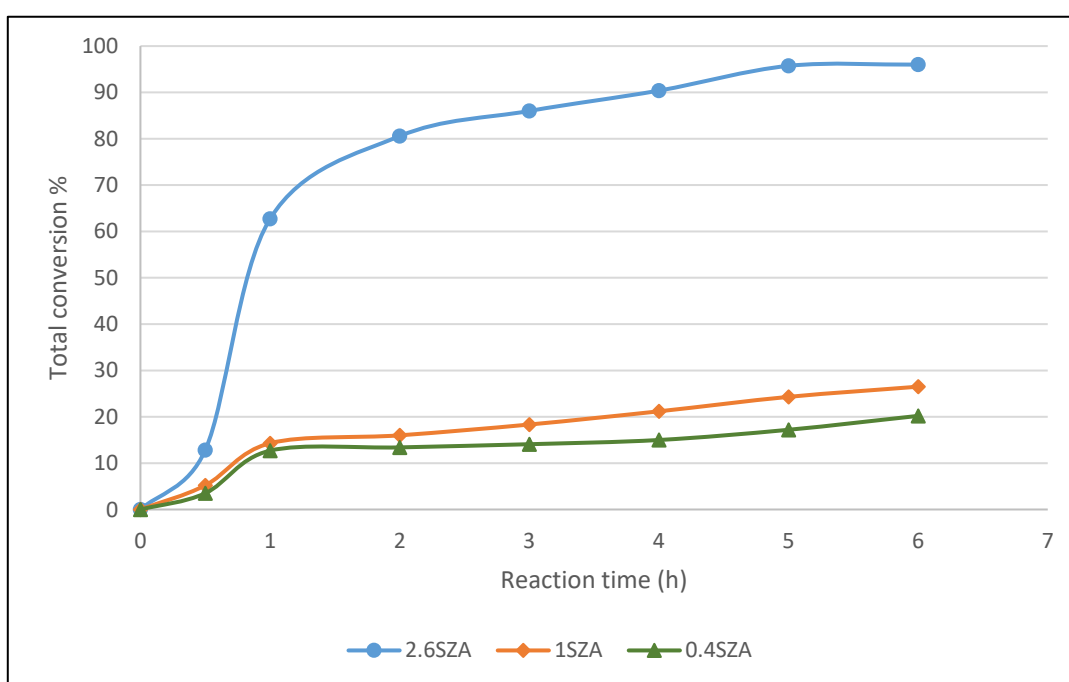


Figure 4-1. Effect of the catalyst metal ratio on conversion during the reaction. Reaction conditions: 10:1 ethanol:WCO molar ratio, 15 wt.%, 75 °C

#### 4.4.2.2 Effect of reaction temperature

The reaction temperature had a significant influence on FAEE conversion. The influence of reaction temperature on WCO conversion was investigated at 55, 65, and 75 °C; while the other parameters were a 10:1 ethanol-to-WCO molar ratio, 15 wt.% catalyst dosage, and 5 h reaction time, as shown in Fig. 4.2. Increasing the reaction temperature from 55 °C to 75 °C increased the reaction conversion from 75% to 95.7% after 5 h of reaction time. Collisions between reactant molecules will increase due to the higher energy input by the temperature increase, which will accelerate the chemical reaction and lead to a higher FAEE conversion (Farooq et al., 2013). Essamlali et al. (2019) reported the same observation. A high temperature could benefit the diffusion of oil that enables more collisions of reactants (ethanol and WCO) over the surface of the heterogeneous catalyst, which accelerates and completes the reaction with high reaction conversion and high diesel production.

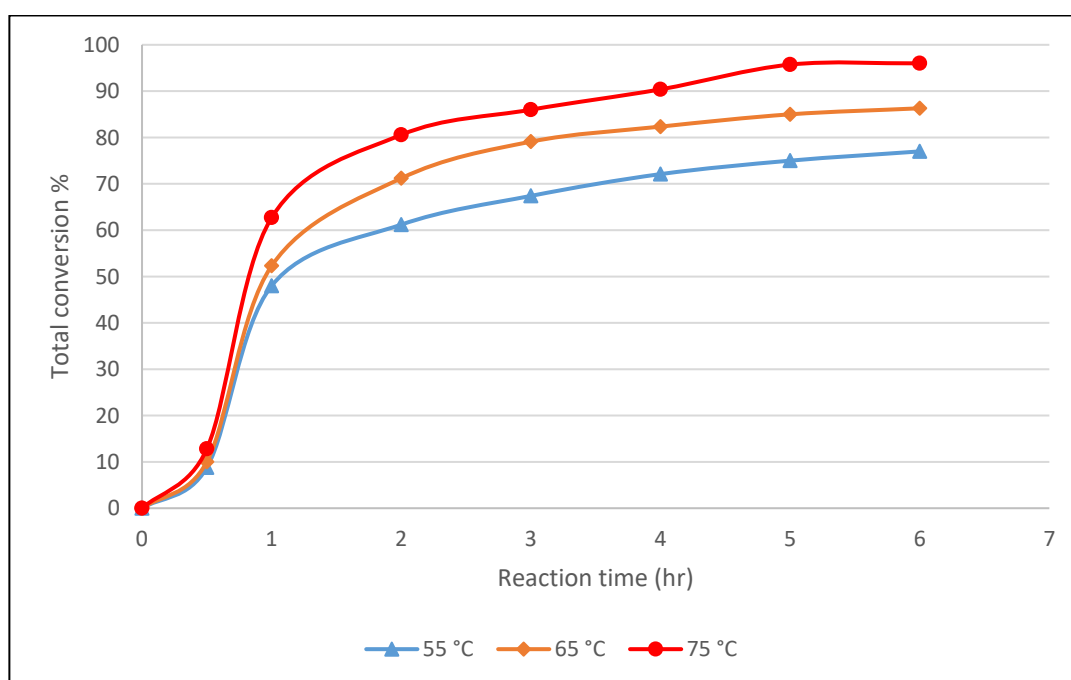


Figure 4-2. Effect of reaction temperature on conversion using the 2.6SZA catalyst. Reaction conditions: 10:1 ethanol:WCO molar ratio, 15 wt.% catalyst, 5 h reaction time.

#### 4.4.2.3 Effect of the ethanol-to-waste cooking oil molar ratio

The effect of the ethanol-to-WCO molar ratio on FAEE production in the presence of catalyst 2.6SZA was investigated at ratios of 5:1 to 15:1 (Fig. 4.3). The reaction was conducted at 75 °C for 5 h with a 15 wt.% catalyst dosage. Increasing FAEE conversion was observed with increasing ethanol loading. The rate of FAEE formation increased from 52.5% to 95.7% with increases in the ethanol-to-WCO ratio of 5:1 to 10:1 (Fig. 4.3). However, further increases in the ratio decreased the conversion to 74.8% as the catalytic activity was inhibited by accumulation of ethanol on the active sites of the catalyst. Also, excessive ethanol can dilute or deactivate a catalyst in such a reaction (Essamlali et al., 2019).

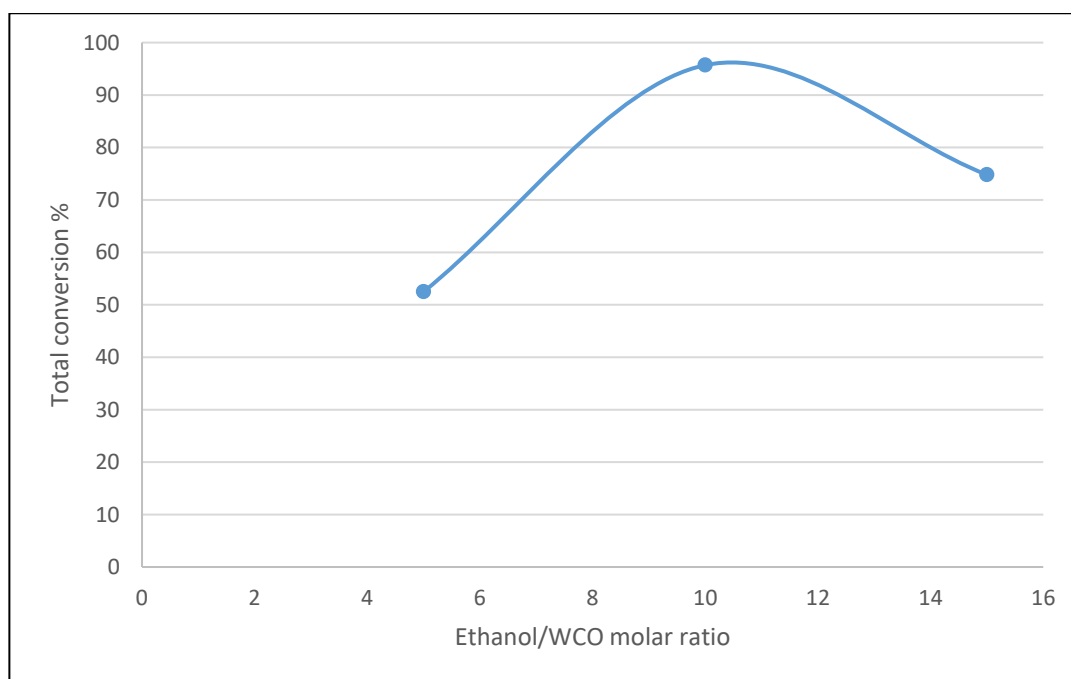


Figure 4-3. Effect of the ethanol/WCO molar ratio on conversion using catalyst 2.6SZA. Reaction conditions: 75 °C, 5 h reaction time, 15 wt.% catalyst.

#### 4.4.2.4 Effect of catalyst loading

The catalyst dosage is one of the important parameters that significantly influenced FAEE conversion during the reaction. The effects of 2.6SZA catalyst loadings of 5 – 15% on FAEE conversion under reaction conditions of 75 °C and a 10:1 ethanol:WCO molar ratio for a 5 h reaction time are presented in Fig. 4.4. The FAEE conversion increased from 9.3% to 95.7% with increases in catalyst loading from 5 wt.% to 15 wt.% because of the increase in the total number of active sites available in the reaction (Alhassan et al., 2015). The significant increase in conversion shows that FAEE production strongly depends on the catalyst dosage (Alhassan et al., 2015).

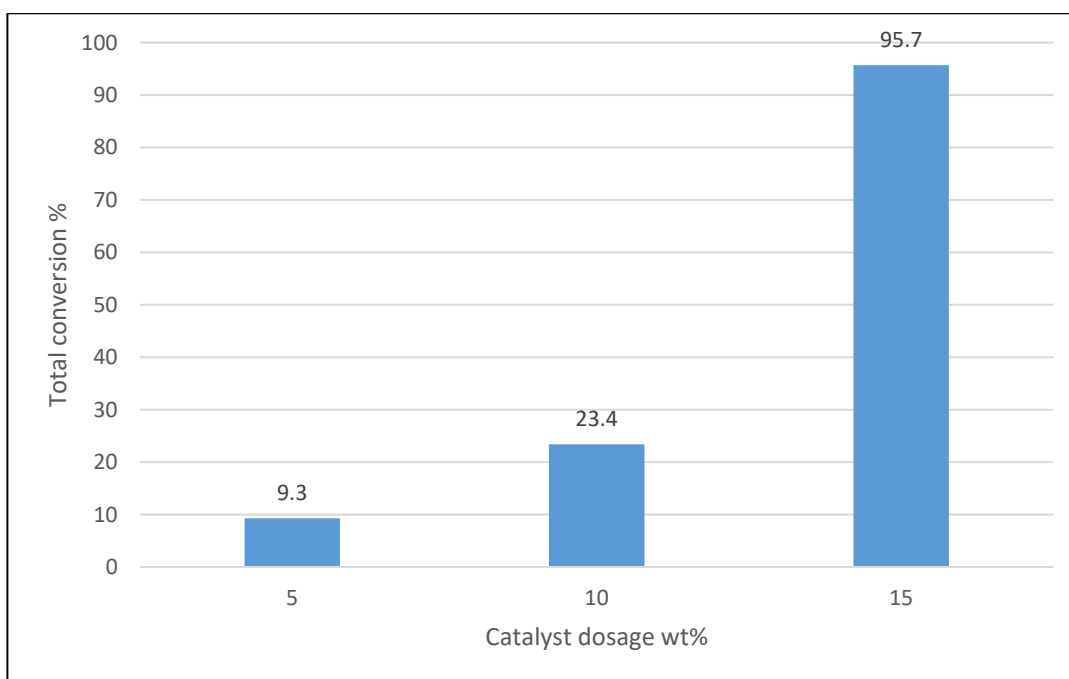


Figure 4-4. Effect of 2.6SZA catalyst loading on conversion. Reaction conditions: 75 °C, 5 h reaction time, 10:1 ethanol:WCO molar ratio.

#### 4.4.2.5 Catalyst activity in simultaneous transesterification and esterification reactions

The catalyst showed high catalytic activity with the TG and FFA in the WCO. The optimal operating conditions for FAEE production using catalyst 2.6SZA were 15% catalyst, an ethanol/WCO molar ratio of 10:1, reaction temperature of 75 °C, and 5 h reaction time, which resulted in FAEE conversion of 95.7%. The bifunctional catalytic activities of the catalyst used in the current research on the transesterification and esterification reactions can be evaluated by separately determining the conversion of each reaction. Because the WCO contained two sources of FAEE production, which were FFA (18 wt.%) and TG (82 wt.%), it is useful to calculate the FAEE conversion of each reaction.

The FFA content of the WCO during the 5 h reaction decreased from 18 wt.% to 4 wt.%, while the concentration of TG declined from 82 wt.% to 0.5 wt.% (Fig. 4.5). The reaction conversions of transesterification and esterification were 99.4% and 77.8 %, respectively. The result indicates that the catalyst used in this study has a high tolerance for FFA and provides high TG conversion. The <sup>1</sup>H NMR spectrum of the final product clearly shows that most of the TG content in the WCO was converted, with the disappearance of the TG peak at 4.25 – 4.35 ppm (Fig. 4.6).

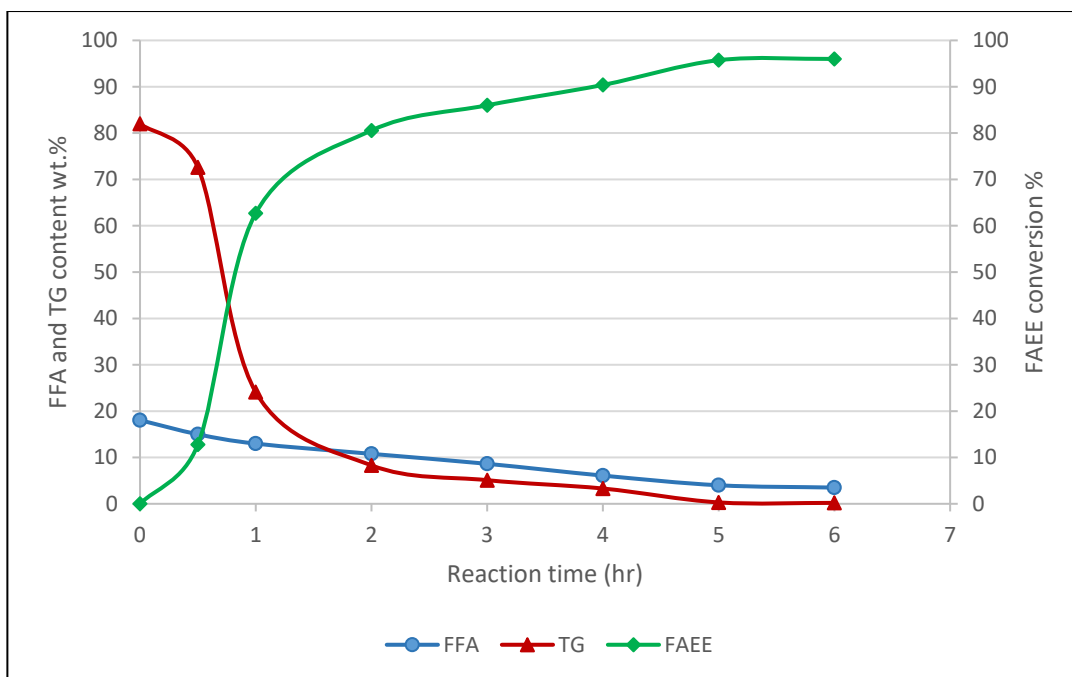


Figure 4-5. FAEE conversion and FFA and TG contents as a function of time. Reaction conditions: 15% catalyst, 10:1 ethanol:WCO molar ratio, 75 °C reaction temperature.

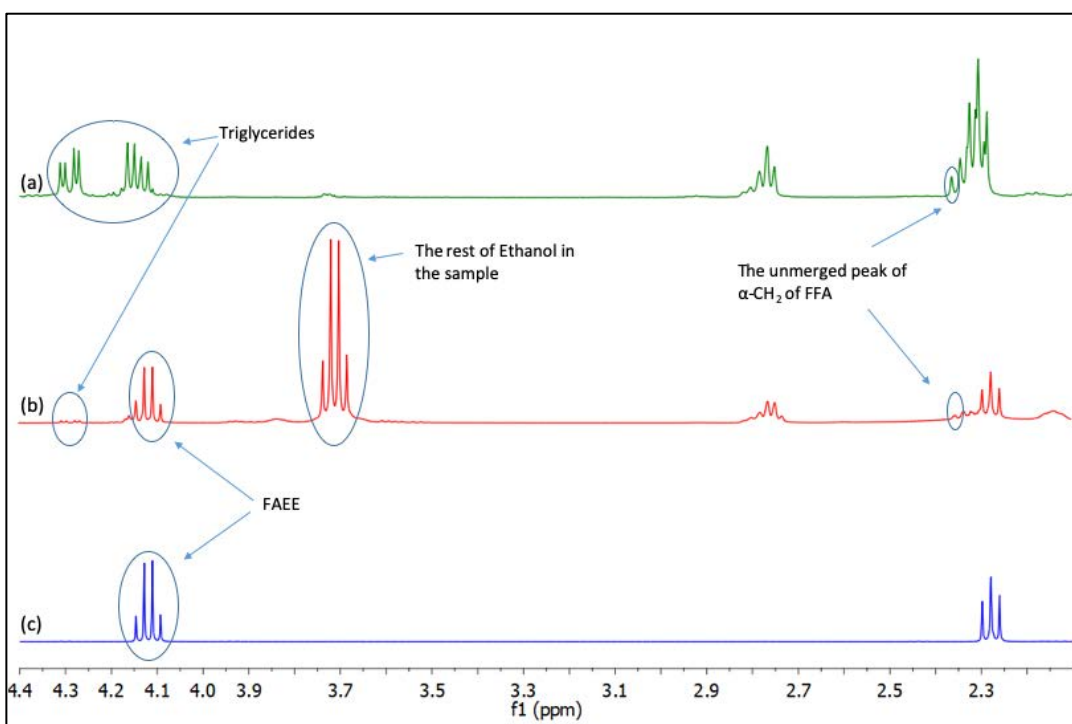


Figure 4-6.  $^1\text{H}$  NMR spectra of the esterification reaction: (a) WCO; (b) final product after reaction and (c) standard ethyl ester for comparison

A comparison of the performance of published catalyst activities with that of the present research in terms of one-step FAEE production from WCO is presented in Table 4.3. Two catalysts achieved greater conversion or yield than the current catalyst. Kaur et al. (2018) reported a W/Ti/SiO<sub>2</sub> catalyst that achieved > 98% conversion with WCO containing 6.8 wt.% FFA. Correspondingly, Borah et al. (2019) reported a Zn/CaO catalyst that achieved 96.74% conversion with WCO containing 0.84 wt.% FFA. However, the WCO used in their studies had FFA contents of 6.8 wt.% and 0.84 wt.%, which is much less than that used in the current research (18 wt.%). This finding indicates that the SrO-ZnO/Al<sub>2</sub>O<sub>3</sub> catalyst achieved high conversion despite a high content of FFA in the WCO due to its bifunctionality.

Table 4.3. Comparison of the studied SrO-ZnO/Al<sub>2</sub>O<sub>3</sub> catalyst with previous catalysts

Catalyst	FFA (wt. %)	Reaction temperature (°C)	Reaction time (h)	Conversion or Yield (%)	Reference
[CTA]MCM-41	1.1	80	3	93	Pirouzmand et al. (2018)
Zn/CaO	0.84	86	4	96.74	Borah et al.(2019)
CaO	1.0	65	5	90	(Maneerung et al. (2016)
W/Ti/SiO <sub>2</sub>	6.8	65	4	> 98	Kaur et al. (2018)
C-SO <sub>3</sub> H	3.9	60	3	95	Nata et al. (2017)
Li/TiO <sub>2</sub>	1.85	55	3	91.73	Alsharifi et al. (2017)
SrO-ZnO/Al <sub>2</sub> O <sub>3</sub>	18	75	5	95.7	Current study

#### 4.4.2.6 Effect of free fatty acid content

The effect of FFA content on reaction time using two feedstocks with different FFA contents, WCO (18 wt.% FFA) and corn oil (0.2 wt.% FFA), is shown in Fig. 4.7. The reaction was carried out at a 10:1 ethanol:WCO molar ratio, 15 wt.% catalyst loading, and 75 °C reaction temperature. Pure corn oil was transesterified and achieved a conversion of 98.5% within 2 h of reaction, while WCO took 5 h to achieve 95.7% conversion. This is interpreted as the acid-catalysed esterification reaction taking a different chemical pathway from base-catalysed transesterification (Kondamudi et al., 2011). The presence of a carboxylic acid group in FFA, which has higher polarity than triglyceride, could cause the partial blockage of catalyst active sites because of its ability to react irreversibly with such sites on the catalyst surface (Kaur et al., 2018). Also, a high FFA content causes soap formation due to strontium leaching, leading to reduced catalyst activity (Roschat et al., 2016).

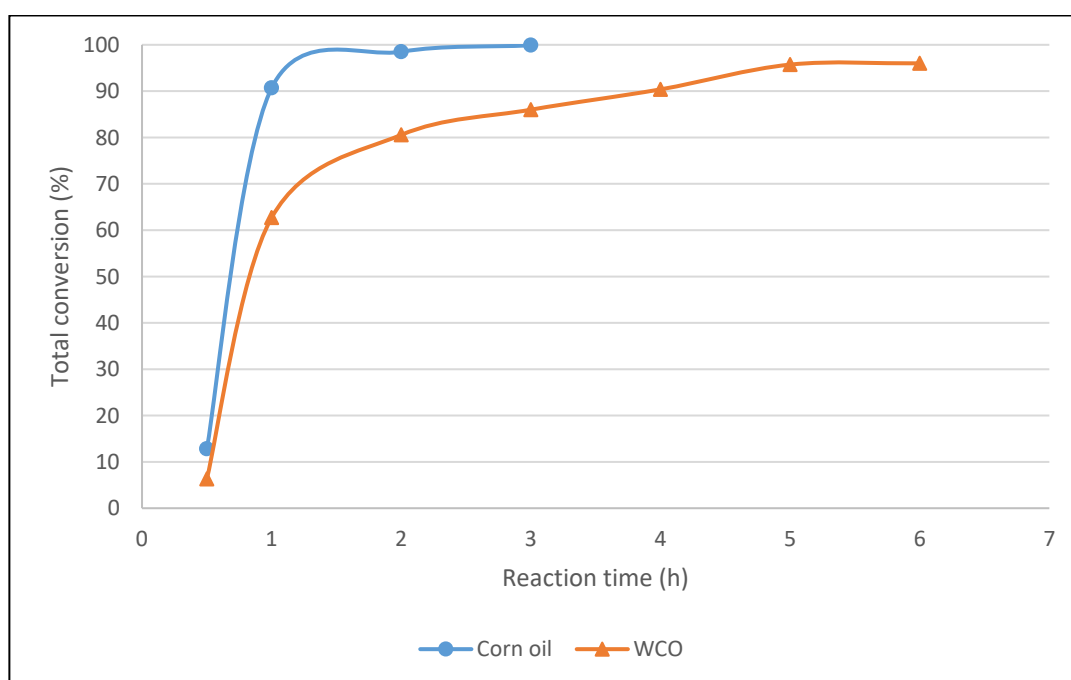
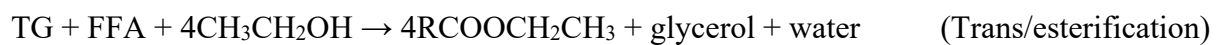
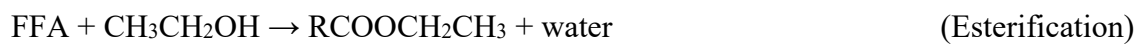
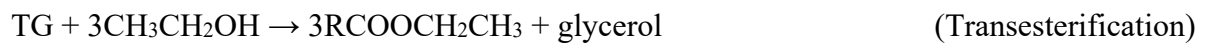


Figure 4-7. Conversion with reaction time with two feedstocks with different FFA contents (waste vegetable oil, WCO = 18% and corn oil = 0.05%)

#### 4.4.3 Kinetic study

For the study of the reaction kinetics, the following assumptions were made. (1) The reaction is carried forward because of using excessive amounts of ethanol. (2) The mass transfer limitation is negligible due to perfect mixing between the reactants and products in the reactor. (3) Transesterification and esterification reactions are both described with pseudo-first-order models with respect to TG and FFA, as reported in previous studies (Al-Sharifi et al., 2019; Fauzi et al., 2014). The aim of the kinetic study was to determine the rate of FAEE formation from the transesterification and esterification of WCO. Each process was investigated separately at a reaction temperature of 75 °C and reaction times of 30 min to 5 h.

The overall reaction of WCO from FFA and TG can be written as:



The pseudo-first-order model of the transesterification reaction is:

$$r_1 = \frac{d[\text{TG}]}{dt} = -k_1[\text{TG}]$$

Integration of the above equation from 0 to  $t$  and  $[\text{TG}]_0$  to  $[\text{TG}]$  for time and triglyceride concentration, respectively, yields:

$$\ln[\text{TG}] = -k_1 t + \ln[\text{TG}]_0$$

$$\ln \frac{[\text{TG}]_0}{[\text{TG}]} = -k_1 t \quad (4.6)$$

For the pseudo-first-order model of esterification reaction:

$$r_2 = \frac{d[\text{FFA}]}{dt} = -k_2[\text{FFA}]$$

Integration of the above equation from 0 to  $t$  and  $[\text{FFA}]_0$  to  $[\text{FFA}]$  for time and triglyceride concentration, respectively, yields:

$$\ln[FFA] = -k_2 t + \ln[FFA]_0$$

$$\ln \frac{[FFA]_0}{[FFA]} = -k_2 t \quad (4.7)$$

Where  $r_1$  and  $r_2$  are the reaction rate (mol.L<sup>-1</sup>.h<sup>-1</sup>), and  $k_1$  and  $k_2$  the reaction rate constants (h<sup>-1</sup>) of the transesterification and esterification reactions, respectively.

The rate constants  $k_1$  and  $k_2$  can be obtained by plotting  $\ln \frac{[TG]_0}{[TG]}$  in Equation (4.8) or  $\ln \frac{[FFA]_0}{[FFA]}$  in Equation (4.9) against time ( $t$ ); respectively, where the slope of the linear equation represents  $k$ .

The fitting of the kinetic first-order models of the transesterification and esterification reactions took into account all data points obtained from 30 min to 5 h. The high  $R^2$  values demonstrate the adequacy of the models. Regressions of the experimental results for transesterification and esterification are shown in Figs. S2 (a) and (b), respectively (Appendix A). The reaction rate constants for the transesterification and esterification reactions are 0.9537 h<sup>-1</sup> and 0.2816 h<sup>-1</sup>, with the  $R^2$  values of the models being 0.9437 and 0.974, respectively. The good fits confirm that both pseudo-first-order models have excellent agreement with experimental data. The Arrhenius equation was applied to calculate the activation energy, as shown below:

$$k = A e^{-E_a/RT} \quad (4.8)$$

By simplifying the equation:

$$\ln k = -\frac{E_a}{RT} + \ln A \quad (4.9)$$

Where  $E_a$  is the activation energy (kJ/mol),  $R$  is the universal gas constant (8.314 J mol<sup>-1</sup> K<sup>-1</sup>),  $k$  is the reaction rate constant (min<sup>-1</sup>),  $A$  is a frequency factor (min<sup>-1</sup>), and  $T$  is the reaction temperature (K). The activation energy ( $E_a$ ) was obtained by plotting  $\ln(k)$  against the reciprocal of temperature ( $1/T$ ), where the slope of the linear equation represents ( $-E_a/R$ ), and the intercept represents  $A$ , as shown in Fig. S3 (Appendix A).

From Fig. S3, the activation energies for the transesterification and esterification reactions using the ZnO-SrO/Al<sub>2</sub>O<sub>3</sub> catalyst were found to be 53.03 kJ/mol and 21.74 kJ/mol, respectively. This suggests that the rate of the transesterification reaction increases more quickly than that of esterification with increasing temperature.

The values of  $k_1$  and  $k_2$  suggest that transesterification of TG occurs faster than esterification of FFA. However, with WCOs that contain both FFA and TG, transesterification and esterification reactions take place in parallel, with little interaction between them. As a result, the FFA content in the feedstock significantly influences the overall reaction time (as discussed in Section 3.2.6).

#### **4.4.4 Reusability of catalyst**

The synthesised SrO-ZnO/Al<sub>2</sub>O<sub>3</sub> catalyst was reused for (trans)esterification reaction under the best operating conditions. The catalyst was collected after reaction and washed with n-hexane three times and methanol to remove any oil and glycerol residue, then dried overnight at 120 °C before reuse in the next experiment. The catalytic activity of the recovered catalyst provided only 19% conversion, which is much less than that over fresh catalyst. This finding indicates that the catalyst synthesized in the current research was significantly deactivated and unable to be used again immediately after the reaction. Furthermore, the metal molar ratio of the catalyst recovered after the reaction was characterized by ICP-OS analysis, as shown in Table 4.4. The results indicate that, with a reduction in the weight percentage, there was significant leaching of strontium after its use in the reaction. There is also some loss of zinc as the Zn to Al ratio is much lower after (6.95) than before reaction (9.07). This reduced the catalytic efficiency of the catalyst, as the amount of strontium directly influences its effectiveness, as shown in Fig. 4.1 and reported by others (Yang et al., 2007).

Table 4.4. ICP-OS analysis of 2.6SZA catalysts before and after use in reaction

Metal	Theoretical amount (wt.%)	Experimental amount before reaction (wt.%)	Experimental amount after reaction (wt.%)
Sr	74.9	70.8	55.5
Zn	21.5	26.3	38.9
Al	3.6	2.9	5.6
Total	100	100	100

Two methods were used to regenerate the used catalyst. Firstly, after being washed and dried, the used catalyst was calcined at 900 °C to remove any organic material on the active sites. However, its conversion was still low. Secondly, used catalyst was immersed in the same solution of precursors described in the experimental section, which is the same method reported by Yang et al. (2007). The results suggest that immersion improved the stability of the catalyst with only a slight decrease in FAEE conversion after two recycles, as shown in Fig. 4.8. In future, different catalyst preparation methods, such as sol-gel or ion exchange, which are expected to decrease the leaching of Sr, should be investigated for further improvement of the reusability or durability of these catalysts (Salinas et al., 2018; Rattanaphra et al., 2019; Jalilnejad Falizi et al., 2019).

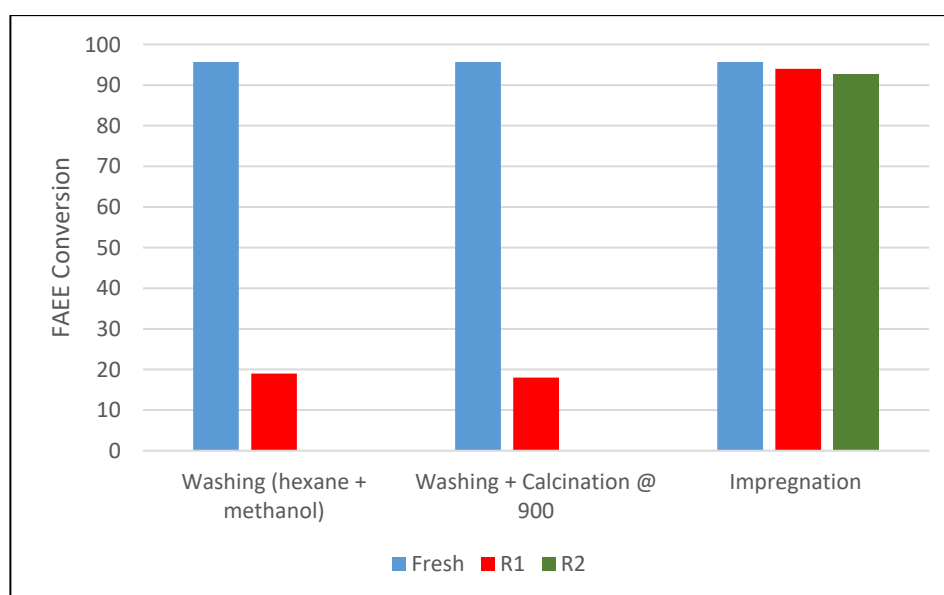


Figure 4-8. Catalyst recycling activity with different methods

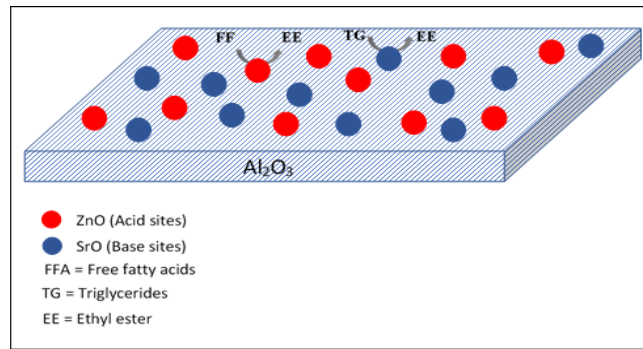
#### 4.4.5 Mechanism of reaction

Reaction mechanisms for trans/esterification reactions over their respective catalysts have been proposed and largely accepted (Wan Omar et al., 2011; Yan et al., 2009). Since little interaction was observed on the production of FAEE from WCO using the bifunctional catalyst, trans/esterification reaction mechanisms that occur on the surface of the bifunctional catalyst are proposed and are illustrated in Fig. 4.9a.

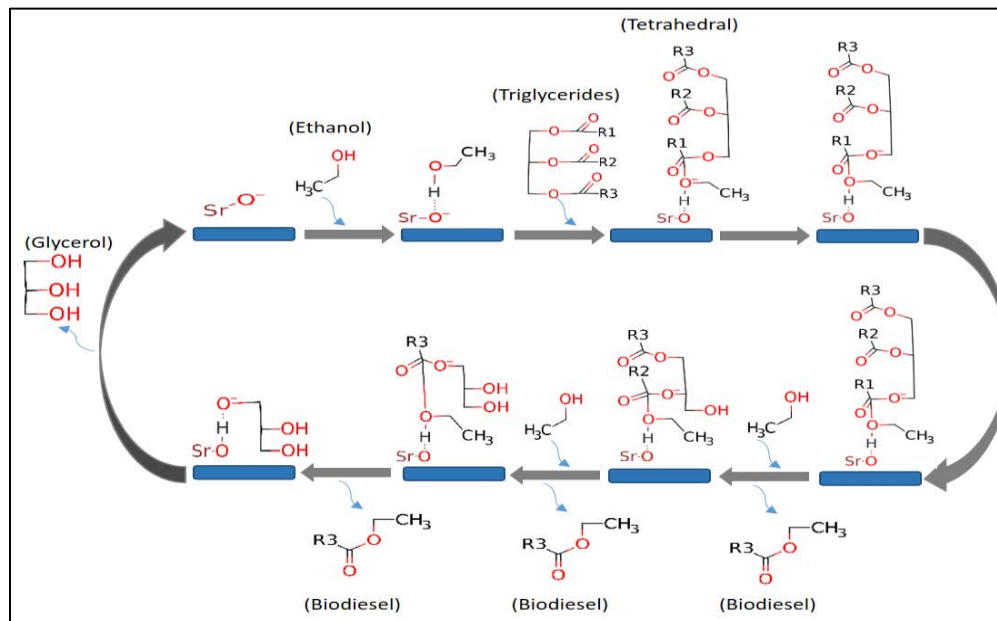
For the transesterification reaction, the Lewis base sites (strontium oxide) produce a reactive nucleophile (ethoxide anion) by absorption of ethanol. The reactive nucleophile of ethanol reacts with the electrophilic carbonyl carbon of the triglyceride to form a tetrahedral intermediate. The reaction extends to di- and triglycerides, then esters are formed by breaking the hydroxyl group, as shown in Fig. 4.9b.

For the esterification reaction, oleic acid and ethanol are absorbed on the Lewis acid sites (zinc oxide). The interaction of the Lewis acidic sites of the catalyst with the carbonyl oxygens of the fatty acid forms the carbocation. A tetrahedral intermediate is produced by attacking the nucleophilic of alcohol to the carbocation. Further, one mole of ester forms after eliminating H<sub>2</sub>O, as shown in Fig. 4.9c.

(a)



(b)



(c)

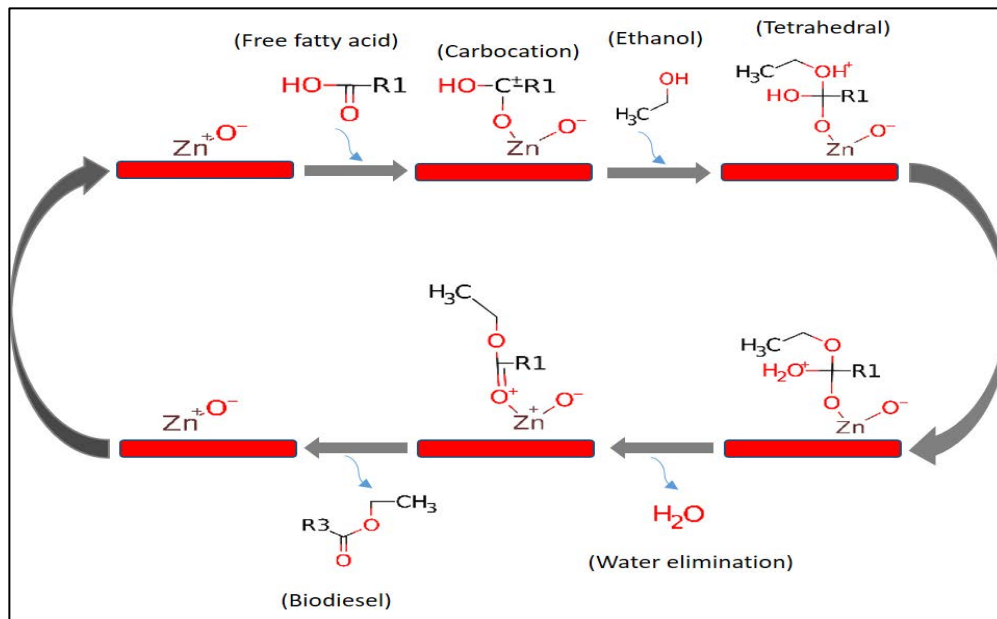


Figure 4-9. Schematic illustrations of (a) an overview of the suggested reaction mechanism, (b) a possible mechanism for transesterification of TG with ethanol, and (c) a possible mechanism for esterification of FFA with ethanol

## 4.5 Conclusion

The production of FAEE from waste cooking oil was investigated using a range of bifunctional strontium-zinc-aluminium mixed oxides. There was a high interaction between the Sr, Al and Zn metal oxides, with catalyst 2.6SZA showing the highest activity. The optimum conditions were found to be a 75 °C reaction temperature, 10:1 ethanol-to-WCO molar ratio, 15 wt.% catalyst loading, and 5 h reaction time. The catalysts showed high catalytic activity in both esterification and transesterification reactions and were highly tolerant to FFA. The strontium-aluminium and zinc oxide distribution provided acid-base active sites on the surface of the catalyst. Consequently, the capability of the catalyst in simultaneous transesterification and esterification reactions was enhanced. The results confirm the potential to produce FAEE from high-FFA WCOs using a mixed-metal oxide of strontium, aluminium and zinc as a bifunctional catalyst. Using relatively inexpensive catalysts such as this is expected to significantly decrease the production cost of FAEE. A major drawback of the synthesized catalyst was that its deactivation was significant and reactivation was required after each use.

## Chapter 5: Conclusions and recommendations

### 5.1 Conclusions

This research aimed to develop a bifunctional catalyst that can catalyse reactions with feedstock containing high acidic oils for biodiesel production. Based on the results obtained from the current research, the following conclusions can be reached.

In the first part of the study, a series of SrO-ZnO/Al<sub>2</sub>O<sub>3</sub> novel bifunctional heterogeneous catalysts with different metal molar ratios were synthesized by a wet impregnation method and calcined at different temperatures. Among the synthesized catalysts, the one with a metal molar ratio Sr:Zn of 2.6:1 and calcined at 900 °C temperature (2.6SZA900) exhibited the best overall catalytic activity in transesterification and esterification reactions, and was able to work under moderate operating conditions. The effectiveness of the bifunctionality of catalyst 2.6SZA900 was demonstrated separately using two types of oils. Oleic acid (representing free fatty acid source) and corn oil (representing triglycerides source) were used for esterification and transesterification reactions for biodiesel production, respectively. It was found that the best operating conditions for transesterification reaction, which achieved 95.1% conversion, were a 10:1 ethanol-to-corn oil molar ratio, 10 wt% catalyst loading, 3 h reaction time and 70 °C reaction temperature. The best operating conditions for esterification reaction, which achieved 71.4% biodiesel conversion, were a 5:1 ethanol-to-oleic acid molar ratio, 10 wt% catalyst loading, 6 h reaction time and 70 °C reaction temperature.

In the second part of the study, the ability of catalyst 2.6SZA900 to catalyze both esterification and transesterification reactions simultaneously was proven with the successful production of biodiesel using high-acidity waste cooking oil as the feedstock. The best operating conditions for the reactions, which achieved 95.7% conversion, were a 10:1 ethanol-

to-oleic acid molar ratio, 15 wt% catalyst loading, 5 h reaction time and 75 °C reaction temperature. The catalyst showed high catalytic activity in both esterification and transesterification reactions and was highly tolerant to free fatty acids.

An in-depth study on the mechanisms of trans/esterification reactions over the SrO-ZnO/Al<sub>2</sub>O<sub>3</sub> bifunctional catalysts was also conducted that provided more insights into the reaction pathway and the functions of the metal oxides. It revealed that base and acid active sites were represented by SrO and ZnO on the surface of the catalyst particles, respectively. The study also determined that the main cause for deactivation was the leaching of strontium. Reactivation of the catalyst could be achieved with a simple immersion of the deactivated catalyst in the same impregnation solution used in the synthesis process.

In summary, catalysts consisted of strontium-aluminium-zinc oxides were proven to be capable of catalyzing simultaneous transesterification and esterification reactions under moderate reaction conditions. The optimized catalyst of this type was shown to be able to produce biodiesel from waste cooking oils containing high content of free fatty acids. It has the potential to be applied at the industrial scale for biodiesel production. The fact that this type of catalysts were relatively inexpensive, and that it could utilize a waste stream as the feedstock, suggests that it has the potential to significantly reduce the production costs of biodiesel.

## **5.2 Future work**

The research conducted in this study has highlighted several areas where further investigations are required to improve the application of the catalysts at an industrial scale.

The most significant drawback of the prepared catalysts in this study is their rapid deactivation due to leaching. One of the futile areas for future work is to improve the longevity of the catalysts by using different preparation methods such as sol-gel and ion-exchange. In

fact, any methods that can reduce the leaching of the active component, in this thesis, strontium, would significantly alleviate the deactivation process and improve the durability of the catalyst.

The focus of this research was on the synthesis of effective catalyst component. Little attention was paid to the specific surface area of the catalysts synthesized. Consequently, the specific surface area of the catalysts synthesized and tested in this study was low compared to that of those used in industry. A higher specific surface area of the catalyst is expected to substantially enhance the catalytic activity of the catalyst.

The thesis work only synthesized and tested one series of bifunctional catalysts consisting of metals of acidic and alkaline in their innate chemical properties, namely, zinc and strontium on alumina. It demonstrated that this type of bifunctional catalysts are able to simultaneously and efficiently catalyze esterification and transesterification reactions, and therefore produce biodiesel from feedstock that contain high levels of free fatty acids. It would be interesting and of practical relevance to develop new bifunctional heterogeneous catalysts using different metal oxides that possess acid-base properties.

## Bibliography

- Aca-Aca, G., Loría-Bastarrachea, M. I., Ruiz-Treviño, F. A., & Aguilar-Vega, M. (2018). Transesterification of soybean oil by PAAc catalytic membrane: Sorption properties and reactive performance for biodiesel production. *Renewable Energy*, 116, 250-257. doi:10.1016/j.renene.2017.09.042
- Al-Dawody, M. F., & Bhatti, S. K. (2014). Experimental and computational investigations for combustion, performance and emission parameters of a diesel engine fueled with soybean biodiesel-diesel blends. *Energy Procedia*, 52, 421-430. doi:10.1016/j.egypro.2014.07.094
- Alcañiz-Monge, J., Bakkali, B. E., Trautwein, G., & Reinoso, S. (2018). Zirconia-supported tungstophosphoric heteropolyacid as heterogeneous acid catalyst for biodiesel production. *Applied Catalysis B: Environmental*, 224, 194-203. doi:10.1016/j.apcatb.2017.10.066
- Alhassan, F. H., Rashid, U., & Taufiq-Yap, Y. H. (2015). Synthesis of waste cooking oil-based biodiesel via effectual recyclable bi-functional Fe<sub>2</sub>O<sub>3</sub>MnOSO<sub>4</sub>·2H<sub>2</sub>O/ZrO<sub>2</sub> nanoparticle solid catalyst. *Fuel*, 142, 38-45. doi:10.1016/j.fuel.2014.10.038
- Al-Sharifi, M., & Znad, H. (2019). Development of a lithium based chicken bone (Li-Cb) composite as an efficient catalyst for biodiesel production. *Renewable Energy*, 136, 856-864. doi:10.1016/j.renene.2019.01.052
- Al-Sharifi, M., Znad, H., Hena, S., & Ang, M. (2017). Biodiesel production from canola oil using novel Li/TiO<sub>2</sub> as a heterogeneous catalyst prepared via impregnation method. *Renewable Energy*, 114, 1077-1089. doi:10.1016/j.renene.2017.07.117
- Alves, C. T., de Oliveira, A. S., Carneiro, S. A. V., Santos, R. C. D., Melo, S. A. B. V. d., Andrade, H. M. C., . . . Torres, E. A. (2012). Transesterification of waste frying oils using ZnAl<sub>2</sub>O<sub>4</sub> as heterogeneous catalyst. *Procedia Engineering*, 42, 1928-1945. doi:10.1016/j.proeng.2012.07.589
- Amani, H., Ahmad, Z., Asif, M., & Hameed, B. H. (2014). Transesterification of waste cooking palm oil by MnZr with supported alumina as a potential heterogeneous catalyst. *Journal of Industrial and Engineering Chemistry*, 20(6), 4437-4442. doi:10.1016/j.jiec.2014.02.012
- Atabani, A. E., Silitonga, A. S., Badruddin, I. A., Mahlia, T. M. I., Masjuki, H. H., & Mekhilef, S. (2012). A comprehensive review on biodiesel as an alternative energy resource and its characteristics. *Renewable and Sustainable Energy Reviews*, 16(4), 2070-2093. doi:10.1016/j.rser.2012.01.003
- Atadashi, I. M., Aroua, M. K., Abdul Aziz, A. R., & Sulaiman, N. M. N. (2013). The effects of catalysts in biodiesel production: A review. *Journal of Industrial and Engineering Chemistry*, 19(1), 14-26. doi:10.1016/j.jiec.2012.07.009
- Azevêdo, S., Santos, Ê., Medeiros, A., Jesus, A., Oliveira, H., & Sousa, E. (2018). Evaluation of the use of *Gossypium hirsutum* oil and supercritical ethanol for the production of ethyl

- esters in non-catalytic process. *The Canadian Journal of Chemical Engineering*, 96(3), 651-658. doi:10.1002/cjce.22950
- B. He, B., P. Singh, A., & C. Thompson, J. (2005). Experimental optimization of a continuous-flow reactive distillation reactor for biodiesel production. *Transactions of the ASAE*, 48(6), 2237-2243. doi:https://doi.org/10.13031/2013.20071
- Balat, M. (2011). Potential alternatives to edible oils for biodiesel production: A review of current work. *Energy Conversion and Management*, 52(2), 1479-1492. doi:10.1016/j.enconman.2010.10.011
- Bancquart, S., Vanhove, C., Pouilloux, Y., & Barrault, J. (2001). Glycerol transesterification with methyl stearate over solid basic catalysts I. Relationship between activity and basicity. *Applied Catalysis a-General*, 218(1-2), 1-11. doi:Doi 10.1016/S0926-860x(01)00579-8
- Baskar, G., & Aiswarya, R. (2016). Trends in catalytic production of biodiesel from various feedstocks. *Renewable and Sustainable Energy Reviews*, 57, 496-504. doi:10.1016/j.rser.2015.12.101
- Bharathiraja, B., Chakravarthy, M., Kumar, R. R., Yuvaraj, D., Jayamuthunagai, J., Kumar, R. P., & Palani, S. (2014). Biodiesel production using chemical and biological methods: A review of process, catalyst, acyl acceptor, source and process variables. *Renewable and Sustainable Energy Reviews*, 38, 368-382. doi:10.1016/j.rser.2014.05.084
- Bildea, C. S., & Kiss, A. A. (2011). Dynamics and control of a biodiesel process by reactive absorption. *Chemical Engineering Research and Design*, 89(2), 187-196. doi:10.1016/j.cherd.2010.05.007
- Boonyuen, S., Smith, S. M., Malaithong, M., Prokaew, A., Cherdhirunkorn, B., & Luengnaruemitchai, A. (2018). Biodiesel production by a renewable catalyst from calcined Turbo jourdani (Gastropoda: Turbinidae) shells. *Journal of Cleaner Production*, 177, 925-929. doi:10.1016/j.jclepro.2017.10.137
- Borah, M. J., Das, A., Das, V., Bhuyan, N., & Deka, D. (2019). Transesterification of waste cooking oil for biodiesel production catalyzed by Zn substituted waste egg shell derived CaO nanocatalyst. *Fuel*, 242, 345-354. doi:10.1016/j.fuel.2019.01.060
- Borges, M. E., & Díaz, L. (2012). Recent developments on heterogeneous catalysts for biodiesel production by oil esterification and transesterification reactions: A review. *Renewable and Sustainable Energy Reviews*, 16(5), 2839-2849. doi:10.1016/j.rser.2012.01.071
- Kusumaningtyas, R. D., Budiman A., Sutijan, Purwono, S., Sawitri, D. R. (2009). Design of Reactive Distillation Process for Sustainable Biodiesel Production from Palm Oil. Paper Presented at the World Congress on Oils and Fats & 28th ISF Congress 27-30 September 2009. Sydney – Australia.
- Abdurakhman, B. Y., Adi Putra, Z., Bilad, M. R., Nordin, N. A. H., & Wirzal, M. D. H. (2018). Techno-economic analysis of biodiesel production process from waste cooking oil using catalytic membrane reactor and realistic feed composition. *Chemical Engineering Research and Design*, 134, 564-574. doi:10.1016/j.cherd.2018.04.044

- Campanati, M., Fornasari, G., & Vaccari, A. (2003). Fundamentals in the preparation of heterogeneous catalysts. *Catalysis Today*, 77(4), 299-314. doi:10.1016/s0920-5861(02)00375-9
- Canakci, M., & Van Gerpen, J. (1999). Biodiesel production via acid catalysis. *Transactions of the American Society of Agricultural Engineers*, 42(5), 1203-1210.
- Cannilla, C., Bonura, G., Costa, F., & Frusteri, F. (2018). Biofuels production by esterification of oleic acid with ethanol using a membrane assisted reactor in vapour permeation configuration. *Applied Catalysis A: General*, 566, 121-129. doi:10.1016/j.apcata.2018.08.014
- Cannilla, C., Bonura, G., Rombi, E., Arena, F., & Frusteri, F. (2010). Highly effective MnCeOx catalysts for biodiesel production by transesterification of vegetable oils with methanol. *Applied Catalysis A: General*, 382(2), 158-166. doi:10.1016/j.apcata.2010.04.031
- Carrero, A., Vicente, G., Rodríguez, R., Linares, M., & del Peso, G. L. (2011). Hierarchical zeolites as catalysts for biodiesel production from *Nannochloropsis* microalga oil. *Catalysis Today*, 167(1), 148-153. doi:10.1016/j.cattod.2010.11.058
- Carvalho, A. K. F., da Conceição, L. R. V., Silva, J. P. V., Perez, V. H., & de Castro, H. F. (2017). Biodiesel production from *Mucor circinelloides* using ethanol and heteropolyacid in one and two-step transesterification. *Fuel*, 202, 503-511. doi:10.1016/j.fuel.2017.04.063
- Chang, F., Zhou, Q., Pan, H., Liu, X.-F., Zhang, H., Xue, W., & Yang, S. (2014). Solid mixed-metal-oxide catalysts for biodiesel production: A review. *Energy Technology*, 2(11), 865-873. doi:10.1002/ente.201402089
- Chen, C. L., Huang, C. C., Tran, D. T., & Chang, J. S. (2012). Biodiesel synthesis via heterogeneous catalysis using modified strontium oxides as the catalysts. *Bioresource Technology* 113, 8-13. doi:10.1016/j.biortech.2011.12.142
- Chisti, Y. (2007). Biodiesel from microalgae. *Biotechnology Advances*, 25(3), 294-306. doi:10.1016/j.biotechadv.2007.02.001
- Chisti, Y. (2008). Biodiesel from microalgae beats bioethanol. *Trends in Biotechnology*, 26(3), 126-131. doi:10.1016/j.tibtech.2007.12.002
- Chroma, M., Pinkas, J., Pakutinskiene, I., Beganskiene, A., & Kareiva, A. (2005). Processing and characterization of sol-gel fabricated mixed metal aluminates. *Ceramics International*, 31(8), 1123-1130. doi:10.1016/j.ceramint.2004.11.012
- Correia, L. M., Campelo, N. d. S., Albuquerque, R. d. F., Cavalcante, C. L., Cecilia, J. A., Rodríguez-Castellón, E., . . . Vieira, R. S. (2015). Calcium/chitosan spheres as catalyst for biodiesel production. *Polymer International*, 64(2), 242-249. doi:10.1002/pi.4782
- Corro, G., Pal, U., & Tellez, N. (2013). Biodiesel production from *Jatropha curcas* crude oil using ZnO/SiO<sub>2</sub> photocatalyst for free fatty acids esterification. *Applied Catalysis B: Environmental*, 129, 39-47. doi:10.1016/j.apcatb.2012.09.004
- Cossio-Vargas, E., Hernandez, S., Segovia-Hernandez, J. G., & Cano-Rodriguez, M. I. (2011). Simulation study of the production of biodiesel using feedstock mixtures of fatty acids in

- complex reactive distillation columns. *Energy*, 36(11), 6289-6297. doi:10.1016/j.energy.2011.10.005
- Da Silva, R. B., Neto, A. F. L., Dos Santos, L. S. S., Lima, J. R. D., Chaves, M. H., Dos Santos, J. R., de Lima, G. M., de Moura, E. M., de Moura, C. V. R. (2008). Catalysts of Cu(II) and Co(II) ions adsorbed in chitosan used in transesterification of soy bean and babassu oils: A new route for biodiesel syntheses. *Bioresource Technology*, 99(15), 6793-6798. doi:10.1016/j.biortech.2008.01.047
- Dai, Y.-M., Wang, Y.-F., & Chen, C.-C. (2018). Synthesis and characterization of magnetic LiFe<sub>5</sub>O<sub>8</sub>-LiFeO<sub>2</sub> as a solid basic catalyst for biodiesel production. *Catalysis Communications*, 106, 20-24. doi:10.1016/j.catcom.2017.12.002
- Demirbas, A. (2007). Importance of biodiesel as transportation fuel. *Energy Policy*, 35(9), 4661-4670. doi:10.1016/j.enpol.2007.04.003
- Demirbas, A. (2009). Progress and recent trends in biodiesel fuels. *Energy Conversion and Management*, 50(1), 14-34. doi:10.1016/j.enconman.2008.09.001
- Demirbas, M. F., Balat, M., & Balat, H. (2009). Potential contribution of biomass to the sustainable energy development. *Energy Conversion and Management*, 50(7), 1746-1760. doi:10.1016/j.enconman.2009.03.013
- Deng, T., Ding, J., Zhao, G., Liu, Y., & Lu, Y. (2018). Catalytic distillation for esterification of acetic acid with ethanol: Promising SS-fiber@HZSM-5 catalytic packings and experimental optimization via response surface methodology. *Journal of Chemical Technology & Biotechnology*, 93(3), 827-841. doi:10.1002/jctb.5436
- Di Serio, M., Tesser, R., Casale, L., D'Angelo, A., Trifuoggi, M., & Santacesaria, E. (2010). Heterogeneous catalysis in biodiesel production: The influence of leaching. *Topics in Catalysis*, 53(11-12), 811-819. doi:10.1007/s11244-010-9467-y
- Di Serio, M., Tesser, R., Pengmei, L., & Santacesaria, E. (2008). Heterogeneous catalysts for biodiesel production. *Energy and Fuels*, 22(1), 207-217. doi:10.1021/ef700250g
- dos Santos, L. K., Hatanaka, R. R., de Oliveira, J. E., & Flumignan, D. L. (2019). Production of biodiesel from crude palm oil by a sequential hydrolysis/esterification process using subcritical water. *Renewable Energy*, 130, 633-640. doi:10.1016/j.renene.2018.06.102
- Duan, Y., Zhu, Z., Cai, K., Tan, X., & Lu, X. (2011). De novo biosynthesis of biodiesel by *Escherichia coli* in optimized fed-batch cultivation. *PLoS One*, 6(5), e20265. doi:10.1371/journal.pone.0020265
- Encinar, J. M., Pardal, A., & Sánchez, N. (2016). An improvement to the transesterification process by the use of co-solvents to produce biodiesel. *Fuel*, 166, 51-58. doi:10.1016/j.fuel.2015.10.110
- Endalew, A. K., Kiros, Y., & Zanzi, R. (2011). Heterogeneous catalysis for biodiesel production from *Jatropha curcas* oil (JCO). *Energy*, 36(5), 2693-2700. doi:10.1016/j.energy.2011.02.010

- Essamlali, Y., Amadine, O., Fihri, A., & Zahouily, M. (2019). Sodium modified fluorapatite as a sustainable solid bi-functional catalyst for biodiesel production from rapeseed oil. *Renewable Energy*, 133, 1295-1307. doi:10.1016/j.renene.2018.08.103
- Falizi N. J., Madenoğlu T. G., Yüksel M., & Kabay N. (2019). Biodiesel production using gel-type cation exchange resin at different ionic forms. *International Journal of Energy Research*, 43, 2188-2199, doi:10.1002/er.4434.
- Farooq, M., Ramli, A., Naeem, A., & Saleem Khan, M. (2016). Effect of different metal oxides on the catalytic activity of  $\gamma$ -Al<sub>2</sub>O<sub>3</sub>-MgO supported bifunctional heterogeneous catalyst in biodiesel production from WCO. *RSC Advances*, 6(2), 872-881. doi:10.1039/c5ra18146a
- Farooq, M., Ramli, A., & Subbarao, D. (2013). Biodiesel production from waste cooking oil using bifunctional heterogeneous solid catalysts. *Journal of Cleaner Production*, 59, 131-140. doi:10.1016/j.jclepro.2013.06.015
- Fawaz, E. G., & Salam, D. A. (2018). Preliminary economic assessment of the use of waste frying oils for biodiesel production in Beirut, Lebanon. *Science of the Total Environment*, 637-638, 1230-1240. doi:10.1016/j.scitotenv.2018.04.421
- Feng, Y., He, B., Cao, Y., Li, J., Liu, M., Yan, F., & Liang, X. (2010). Biodiesel production using cation-exchange resin as heterogeneous catalyst. *Bioresource Technology*, 101(5), 1518-1521. doi:10.1016/j.biortech.2009.07.084
- Ghesti, G. F., de Macedo, J. L., Resck, I. S., Dias, J. A., & Dias, S. C. L. (2007). FT-Raman spectroscopy quantification of biodiesel in a progressive soybean oil transesterification reaction and its correlation with <sup>1</sup>H NMR spectroscopy methods. *Energy & Fuels*, 21(5), 2475-2480. doi:10.1021/ef060657r
- Go, A. W., Sutanto, S., Ong, L. K., Tran-Nguyen, P. L., Ismadji, S., & Ju, Y.-H. (2016). Developments in in-situ (trans) esterification for biodiesel production: A critical review. *Renewable and Sustainable Energy Reviews*, 60, 284-305. doi:10.1016/j.rser.2016.01.070
- Guo, J., Lou, H., Zhao, H., Wang, X., & Zheng, X. (2004). Novel synthesis of high surface area MgAl<sub>2</sub>O<sub>4</sub> spinel as catalyst support. *Materials Letters*, 58(12-13), 1920-1923. doi:10.1016/j.matlet.2003.12.013
- Gurunathan, B., & Ravi, A. (2015). Process optimization and kinetics of biodiesel production from neem oil using copper doped zinc oxide heterogeneous nanocatalyst. *Bioresource Technology*, 190, 424-428. doi:10.1016/j.biortech.2015.04.101
- Huang, G., Chen, F., Wei, D., Zhang, X., & Chen, G. (2010). Biodiesel production by microalgal biotechnology. *Applied Energy*, 87(1), 38-46. doi:10.1016/j.apenergy.2009.06.016
- Huang, J., Xia, J., Jiang, W., Li, Y., & Li, J. (2015). Biodiesel production from microalgae oil catalyzed by a recombinant lipase. *Bioresource Technology*, 180, 47-53. doi:10.1016/j.biortech.2014.12.072
- Hwang, H. T., Qi, F., Yuan, C., Zhao, X., Ramkrishna, D., Liu, D., & Varma, A. (2014). Lipase-catalyzed process for biodiesel production: Protein engineering and lipase production. *Biotechnology and Bioengineering*, 111(4), 639-653. doi:10.1002/bit.25162

- Jeong, S.-H., Lee, H.-S., Kim, D.-K., Lee, J.-P., Park, J.-Y., Hwang, K.-R., & Lee, J.-S. (2017). Biodiesel production from high free fatty acid oils using a bifunctional solid catalyst. *Topics in Catalysis*, 60(9-11), 651-657. doi:10.1007/s11244-017-0772-6
- Jiang, W., Lu, H. F., Qi, T., Yan, S. L., & Liang, B. (2010). Preparation, application, and optimization of Zn/Al complex oxides for biodiesel production under sub-critical conditions. *Biotechnology Advances*, 28(5), 620-627. doi:10.1016/j.biotechadv.2010.05.011
- Kaur, M., Malhotra, R., & Ali, A. (2018). Tungsten supported Ti/SiO<sub>2</sub> nanoflowers as reusable heterogeneous catalyst for biodiesel production. *Renewable Energy*, 116, 109-119. doi:10.1016/j.renene.2017.09.065
- Kiss, A. A., & Bildea, C. S. (2012). A review of biodiesel production by integrated reactive separation technologies. *Journal of Chemical Technology & Biotechnology*, 87(7), 861-879. doi:10.1002/jctb.3785
- Kiss, A. A., Omota, F., Dimian, A. C., & Rothenberg, G. (2006). The heterogeneous advantage: Biodiesel by catalytic reactive distillation. *Topics in Catalysis*, 40(1-4), 141-150. doi:10.1007/s11244-006-0116-4
- Knothe, G. (2010). Biodiesel and renewable diesel: A comparison. *Progress in Energy and Combustion Science*, 36(3), 364-373. doi:10.1016/j.pecs.2009.11.004
- Kondamudi, N., Mohapatra, S. K., & Misra, M. (2011). Quintinite as a bifunctional heterogeneous catalyst for biodiesel synthesis. *Applied Catalysis A: General*, 393(1-2), 36-43. doi:10.1016/j.apcata.2010.11.025
- Kumar, D., Singh, B., & Korstad, J. (2017). Utilization of lignocellulosic biomass by oleaginous yeast and bacteria for production of biodiesel and renewable diesel. *Renewable and Sustainable Energy Reviews*, 73, 654-671. doi:10.1016/j.rser.2017.01.022
- Lee, A. F., Bennett, J. A., Manayil, J. C., & Wilson, K. (2014). Heterogeneous catalysis for sustainable biodiesel production via esterification and transesterification. *Chemical Society Reviews*, 43(22), 7887-7916. doi:10.1039/c4cs00189c
- Lee, H. V., Juan, J. C., & Taufiq-Yap, Y. H. (2015). Preparation and application of binary acid–base CaO–La<sub>2</sub>O<sub>3</sub> catalyst for biodiesel production. *Renewable Energy*, 74, 124-132. doi:10.1016/j.renene.2014.07.017
- Lee, J. S., & Saka, S. (2010). Biodiesel production by heterogeneous catalysts and supercritical technologies. *Bioresource Technology*, 101(19), 7191-7200. doi:10.1016/j.biortech.2010.04.071
- Lee, K. T., Lim, S., Pang, Y. L., Ong, H. C., & Chong, W. T. (2014). Integration of reactive extraction with supercritical fluids for process intensification of biodiesel production: Prospects and recent advances. *Progress in Energy and Combustion Science*, 45, 54-78. doi:10.1016/j.pecs.2014.07.001
- Leung, D. Y. C., Wu, X., & Leung, M. K. H. (2010). A review on biodiesel production using catalyzed transesterification. *Applied Energy*, 87(4), 1083-1095. doi:10.1016/j.apenergy.2009.10.006

- Li, H., Niu, S., Lu, C., & Li, J. (2016). Calcium oxide functionalized with strontium as heterogeneous transesterification catalyst for biodiesel production. *Fuel*, 176, 63-71. doi:10.1016/j.fuel.2016.02.067
- Liu, X., He, H., Wang, Y., & Zhu, S. (2007). Transesterification of soybean oil to biodiesel using SrO as a solid base catalyst. *Catalysis Communications*, 8(7), 1107-1111. doi:10.1016/j.catcom.2006.10.026
- Macario, A., Giordano, G., Onida, B., Cocina, D., Tagarelli, A., & Giuffrè, A. M. (2010). Biodiesel production process by homogeneous/heterogeneous catalytic system using an acid–base catalyst. *Applied Catalysis A: General*, 378(2), 160-168. doi:10.1016/j.apcata.2010.02.016
- Maneerung, T., Kawi, S., Dai, Y., & Wang, C.-H. (2016). Sustainable biodiesel production via transesterification of waste cooking oil by using CaO catalysts prepared from chicken manure. *Energy Conversion and Management*, 123, 487-497. doi:10.1016/j.enconman.2016.06.071
- Marchetti, J. M., Miguel, V. U., & Errazu, A. F. (2007). Possible methods for biodiesel production. *Renewable and Sustainable Energy Reviews*, 11(6), 1300-1311. doi:10.1016/j.rser.2005.08.006
- Mardhiah, H. H., Ong, H. C., Masjuki, H. H., Lim, S., & Lee, H. V. (2017). A review on latest developments and future prospects of heterogeneous catalyst in biodiesel production from non-edible oils. *Renewable and Sustainable Energy Reviews*, 67, 1225-1236. doi:10.1016/j.rser.2016.09.036
- Meng, X., Yang, J., Xu, X., Zhang, L., Nie, Q., & Xian, M. (2009). Biodiesel production from oleaginous microorganisms. *Renewable Energy*, 34(1), 1-5. doi:10.1016/j.renene.2008.04.014
- Meng, Y. L., Wang, B. Y., Li, S. F., Tian, S. J., & Zhang, M. H. (2013). Effect of calcination temperature on the activity of solid Ca/Al composite oxide-based alkaline catalyst for biodiesel production. *Bioresource Technology*, 128, 305-309. doi:10.1016/j.biortech.2012.10.152
- Meshram, D., Thote, S., Singh, N., & Pakhare, K. (2013). Algae fuel technology: Concept of revolutionary future. *Research and Development (IJAERD)*, 3(3), 15-28.
- Mierczynski, P., Chalupka, K. A., Maniukiewicz, W., Kubicki, J., Szyrkowska, M. I., & Maniecki, T. P. (2015). SrAl<sub>2</sub>O<sub>4</sub> spinel phase as active phase of transesterification of rapeseed oil. *Applied Catalysis B: Environmental*, 164, 176-183. doi:10.1016/j.apcatb.2014.09.003
- Mohammad Fauzi, A. H., Amin, N. A. S., & Mat, R. (2014). Esterification of oleic acid to biodiesel using magnetic ionic liquid: Multi-objective optimization and kinetic study. *Applied Energy*, 114, 809-818. doi:10.1016/j.apenergy.2013.10.011
- Mohammadshirazi, A., Akram, A., Rafiee, S., & Bagheri Kalhor, E. (2014). Energy and cost analyses of biodiesel production from waste cooking oil. *Renewable and Sustainable Energy Reviews*, 33, 44-49. doi:10.1016/j.rser.2014.01.067
- Moser, B. R. (2009). Biodiesel production, properties, and feedstocks. *In Vitro Cellular & Developmental Biology - Plant*, 45(3), 229-266. doi:10.1007/s11627-009-9204-z

- Muniyappa, P. R., Brammer, S. C., & Nouredini, H. (1996). Improved conversion of plant oils and animal fats into biodiesel and co-product. *Bioresource Technology*, 56(1), 19-24. doi:10.1016/0960-8524(95)00178-6
- Muthia, R., Reijneveld, A. G. T., van der Ham, A. G. J., ten Kate, A. J. B., Bargeman, G., Kersten, S. R. A., & Kiss, A. A. (2018). Novel method for mapping the applicability of reactive distillation. *Chemical Engineering and Processing - Process Intensification*, 128, 263-275. doi:10.1016/j.cep.2018.04.001
- Mythili, R., Venkatachalam, P., Subramanian, P., & Uma, D. (2014). Production characterization and efficiency of biodiesel: A review. *International Journal of Energy Research*, 38(10), 1233-1259. doi:10.1002/er.3165
- Nata, I. F., Putra, M. D., Irawan, C., & Lee, C.-K. (2017). Catalytic performance of sulfonated carbon-based solid acid catalyst on esterification of waste cooking oil for biodiesel production. *Journal of Environmental Chemical Engineering*, 5(3), 2171-2175. doi:10.1016/j.jece.2017.04.029
- Nielsen, P. M., Brask, J., & Fjerbaek, L. (2008). Enzymatic biodiesel production: Technical and economical considerations. *European Journal of Lipid Science and Technology*, 110(8), 692-700. doi:10.1002/ejlt.200800064
- Noriega, M. A., Narváez, P. C., & Habert, A. C. (2018). Simulation and validation of biodiesel production in liquid-liquid film reactors integrated with PES hollow fibers membranes. *Fuel*, 227, 367-378. doi:10.1016/j.fuel.2018.04.101
- Noshadi, I., Amin, N. A. S., & Parnas, R. S. (2012). Continuous production of biodiesel from waste cooking oil in a reactive distillation column catalyzed by solid heteropolyacid: Optimization using response surface methodology (RSM). *Fuel*, 94, 156-164. doi:10.1016/j.fuel.2011.10.018
- Nyström, R., Sadiktsis, I., Ahmed, T. M., Westerholm, R., Koegler, J. H., Blomberg, A., . . . Boman, C. (2016). Physical and chemical properties of RME biodiesel exhaust particles without engine modifications. *Fuel*, 186, 261-269. doi:10.1016/j.fuel.2016.08.062
- Parawira, W. (2009). Biotechnological production of biodiesel fuel using biocatalysed transesterification: A review. *Critical Reviews in Biotechnology*, 29(2), 82-93. doi:10.1080/07388550902823674
- Park, Y. M., Lee, J. Y., Chung, S. H., Park, I. S., Lee, S. Y., Kim, D. K., . . . Lee, K. Y. (2010). Esterification of used vegetable oils using the heterogeneous WO<sub>3</sub>/ZrO<sub>2</sub> catalyst for production of biodiesel. *Bioresource Technology*, 101 Suppl 1, S59-61. doi:10.1016/j.biortech.2009.04.025
- Pasupulety, N., Gunda, K., Liu, Y., Rempel, G. L., & Ng, F. T. T. (2013). Production of biodiesel from soybean oil on CaO/Al<sub>2</sub>O<sub>3</sub> solid base catalysts. *Applied Catalysis A: General*, 452, 189-202. doi:10.1016/j.apcata.2012.10.006
- Peng, B.-X., Shu, Q., Wang, J.-F., Wang, G.-R., Wang, D.-Z., & Han, M.-H. (2008). Biodiesel production from waste oil feedstocks by solid acid catalysis. *Process Safety and Environmental Protection*, 86(6), 441-447. doi:10.1016/j.psep.2008.05.003

- Pérez-Cisneros, E. S., Mena-Espino, X., Rodríguez-López, V., Sales-Cruz, M., Viveros-García, T., & Lobo-Oehmichen, R. (2016). An integrated reactive distillation process for biodiesel production. *Computers & Chemical Engineering*, 91, 233-246. doi:10.1016/j.compchemeng.2016.01.008
- Petchsoongsakul, N., Ngaosuwan, K., Kiatkittipong, W., Aiouache, F., & Assabumrungrat, S. (2017). Process design of biodiesel production: Hybridization of ester- and transesterification in a single reactive distillation. *Energy Conversion and Management*, 153, 493-503. doi:10.1016/j.enconman.2017.10.013
- Pinzi, S., Leiva, D., López-García, I., Redel-Macías, M. D., & Dorado, M. P. (2014). Latest trends in feedstocks for biodiesel production. *Biofuels, Bioproducts and Biorefining*, 8(1), 126-143. doi:10.1002/bbb.1435
- Pirouzmand, M., Anakhaton, M. M., & Ghasemi, Z. (2018). One-step biodiesel production from waste cooking oils over metal incorporated MCM-41; positive effect of template. *Fuel*, 216, 296-300. doi:10.1016/j.fuel.2017.11.138
- Pourzolfaghar, H., Abnisa, F., Daud, W. M. A. W., & Aroua, M. K. (2016). A review of the enzymatic hydroesterification process for biodiesel production. *Renewable and Sustainable Energy Reviews*, 61, 245-257. doi:10.1016/j.rser.2016.03.048
- Pradana, Y. S., Hidayat, A., Prasetya, A., & Budiman, A. (2017). Biodiesel production in a reactive distillation column catalyzed by heterogeneous potassium catalyst. *Energy Procedia*, 143, 742-747. doi:10.1016/j.egypro.2017.12.756
- Qiul, J., Fan, X., & Zou, H. (2011). Development of biodiesel from inedible feedstock through various production processes. *Review. Chemistry and Technology of Fuels and Oils*, 47(2), 102-111. doi:10.1007/s10553-011-0266-3
- Rafiei, S., Tangestaninejad, S., Horcajada, P., Moghadam, M., Mirkhani, V., Mohammadpoor-Baltork, I., . . . Zadehahmadi, F. (2018). Efficient biodiesel production using a lipase@ZIF-67 nanobioreactor. *Chemical Engineering Journal*, 334, 1233-1241. doi:10.1016/j.cej.2017.10.094
- Ramachandran, K., Suganya, T., Nagendra Gandhi, N., & Renganathan, S. (2013). Recent developments for biodiesel production by ultrasonic assist transesterification using different heterogeneous catalyst: A review. *Renewable and Sustainable Energy Reviews*, 22, 410-418. doi:10.1016/j.rser.2013.01.057
- Ramu, S., Lingaiah, N., Prabhavathi Devi, B. L. A., Prasad, R. B. N., Suryanarayana, I., & Sai Prasad, P. S. (2004). Esterification of palmitic acid with methanol over tungsten oxide supported on zirconia solid acid catalysts: Effect of method of preparation of the catalyst on its structural stability and reactivity. *Applied Catalysis A: General*, 276(1-2), 163-168. doi:10.1016/j.apcata.2004.08.002
- Rashtizadeh, E., Farzaneh, F., & Talebpour, Z. (2014). Synthesis and characterization of Sr3Al2O6 nanocomposite as catalyst for biodiesel production. *Bioresource Technology*, 154, 32-37. doi:10.1016/j.biortech.2013.12.014

- Rattanaphra, D., Soodjit, P., Thanapimmetha, A., Saisriyoot, M., & Srinophakun, P. (2019). Synthesis, characterization and catalytic activity studies of lanthanum oxide from Thai monazite ore for biodiesel production. *Renewable Energy* 131, 1128-1137. doi: 10.1016/j.renene.2018.08.066.
- Rodolfi, L., Chini Zittelli, G., Bassi, N., Padovani, G., Biondi, N., Bonini, G., & Tredici, M. R. (2009). Microalgae for oil: Strain selection, induction of lipid synthesis and outdoor mass cultivation in a low-cost photobioreactor. *Biotechnology and Bioengineering*, 102(1), 100-112. doi:10.1002/bit.22033
- Roschat, W., Siritanon, T., Yoosuk, B., & Promarak, V. (2016). Rice husk-derived sodium silicate as a highly efficient and low-cost basic heterogeneous catalyst for biodiesel production. *Energy Conversion and Management*, 119, 453-462. doi:10.1016/j.enconman.2016.04.071
- Ruhul, A. M., Kalam, M. A., Masjuki, H. H., Fattah, I. M. R., Reham, S. S., & Rashed, M. M. (2015). State of the art of biodiesel production processes: A review of the heterogeneous catalyst. *RSC Advances*, 5(122), 101023-101044. doi:10.1039/c5ra09862a
- Sádaba, I., López Granados, M., Riisager, A., & Taarning, E. (2015). Deactivation of solid catalysts in liquid media: The case of leaching of active sites in biomass conversion reactions. *Green Chemistry*, 17(8), 4133-4145. doi:10.1039/c5gc00804b
- Salinas, D., Sepúlveda, C., Escalona, N., Gfierro, J. L., & Pecchi, G. (2018). Sol-gel La<sub>2</sub>O<sub>3</sub>-ZrO<sub>2</sub> mixed oxide catalysts for biodiesel production. *Journal of Energy Chemistry*, 27 (2), 565-572. doi:10.1016/j.jechem.2017.11.003.
- Sani, Y. M., Daud, W. M. A. W., & Abdul Aziz, A. R. (2013). Solid acid-catalyzed biodiesel production from microalgal oil: The dual advantage. *Journal of Environmental Chemical Engineering*, 1(3), 113-121. doi:10.1016/j.jece.2013.04.006
- Satyarthi, J. K., Srinivas, D., & Ratnasamy, P. (2009). Estimation of free fatty acid content in oils, fats, and biodiesel by <sup>1</sup>H NMR spectroscopy. *Energy & Fuels*, 23(4), 2273-2277. doi:10.1021/ef801011v
- Sbihi, H. M., Nehdi, I. A., Blidi, L. E., Rashid, U., & Al-Resayes, S. I. (2015). Lipase/enzyme catalyzed biodiesel production from Prunus mahaleb: A comparative study with base catalyzed biodiesel production. *Industrial Crops and Products*, 76, 1049-1054. doi:10.1016/j.indcrop.2015.08.023
- Semwal, S., Arora, A. K., Badoni, R. P., & Tuli, D. K. (2011). Biodiesel production using heterogeneous catalysts. *Bioresource Technology*, 102(3), 2151-2161. doi:10.1016/j.biortech.2010.10.080
- Sharma, Y. C., Singh, B., & Korstad, J. (2011). Latest developments on application of heterogenous basic catalysts for an efficient and eco friendly synthesis of biodiesel: A review. *Fuel*, 90(4), 1309-1324. doi:10.1016/j.fuel.2010.10.015
- Sharma, Y. C., Singh, B., & Upadhyay, S. N. (2008). Advancements in development and characterization of biodiesel: A review. *Fuel*, 87(12), 2355-2373. doi:10.1016/j.fuel.2008.01.014

- Shi, S., Valle-Rodriguez, J. O., Khoomrung, S., Siewers, V., & Nielsen, J. (2012). Functional expression and characterization of five wax ester synthases in *Saccharomyces cerevisiae* and their utility for biodiesel production. *Biotechnol Biofuels*, 5, 7. doi:10.1186/1754-6834-5-7
- Shi, S., Valle-Rodriguez, J. O., Siewers, V., & Nielsen, J. (2011). Prospects for microbial biodiesel production. *Journal of Biotechnology*, 6(3), 277-285. doi:10.1002/biot.201000117
- Songstad, D. D., Lakshmanan, P., Chen, J., Gibbons, W., Hughes, S., & Nelson, R. (2009). Historical perspective of biofuels: Learning from the past to rediscover the future. *In Vitro Cellular & Developmental Biology - Plant*, 45(3), 189-192. doi:10.1007/s11627-009-9218-6
- Steen, E. J., Kang, Y., Bokinsky, G., Hu, Z., Schirmer, A., McClure, A., . . . Keasling, J. D. (2010). Microbial production of fatty-acid-derived fuels and chemicals from plant biomass. *Nature*, 463(7280), 559-562. doi:10.1038/nature08721
- Su, M., Yang, R., & Li, M. (2013). Biodiesel production from hempseed oil using alkaline earth metal oxides supporting copper oxide as bi-functional catalysts for transesterification and selective hydrogenation. *Fuel*, 103, 398-407. doi:10.1016/j.fuel.2012.07.009
- Sun, C., Qiu, F., Yang, D., & Ye, B. (2014). Preparation of biodiesel from soybean oil catalyzed by Al-Ca hydrotalcite loaded with K<sub>2</sub>CO<sub>3</sub> as heterogeneous solid base catalyst. *Fuel Processing Technology*, 126, 383-391. doi:10.1016/j.fuproc.2014.05.021
- Talebian-Kiakalaieh, A., Amin, N. A. S., & Mazaheri, H. (2013). A review on novel processes of biodiesel production from waste cooking oil. *Applied Energy*, 104, 683-710. doi:10.1016/j.apenergy.2012.11.061
- Tamborini, L. H., Casco, M. E., Militello, M. P., Silvestre-Albero, J., Barbero, C. A., & Acevedo, D. F. (2016). Sulfonated porous carbon catalysts for biodiesel production: Clear effect of the carbon particle size on the catalyst synthesis and properties. *Fuel Processing Technology*, 149, 209-217. doi:10.1016/j.fuproc.2016.04.006
- Tang, Z.-E., Lim, S., Pang, Y.-L., Ong, H.-C., & Lee, K.-T. (2018). Synthesis of biomass as heterogeneous catalyst for application in biodiesel production: State of the art and fundamental review. *Renewable and Sustainable Energy Reviews*, 92, 235-253. doi:10.1016/j.rser.2018.04.056
- Taufiq-Yap, Y. H., Teo, S. H., Rashid, U., Islam, A., Hussien, M. Z., & Lee, K. T. (2014). Transesterification of *Jatropha curcas* crude oil to biodiesel on calcium lanthanum mixed oxide catalyst: Effect of stoichiometric composition. *Energy Conversion and Management*, 88, 1290-1296. doi:10.1016/j.enconman.2013.12.075
- Teo, W. S., Ling, H., Yu, A. Q., & Chang, M. W. (2015). Metabolic engineering of *Saccharomyces cerevisiae* for production of fatty acid short- and branched-chain alkyl esters biodiesel. *Biotechnology for Biofuels*, 8, 177. doi:10.1186/s13068-015-0361-5
- Thliveros, P., Uckun Kiran, E., & Webb, C. (2014). Microbial biodiesel production by direct methanolysis of oleaginous biomass. *Bioresource Technology*, 157, 181-187. doi:10.1016/j.biortech.2014.01.111

- Tran, D.-T., Chang, J.-S., & Lee, D.-J. (2017). Recent insights into continuous-flow biodiesel production via catalytic and non-catalytic transesterification processes. *Applied Energy*, 185, 376-409. doi:10.1016/j.apenergy.2016.11.006
- Umdu, E. S., Tuncer, M., & Seker, E. (2009). Transesterification of *Nannochloropsis oculata* microalga's lipid to biodiesel on Al<sub>2</sub>O<sub>3</sub> supported CaO and MgO catalysts. *Bioresource Technology*, 100(11), 2828-2831. doi:10.1016/j.biortech.2008.12.027
- Verma, P., & Sharma, M. P. (2016). Review of process parameters for biodiesel production from different feedstocks. *Renewable and Sustainable Energy Reviews*, 62, 1063-1071. doi:10.1016/j.rser.2016.04.054
- Vieira, S. S., Graça, I., Fernandes, A., Lopes, J. M. F. M., Ribeiro, M. F., & Magriotis, Z. M. (2018). Influence of calcination temperature on catalytic, acid and textural properties of SO<sub>4</sub><sup>2-</sup>/La<sub>2</sub>O<sub>3</sub> /HZSM-5 type catalysts for biodiesel production by esterification. *Microporous and Mesoporous Materials*, 270, 189-199. doi:10.1016/j.micromeso.2018.05.021
- Vijaya, J. J., Kennedy, L. J., Sekaran, G., & Nagaraja, K. S. (2008). Synthesis, characterization and humidity sensing properties of Cu–Sr–Al mixed metal oxide composites. *Materials Research Bulletin*, 43(2), 473-482. doi:10.1016/j.materresbull.2007.02.030
- Wan Omar, W. N. N., & Amin, N. A. S. (2011). Biodiesel production from waste cooking oil over alkaline modified zirconia catalyst. *Fuel Processing Technology*, 92(12), 2397-2405. doi:10.1016/j.fuproc.2011.08.009
- Wang, Y.-T., Fang, Z., & Yang, X.-X. (2017). Biodiesel production from high acid value oils with a highly active and stable bifunctional magnetic acid. *Applied Energy*, 204, 702-714. doi:10.1016/j.apenergy.2017.07.060
- Wang, Y.-T., Fang, Z., Yang, X.-X., Yang, Y.-T., Luo, J., Xu, K., & Bao, G.-R. (2018). One-step production of biodiesel from *Jatropha* oils with high acid value at low temperature by magnetic acid-base amphoteric nanoparticles. *Chemical Engineering Journal*, 348, 929-939. doi:10.1016/j.cej.2018.05.039
- Wen, Z., Yu, X., Tu, S. T., Yan, J., & Dahlquist, E. (2010). Biodiesel production from waste cooking oil catalyzed by TiO<sub>2</sub>-MgO mixed oxides. *Bioresource Technology*, 101(24), 9570-9576. doi:10.1016/j.biortech.2010.07.066
- Wierzbicki, M., Niraula, N., Yarrabothula, A., Layton, D. S., & Trinh, C. T. (2016). Engineering an *Escherichia coli* platform to synthesize designer biodiesels. *Journal of Biotechnology*, 224, 27-34. doi:10.1016/j.jbiotec.2016.03.001
- Wu, L., Wei, T., Lin, Z., Zou, Y., Tong, Z., & Sun, J. (2016). Bentonite-enhanced biodiesel production by NaOH-catalyzed transesterification: Process optimization and kinetics and thermodynamic analysis. *Fuel*, 182, 920-927. doi:10.1016/j.fuel.2016.05.065
- Xu, H., Zhang, Y., Wu, H., Liu, Y., Li, X., Jiang, J., . . . Wu, P. (2011). Postsynthesis of mesoporous MOR-type titanosilicate and its unique catalytic properties in liquid-phase oxidations. *Journal of Catalysis*, 281(2), 263-272. doi:10.1016/j.jcat.2011.05.009

- Xu, Y., Peng, W., Wang, S., Xiang, X., & Lu, P. (2006). Synthesis of SrAl<sub>2</sub>O<sub>4</sub> and SrAl<sub>12</sub>O<sub>19</sub> via ethylenediaminetetraacetic acid precursor. *Materials Chemistry and Physics*, 98(1), 51-54. doi:10.1016/j.matchemphys.2005.08.065
- Xue, B.-j., Luo, J., Zhang, F., & Fang, Z. (2014). Biodiesel production from soybean and Jatropha oils by magnetic CaFe<sub>2</sub>O<sub>4</sub>-Ca<sub>2</sub>Fe<sub>2</sub>O<sub>5</sub>-based catalyst. *Energy*, 68, 584-591. doi:10.1016/j.energy.2014.02.082
- Yadav, M., & Sharma, Y. C. (2018). Process optimization and catalyst poisoning study of biodiesel production from kusum oil using potassium aluminum oxide as efficient and reusable heterogeneous catalyst. *Journal of Cleaner Production*, 199, 593-602. doi:10.1016/j.jclepro.2018.07.052
- Yahya, N. Y., Ngadi, N., Wong, S., & Hassan, O. (2018). Transesterification of used cooking oil (UCO) catalyzed by mesoporous calcium titanate: Kinetic and thermodynamic studies. *Energy Conversion and Management*, 164, 210-218. doi:10.1016/j.enconman.2018.03.011
- Yan, S., Salley, S. O., & Simon Ng, K. Y. (2009). Simultaneous transesterification and esterification of unrefined or waste oils over ZnO-La<sub>2</sub>O<sub>3</sub> catalysts. *Applied Catalysis A: General*, 353(2), 203-212. doi:10.1016/j.apcata.2008.10.053
- Yang, R., Su, M., Li, M., Zhang, J., Hao, X., & Zhang, H. (2010). One-pot process combining transesterification and selective hydrogenation for biodiesel production from starting material of high degree of unsaturation. *Bioresource Technology*, 101(15), 5903-5909. doi:10.1016/j.biortech.2010.02.095
- Yang, Z., & Xie, W. (2007). Soybean oil transesterification over zinc oxide modified with alkali earth metals. *Fuel Processing Technology*, 88(6), 631-638. doi:10.1016/j.fuproc.2007.02.006
- Ye, B., Qiu, F., Sun, C., Li, Y., & Yang, D. (2014). Biodiesel production from soybean oil using heterogeneous solid base catalyst. *Journal of Chemical Technology & Biotechnology*, 89(7), 988-997. doi:10.1002/jctb.4190
- Yilmaz, N., Ileri, E., & Atmanli, A. (2016). Performance of biodiesel/higher alcohols blends in a diesel engine. *International Journal of Energy Research*, 40(8), 1134-1143. doi:10.1002/er.3513
- Yusuf, N. N. A. N., Kamarudin, S. K., & Yaakub, Z. (2011). Overview on the current trends in biodiesel production. *Energy Conversion and Management*, 52(7), 2741-2751. doi:10.1016/j.enconman.2010.12.004
- Zhang, F., Fang, Z., & Wang, Y.-T. (2015). Biodiesel production directly from oils with high acid value by magnetic Na<sub>2</sub>SiO<sub>3</sub>@Fe<sub>3</sub>O<sub>4</sub>/C catalyst and ultrasound. *Fuel*, 150, 370-377. doi:10.1016/j.fuel.2015.02.032
- Zhang, F., Tian, X.-F., Fang, Z., Shah, M., Wang, Y.-T., Jiang, W., & Yao, M. (2017). Catalytic production of Jatropha biodiesel and hydrogen with magnetic carbonaceous acid and base synthesized from Jatropha hulls. *Energy Conversion and Management*, 142, 107-116. doi:10.1016/j.enconman.2017.03.026

- Zhang, F., Wu, X.-H., Yao, M., Fang, Z., & Wang, Y.-T. (2016). Production of biodiesel and hydrogen from plant oil catalyzed by magnetic carbon-supported nickel and sodium silicate. *Green Chemistry*, 18(11), 3302-3314. doi:10.1039/c5gc02680f
- Zhu, H., Wu, Z., Chen, Y., Zhang, P., Duan, S., Liu, X., & Mao, Z. (2006). Preparation of biodiesel catalyzed by solid super base of calcium oxide and its refining process. *Chinese Journal of Catalysis*, 27(5), 391-396. doi:10.1016/s1872-2067(06)60024-7
- Zimmerman, W. B., & Kokoo, R. (2018). Esterification for biodiesel production with a phantom catalyst: Bubble mediated reactive distillation. *Applied Energy*, 221, 28-40. doi:10.1016/j.apenergy.2018.03.147

## Appendix A: Supplementary materials

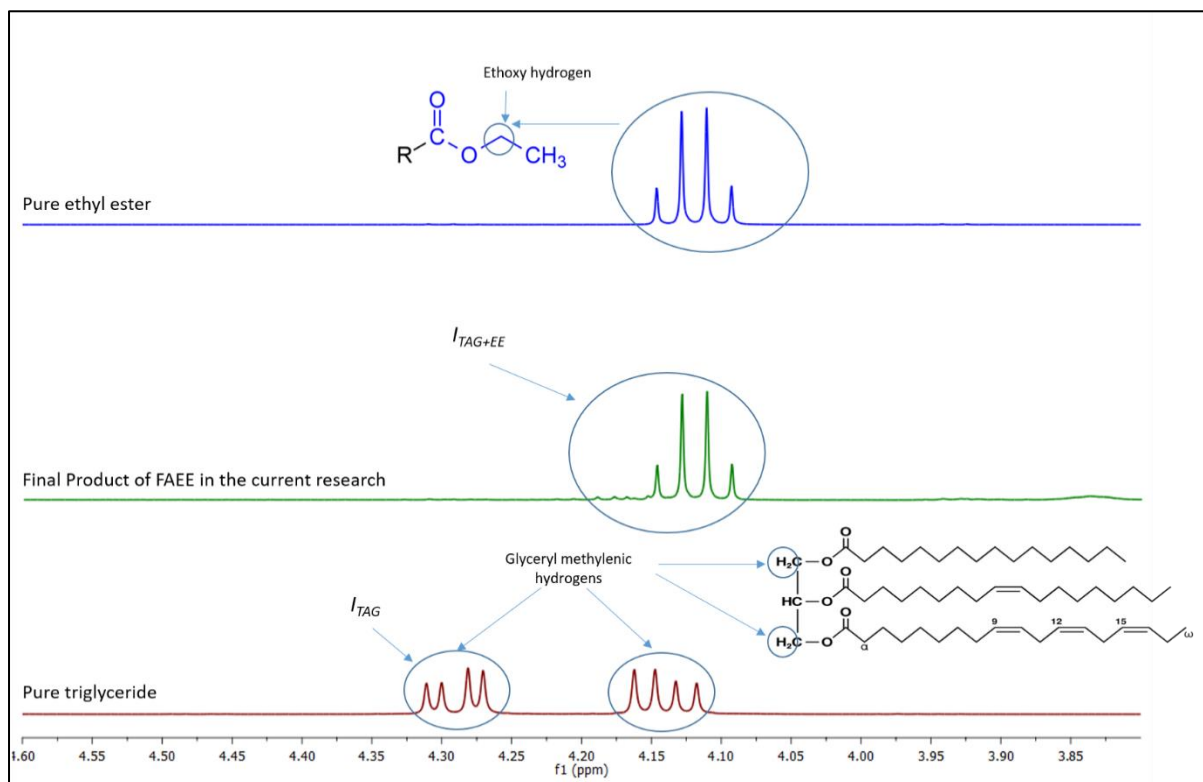
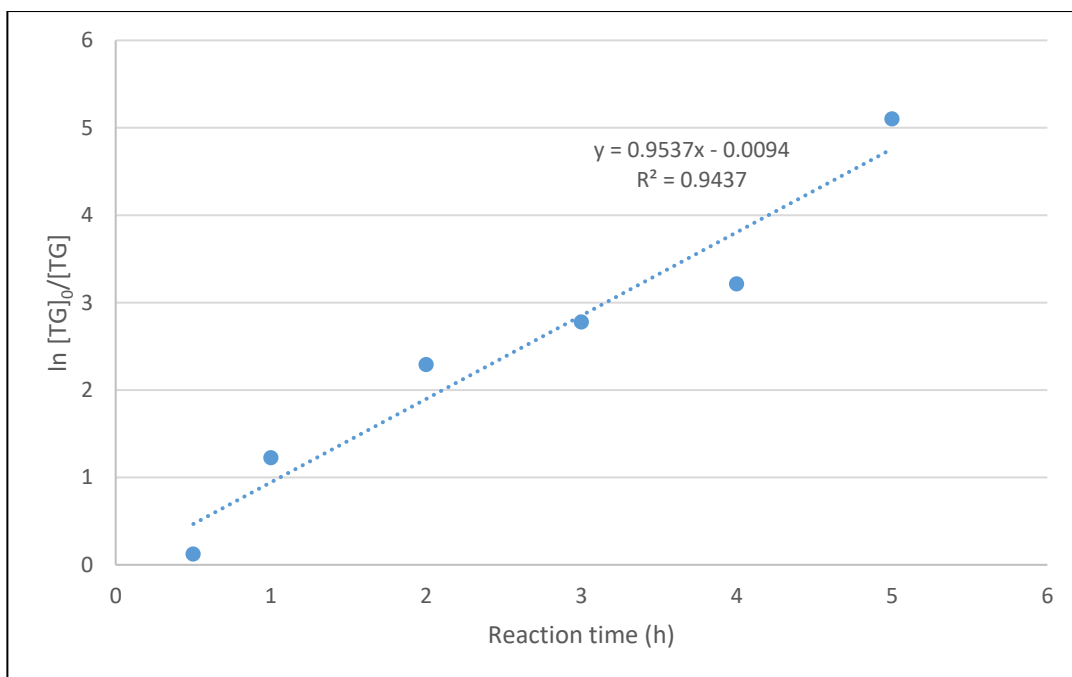
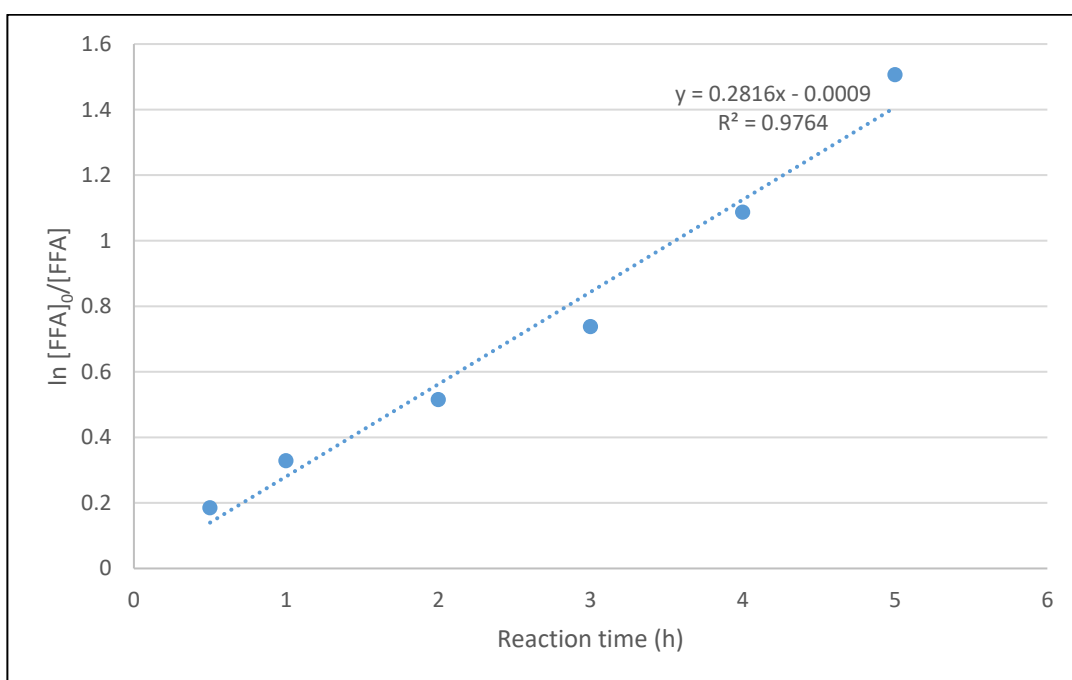


Figure S 1. <sup>1</sup>H NMR spectra for FAEE product with pure ethyl ester and pure triglycerides for comparison

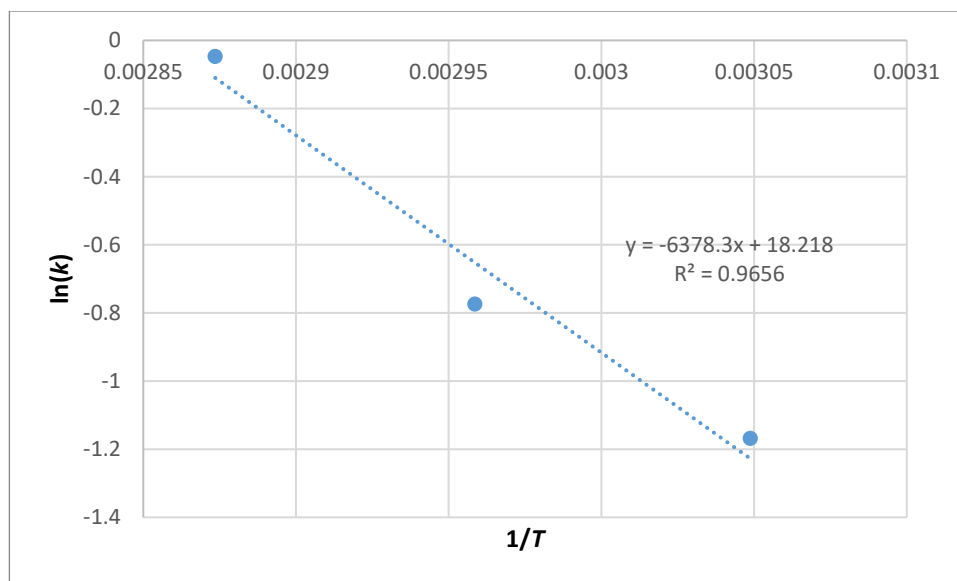


(a)

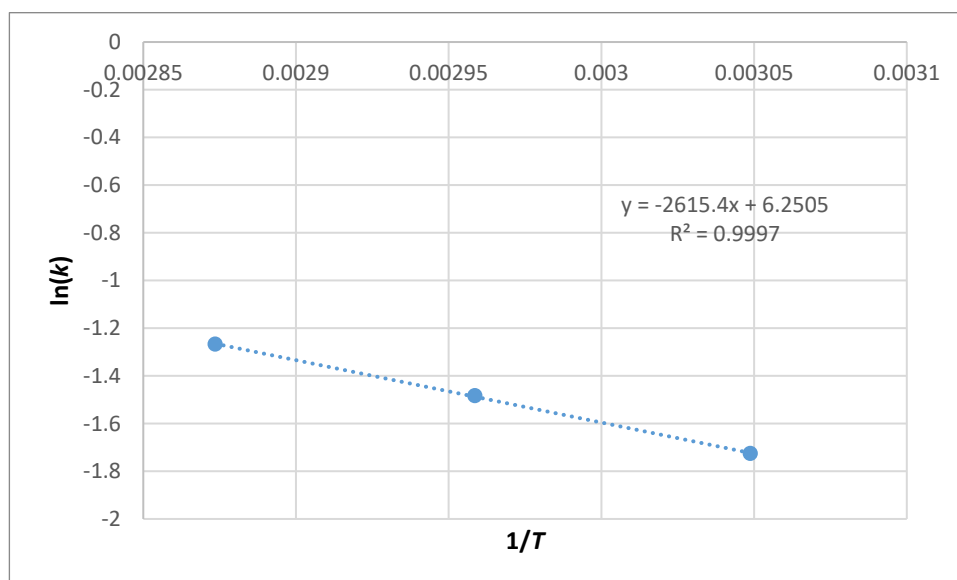


(b)

Figure S 2. Kinetic pseudo-first-order models fitted to data from a) transesterification and b) esterification reactions



(a)



(b)

Figure S 3. Pseudo-first-order models of the activation energies of a) transesterification and b) esterification reactions

### **ASTM D6751:**

For determining the acid number, 2 g of oil sample are dissolved in 100 mL of beaker. Add 75 ml of ethanol/diethyl ether mixture (1:1). The titrant is a potassium hydroxide with molarity (0.1 mol/L). The acid number was calculated as follows:

$$\text{Acid value} = \frac{\text{volume of KOH}(ml) \times N \text{ KOH} \left(\frac{mmol}{ml}\right) \times 56.1\left(\frac{mg}{mmol}\right)}{\text{sample weight (g)}}$$

### **ASTM D 5558:**

5g of sample to 50 mL of the alcoholic KOH in 100 ml 2 neck reactor. Connect air condensers to the reactor and boil the solution gently but steadily until the sample is completely saponified. After the reactor and condenser have cooled somewhat. Then disconnect the flask, add approximately 1 mL of indicator, and titrate the solution with 0.5 N HCl until the pink color has just disappeared. Calculate the saponification number as follows:

$$\text{saponification value} = 28.05 \frac{A - B}{\text{weight sample}}$$

where:

A = titration of blank, and

B = titration of sample.

### **ASTM D 1744:**

- 1) Sample 0.1 ~ 2.5g of test oil in a 5mL syringe.
- 2) Weigh the syringe on a balance of which resolution is to the nearest 0.1mg.
- 3) Discharge the sample into the titration cell to dissolve in the solvent.
- 4) Press Start key of the titrator.
- 5) Weigh the syringe of above 3).
- 6) Enter Wt1 with weighed above 2) and Wt2 with 5).

7) The endpoint is automatically detected, from which water content can be obtained.

$$\text{Moisture \%} = \frac{\text{Data} \times F - \text{Blank}}{Wt1 - Wt2} \times 0.1$$

where:

Data = Titration volume (mL)

F = Reagent factor (mg H<sub>2</sub>O/mL)

Blank = Blank level (mg)

Wt1 = Sample + Syringe weight (g)

Wt2 = Empty syringe (g)

**ASTM D 1298-99:**

The density is measured by using a hydrometer cylinder. Lower the appropriate hydrometer into the liquid and release when in a position equilibrium. Then read the density as it appears in the hydrometer scale.